Author:
Thirthagiri, Eswary

Title:
Mechanisms of genomic instability in oral cancer

MECHANISMS OF GENOMIC INSTABILITY IN ORAL CANCER

by

Eswary Thirthagiri

A dissertation submitted to the University of Bristol

in accordance with the requirements of the degree of

Doctor of Philosophy in the Faculty of Medicine

December 2004

Department of Oral and Dental Science

Division of Oral Medicine, Pathology and Microbiology

Bristol Dental Hospital and School

University of Bristol

Word Count: 36, 423

ABSTRACT

Chromosomal instability (CIN), characterised by alterations in structure and number of chromosomes, is a feature common to oral cancer. The mechanism(s) underlying this phenomenon, however, is unknown. This study examined the mitotic and tetraploidy checkpoints and centrosomes in a panel of seven human oral squamous cell carcinoma (OSCC)-derived cell lines. The results showed that the mitotic checkpoint was attenuated in five cell lines and indicated that the tetraploidy checkpoint was defective in two cell lines. Numerical and morphological centrosome abnormalities were observed in five of the seven cell lines. The centrosomes were able to nucleate microtubules in all cells but defects in the ability of cells to monitor the numbers of microtubules nucleated were observed in two cell lines. Analysis of clonal cell populations further showed that cells containing centrosome abnormalities might have an intrinsic inability to maintain normal centrosome numbers.

Centrosome abnormalities were also examined in archival paraffin-embedded oral tissues. Centrosome abnormalities were detected in 100% of dysplasias (28/28) and OSCCs (17/17). The percentage of cells with abnormal centrosomes increased during the transition from dysplasia to SCC and correlated with a loss of tumour cell differentiation. The results suggest that these abnormalities appear early in the development of oral cancer and contribute to tumour aggressiveness. Centrosome abnormalities in dysplasias occurred irrespective of ploidy status, indicating that these abnormalities precede CIN during disease progression.

In an attempt to develop an *in vitro* model of CIN, human immortalised normal oral keratinocytes were treated with the carcinogen 2-amino-1-methyl-6-phenylimidazo[4,5-b]pyridine (PhIP). Development of PhIP resistance resulted in consistent chromosomal gains and not a dynamic CIN. The response of the PhIP-resistant clones to irradiation induced DNA damage, in terms of cell viability, induction of apoptosis, activation of the p53 pathway and cell cycle arrest was similar to parental control cells indicating that the induction of PhIP-resistance was not associated with resistance to other forms of DNA damage.

ACKNOWLEDGEMENTS

I wish to express my sincere gratitude to my supervisor, Dr. Ian Paterson, Senior Lecturer in Cancer Research, University of Bristol, for his guidance and advice throughout this period of study. I would also like to thank Prof. Stephen Prime, Head of the Dental School, University of Bristol, for his support and encouragement during the course of my work.

I would like to acknowledge Dr. Max Robinson for his guidance for my *in vivo* work on oral cancer, Dr. Angela Hague and Dr. Maria Davies for their advice on cell cycle analysis and molecular biology, respectively. I would also like to thank Mrs Andrea Stone, Miss Suzanne Huntley and Dr Lee San San for technical advice during the course of my studies and to Mr. Nye Fathers for his help with photography.

I would like to thank my collaborators, Dr. Paul Murray (University of Birmingham) and Dr. Jon Sudbo (University of Oslo), whose help facilitated studies on genomic instability in oral cancer. Finally, I would like to thank the Cancer Research Initiatives Foundation, Malaysia, for partially sponsoring my research for the past 3 years.

DECLARATION

Except for help listed in the acknowledgement, the contents of this dissertation are entirely my own work.

This work has not previously been submitted, in part or in full, for a degree or diploma of this or any other university or examining board.

The views expressed in this dissertation are my own and not those of the University of Bristol.

Signed.....

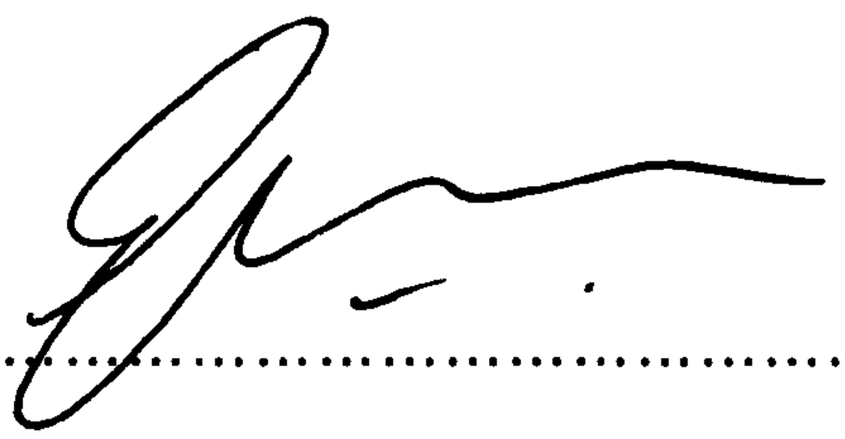

Eswary Thirthagiri

Division of Oral Medicine, Pathology and Microbiology
Department of Oral and Dental Science
Bristol Dental Hospital and School
University of Bristol

December 2004

CONTENTS

Section **Page**

Abstract.....ii

Acknowledgements.....iii

Declaration.....iv

Contents.....v

List of Figures.....xiv

List of Tables.....xvii

List of Abbreviations.....xviii

CHAPTER ONE: INTRODUCTION.....1

1.1 GENERAL INTRODUCTION.....2

1.2 CURRENT THEORIES FOR THE EVOLUTION OF CANCER.....3

1.3 GENOMIC INSTABILITY.....4

1.3.1 Microsatellite instability (MIN).....5

1.3.2 Chromosomal instability (CIN).....6

1.4 HYPOTHETICAL MODEL OF INITIATION AND PROGRESSION OF CIN.....6

1.5 MECHANISMS UNDERLYING CIN.....7

1.5.1 Mitotic and post-mitotic checkpoints.....7

CONTENTS

1.5.1.1 Mitotic checkpoint 8

1.5.1.2 Tetraploidy checkpoint 9

1.5.1.3 Cell cycle checkpoints and cancer 9

1.5.2 Centrosomes 11

1.5.2.1 Centrosome physiology 12

1.5.2.2 Centrosome duplication and regulation 12

1.5.2.3 Mechanisms of centrosome deregulation 13

1.5.2.4 Centrosome abnormalities and cancer 14

1.5.3 Telomeric attrition 16

1.6 *IN VITRO* MODELS OF CIN 17

1.7 ORAL CANCER 18

1.7.1 Pathology 18

1.7.2 Oral premalignant lesions 19

1.7.3 Molecular pathology of oral cancer 20

1.7.4 Markers of malignant development in oral precursor lesions 21

1.7.4.1 Loss of heterozygosity (LOH) 22

1.7.4.2 p53 23

1.7.4.3 Aneuploid status 24

1.8 GENERAL AIMS 25

1.9 HYPOTHESIS 27

1.10 OBJECTIVES 27

CONTENTS

CHAPTER TWO: MATERIALS AND METHODS.....31

2.1 CELL LINES.....32

2.1.1 OSCC-derived cell lines.....32

2.1.2 Normal and immortalised human oral keratinocytes.....33

2.1.3 Control cell lines.....33

2.2 TISSUES.....34

2.3 MATERIALS.....34

2.4 CELL CULTURE TECHNIQUES.....34

2.4.1 3T3 feeder cells.....34

2.4.2 Primary culture of normal oral keratinocytes.....35

2.4.3 Maintenance of cultured cells.....36

2.4.3.1 Normal oral keratinocytes.....36

2.4.3.2 Tumour-derived epithelial cell lines.....37

2.4.3.3 Immortalised normal oral cells.....37

2.4.4 Sub-culture and cell number determination.....37

2.4.5 Storage and retrieval of cell.....38

2.4.6 Microscopy.....39

2.4.7 Mycoplasma testing and treatment.....39

2.4.8 Transfection of cell lines.....40

2.4.9 Cell cloning of transfectants.....41

2.4.10 Irradiation of cell cultures.....41

CONTENTS

2.4.11 MTT assay.....42

2.4.12 Assessment of apoptosis.....42

2.5 FLUORESCENCE ACTIVATED CELL SORTING (FACS).....43

2.6 CELL CYCLE CHECKPOINT ANALYSES.....43

2.6.1 Mitotic checkpoint analysis.....43

2.6.2 Tetraploidy checkpoint analysis.....44

2.7 IMMUNOFLUORESCENCE.....44

2.7.1 Centrosome abnormalities in OSCC-derived cell lines.....44

2.7.2 Centrosome abnormalities in paraffin embedded oral archival material.....45

2.7.3 Microtubule nucleation assay.....46

2.7.4 Mitotic index.....47

2.8 CLONING OF CETN2.....47

2.8.1 Transformation of competent *E.coli* with plasmid DNA.....47

2.8.2 Purification of plasmid DNA.....48

2.8.2.1 Small-scale.....48

2.8.2.2 Large scale.....49

2.8.3 RNA extraction.....51

2.8.4 Reverse transcriptase - Polymerase Chain Reaction (RT-PCR)....51

2.8.5 Expression vector: pEGFP-C1.....53

2.8.6 Restriction digestion and agarose gel electrophoresis.....53

CONTENTS

2.8.7 Purification of DNA from agarose gels.....54

2.8.8 Ligation.....55

2.8.9 Sequencing.....55

2.9 WESTERN BLOTTING.....55

2.9.1 Preparation of protein samples.....55

2.9.2 Polyacrylamide gel electrophoresis.....56

2.10 TREATMENT OF CELLS WITH THE CHEMICAL CARCINOGEN PHIP.....58

2.11 COMPARATIVE GENOMIC HYBRIDISATION (CGH).....59

2.12 DNA PLOIDY ANALYSIS OF ARCHIVAL ORAL TISSUES.....61

CHAPTER THREE: THE ANALYSIS OF THE MITOTIC AND TETRAPLOIDY CHECKPOINTS IN HUMAN OSCC-DERIVED CELL LINES.....65

3.1 INTRODUCTION.....66

3.2 RESULTS.....67

3.2.1 Basal expression of hMLH1 and hMSH2 proteins in human OSCC-derived cell lines.....67

3.2.2 Analysis of the mitotic checkpoint.....68

CONTENTS

3.2.2.1 Cell cycle analysis.....68

3.2.2.2 Mitotic indice.....69

3.2.3 Tetraploidy checkpoint analysis.....70

3.3 SUMMARY.....71

CHAPTER FOUR: THE ANALYSIS OF CENTROSOME ABNORMALITIES IN HUMAN OSCC-DERIVED CELL LINES.....82

4.1 INTRODUCTION.....83

4.2 RESULTS.....84

4.2.1 Centrosome identification and evaluation criteria.....84

4.2.2 Analysis of centrosome abnormalities in human OSCC-derived cell lines.....85

4.2.3 Analysis of centrosome function in human OSCC-derived cell lines.....86

4.2.4 Analysis of centrosome stability in the H413 OSCC-derived cell line exhibiting high centrosome abnormalities.....87

4.3 SUMMARY.....88

CONTENTS

CHAPTER FIVE: CENTROSOME ABNORMALITIES AND DNA PLOIDY IN ORAL PREMALIGNANT LESIONS AND CARCINOMAS.....96

5.1 INTRODUCTION.....97

5.2 RESULTS.....98

5.2.1 Centrosome identification and evaluation criteria in paraffin embedded archival oral tissue.....98

5.2.2 Centrosome defects in oral dysplasias and carcinomas.....99

5.2.3 Ploidy status of oral premalignant lesions.....100

5.3 SUMMARY.....102

CHAPTER SIX: THE DEVELOPMENT OF PHIP RESISTANCE IN IMMORTALISED HUMAN NORMAL ORAL KERATINOCYTES RESULTS IN STABLE CHROMOSOME NUMBER ALTERATIONS BUT DOES NOT AFFECT THE RESPONSE TO IRRADIATION-INDUCED DNA DAMAGE.....108

6.1 INTRODUCTION.....109

6.2 RESULTS.....110

6.2.1 Generating PhIP-resistant clones.....110

6.2.2 Cytogenetic analysis of PhIP-resistant clones.....110

6.2.3 Response to DNA damage in PhIP-resistant clones.....111

CONTENTS

6.2.3.1 Cell viability.....112

6.2.3.2 Apoptosis.....112

6.2.3.3 p53 pathway.....113

6.2.3.4 Cell cycle.....113

6.3 SUMMARY.....114

CHAPTER SEVEN: DISCUSSION.....123

7.1 INTRODUCTION.....124

7.2 ANALYSIS OF THE CHROMOSOMAL SEGREGATION MACHINERY IN HUMAN OSCC-DERIVED CELL LINES.....125

7.2.1 Genetic instability in human OSCC-derived cell lines.....125

7.2.2 Analysis of the mitotic and tetraploidy checkpoints in human OSCC-derived cell lines.....126

7.2.2.1 Mitotic checkpoint.....126

7.2.2.2 Tetraploidy checkpoint.....128

7.2.3 Analysis of centrosome abnormalities in human OSCC-derived cell lines.....130

7.3 ANALYSIS OF CENTROSOME ABNORMALITIES AND DNA PLOIDY IN ORAL DYSPLASIAS AND SCCs.....135

7.4 THE DEVELOPMENT OF AN *IN VITRO* MODEL OF CIN IN IMMORTALISED HUMAN NORMAL ORAL KERATINOCYTES.....139

CONTENTS

7.5 CONCLUDING REMARKS.....143

7.6 FUTURE WORK.....145

REFERENCE.....147

APPENDICES.....164

APPENDIX I: INDEX OF MAIN SUPPLIER.....165

APPENDIX II: CETN2 SEQUENCE.....169

APPENDIX III: PUBLICATIONS ARISING DURING CANDIDATURE.....170

LIST OF FIGURES

Figure 1.1 A two-stage model for how carcinogens may cause cancer via aneuploidy.....28

Figure 1.2 The centrosome duplication cycle in animal cells.....29

Figure 1.3 Defects in cell division as a major route to numerical centrosome aberrations and aneuploidy.....30

Figure 2.1 Mammalian expression vector pEGFP-C1.....64

Figure 3.1 Western blot analysis of the expression of hMLH1 and hMSH2 proteins.....73

Figure 3.2 Cell cycle analysis of HCT116 cells indicating an intact mitotic checkpoint.....74

Figure 3.3 Cell cycle analysis of the H-series of OSCC-derived cell lines exhibiting G0/G1 and G2/M arrest following 18 hours incubation in 0.2 μg/ml nocodazole.....75

Figure 3.4 Cell cycle analysis of the H-series of OSCC-derived cell lines exhibiting G2/M arrest and DNA reduplication following 36 hours incubation in 0.2 μg/ml nocodazole.....76

Figure 3.5 Cell cycle analysis of H376 cells exhibiting DNA reduplication following 36 hours incubation in 0.2 μg/ml nocodazole.....77

Figure 3.6 Immunofluorescence image of anti-phospho histone H3 stained HCT116 cells.....78

Figure 3.7 Mitotic index of the H-series of OSCC-derived cell lines during incubation in 0.2 μg/ml nocodazole.....79

LIST OF FIGURES

Figure 3.8 Cell cycle analysis of H400 cells following pre-synchronization with nocodazole and DCB treatment.....80

Figure 3.9 Cell cycle analysis of H357 and H376 cells after 18 hours following release from DCB.....81

Figure 4.1 Immunofluorescence detection of centrosomes in normal human oral keratinocytes.....90

Figure 4.2 Types of centrosome abnormalities observed in the aneuploid H103 cell line.....91

Figure 4.3 Time course of microtubule nucleation in HCT116 cells showing centrosomes nucleating microtubules after 2 minutes release from nocodazole induced microtubule depolymerization.....93

Figure 4.4 Time course of microtubule nucleation in H157 cells showing centrosomes lacking microtubule nucleation and a H413 cell showing excessive microtubule nucleation after 2 minutes release from nocodazole-induced microtubule depolymerization.....94

Figure 4.5 Immunofluorescence co-localization of CETN2-EGFP signals with antibody against γ-tubulin of the centrosome to authenticate CETN2 targeting to the centrosome in a clonal population of transfected H413 cells.....95

Figure 5.1 Centrosomes in paraffin embedded normal oral tissue.....103

Figure 5.2 Mitotic figures observed in oral carcinomas.....104

Figure 5.3 Centrosomal abnormalities observed in oral carcinomas.....105

Figure 5.4 Centrosome abnormalities correlate with a loss of differentiation in oral SCCs.....106

LIST OF FIGURES

Figure 6.1 Resistance to PhIP.....115

Figure 6.2 MTT assay for analysis of cell viability following irradiation.....117

Figure 6.3 FACS analysis of apoptotic cells following irradiation of OKF6/TERT-1 parental cells.....118

Figure 6.4 FACS analysis of apoptotic cells following irradiation of a PhIP resistant clone 18.....119

Figure 6.5 Western blot analysis of p53, p21 and MDM2 induction, in PhIP resistant clone 18 following 5Gy irradiation.....120

Figure 6.6 FACS analysis of cell cycle arrest in parental OKF6/TERT-1 cells.....121

Figure 6.7 FACS analysis of cell cycle arrest in PhIP resistant clone 18.....122

LIST OF TABLES

Table 2.1 Clinical features of human oral squamous cell carcinomas from which the cell lines were derived.....62

Table 2.2 Characteristics of the human oral squamous cell carcinoma cell lines.....63

Table 4.1 Degree of hyperamplification and microtubule nucleation function of the centrosomes in human OSCC-derived and control cell lines.....92

Table 5.1 Ploidy status of moderate and severe oral dysplasias.....107

Table 6.1 Chromosomal alterations in PhIP resistant clones.....116

LIST OF ABBREVIATIONS

BSA	Bovine serum albumin
cDNA	Complementary DNA
CETN-2	Centrin-2
CGH	Comparative genomic hybridisation
CIN	Chromosomal instability
Cy3	Fluorescent cyanine dye
DAPI	4,6-diamino-2-phenylindole
DCB	Dihydrocytochalasin B
ddH_2O	Double distilled water
DMEM	Dulbecco's modified Eagle's medium
DMSO	Dimethylsulphoxide
DNA	Deoxyribonucleic acid
E. coli	Escherichia coli
EGF	Epidermal growth factor
EGFP	Enhanced green fluorescence protein
FACS	Fluorescence activated cell sorting
FBS	Foetal bovine serum
FISH	Fluorescence in situ hybridisation
FITC	Fluoresceine isothiocyanate
G418	Geneticin sulphate
HTERT	Human telomerase reverse transcriptase
HNPCC	Hereditary non-poliposis colorectal cancer
KSFM	Keratinocyte serum free medium
LOH	Loss of heterozygosity
MIN	Microsatellite instability

LIST OF ABBREVIATIONS

MMR	Mismatch repair
mRNA	Messenger ribonucleic acid
MTT	3-[4,5-Dimethylthiazol-2yl]-2,5-diphenyltetrazolium bromide
PhIP	2-amino-1-methyl-6-phenylimidazo[4,5-b]pyridine
PI	Propidium iodide
RNAse	Ribonuclease
RT-PCR	Reverse transcriptase-Polymerase chain reaction
OSCC	Oral squamous cell carcinoma

CHAPTER ONE

INTRODUCTION

1.1 GENERAL INTRODUCTION

There is increasing evidence that the majority of cancers are genetically unstable and exhibit an abnormal chromosome content, a phenomenon referred to as aneuploidy (Rajagopalan *et al.*, 2004). Based on the numerous studies, which have demonstrated large-scale genomic alterations in solid tumours, a theory known as the aneuploidy hypothesis is being recognised as a plausible explanation for the complex karyotypes observed in cancer. The underlying mechanism(s) responsible for this phenomenon, however, remains to be determined. It has been postulated that defects in the machineries monitoring chromosome segregation and structure could lead to aneuploidy and recent studies indicate that abnormalities of the mitotic and tetraploidy checkpoints and centrosomes may be the underlying cause of genomic instability in a variety of cancers.

Recently, the aneuploid status of premalignant lesions of the oral cavity has been shown to predict malignant progression and patient survival (Sudbo *et al.*, 2001a; 2001b; 2004), indicating that aneuploidy could be used as a diagnostic and prognostic marker. Even though a correlation between aneuploidy and malignant progression has been established in oral cancer, very little is known of the underlying mechanisms responsible for this genetic instability and this forms the basis of the present study.

1.2 CURRENT THEORIES FOR THE EVOLUTION OF CANCER

A common characteristic of solid tumours is a complex karyotype. A genomic destabilisation-initiated carcinogenesis model has been postulated to explain the complex and highly varied karyotypes and phenotypes of these tumours. Two main theories, namely the gene mutation (Zimonjic *et al.*, 2001) and aneuploidy (Li *et al.*, 2000) hypothesis, have been proposed to explain the genomic destabilisation observed in cancers.

The proponents of the mutation hypothesis suggest that the accumulation of somatic mutations is responsible for carcinogenesis. The hypothesis predicts that carcinogens function as mutagens, creating cancer specific mutations with oncogenic properties. The hypothesis is questioned, however, due to the emergence of nongenotoxic carcinogens, the absence of cancer-specific gene mutations and the long latency period between carcinogen treatment and emergence of cancer (Duesberg and Rasnick, 2000). Because the normal rate of mutation could not account for the multiple mutations observed in cancer, Loeb and co-workers (Loeb, 2001; Loeb *et al.*, 2003) put forward the mutator phenotype theory in support of the mutation theory. They proposed that mutations in genes responsible for the maintenance of genomic stability results in an increased mutation rate and this, in turn, drives tumour progression. Other mathematical models of tumorigenesis have favoured the selection of advantageous mutations over increased mutation rates (Tomlinson *et al.*, 1996), suggesting that most tumours start with a normal intrinsic mutation rate but the subsequent clonal expansion of advantageous mutations drives tumorigenesis.

Recently, the aneuploidy hypothesis was revived as an alternative explanation for the complex karyotypes observed in most solid tumours (Li *et al.*, 2000). In this theory, genomic destabilisation occurs as a result of alterations in the proteins that segregate, synthesize and repair chromosomes, resulting in an altered chromosome number or structure and an increased spontaneous rate of gene mutations following every cell division, producing new genomically unstable preneoplastic and neoplastic progeny cells that do not resemble their precursor cells. These progeny cells are constantly evolving due to their unstable genome to create progenies with new karyotypes (Duesberg and Rasnick, 2000; Duesberg and Li, 2003; Duesberg *et al.*, 2004). Consistently, both karyotypic (Duesberg *et al.*, 1998) and chromosome structure (Fabarious *et al.*, 2003) instability has been shown to be proportional to the degree of aneuploidy; the more aneuploid the cell, the more unstable the genotype.

In view of the ongoing debate, the field of genomic instability is highly controversial. In spite of reports of independent mechanisms leading to genetic instability, it is possible that the mutation and aneuploidy hypotheses are not mutually exclusive and could potentially synergise to promote the destabilization of the genome.

1.3 GENOMIC INSTABILITY

To date, genomic instability has been shown to exist at two distinct levels. In a small subset of tumours, the instability is observed at the nucleotide level and results in base substitution, deletion or insertion of a few nucleotides, whilst in most other cancers, the instability is observed at the chromosomal level, resulting in loss of heterozygosity (LOH), structural abnormalities and losses

and gains of whole chromosomes (Lengaur *et al.*, 1998). Studies on colorectal tumours have confirmed that genetic instability occurs in two mutually exclusive forms namely, microsatellite instability (MIN) or chromosomal instability (CIN; Lengaur *et al.*, 1997).

1.3.1 Microsatellite instability (MIN)

The MIN phenotype was described in cancer following the discovery of a subset of hereditary non-polyposis colorectal cancers (HNPCC) exhibiting germline mutations of mismatch repair (MMR) genes, namely *hMSH2*, *hMSH6*, *hMLH1*, *hPMS1* and *hPMS2* (Buermeyer *et al.*, 1999).

The MMR pathway functions to remove nucleotides mispaired by DNA polymerases and insertion/deletion loops (1-10bp) that results from slippage during replication of repetitive sequences or recombination (Hoeijmakers, 2001). Inactivating alterations of the MMR genes leads to an inability to recognize and repair errors that occur during DNA replication. Mutations in the *hMLH1* and *hMSH2* genes account for the majority of mismatch repair defects (Buermeyer *et al.*, 1999; Jiricny and Lahti, 2000). Simple repeat sequences or microsatellites at both the non-coding and coding regions of genes are specific targets for mutations in MIN cells (Yamasaki and Mironov, 2000) giving rise to mutations at the nucleotide level (Jiricny, 1998) resulting in an elevated nucleotide mutation rate. The majority of MIN cancers are diploid or near diploid and exhibit normal rates of gross chromosomal change.

1.3.2 Chromosomal instability (CIN)

CIN is defined as an accelerated rate of gains or losses of whole or large portions of chromosomes (Rajagopalan *et al.*, 2004). CIN manifests itself at the chromosomal level and is characterized at the cytogenetic level by marked aneuploidy, caused by DNA amplifications, chromosomal loss or gain, and allelic losses of chromosome arms (Lengauer *et al.*, 1998). However, the existence of aneuploidy in the static state of the cell, does not indicate the presence of CIN, as CIN is a measure of flux in the karyotype leading to a nondiploid genome (Lengaur *et al.*, 1997). CIN tumours are usually MMR proficient.

The presence of aneuploidy early in human neoplasia suggests that CIN could be the cause and not the consequence of the carcinogenic process (Shih *et al.*, 2001). Further, support from mathematical models of cancer initiation indicates that the first event in many sporadic cancers is a heritable alteration that affects genetic instability (Nowak *et al.*, 2002), suggesting that CIN is an early event and the driving force of cancer progression (Komarova *et al.*, 2003).

1.4 HYPOTHETICAL MODEL OF INITIATION AND PROGRESSION OF CIN

A two-stage mechanism has been proposed to explain the complex karyotype of the aneuploid cell (Figure 1.1; Duesberg and Rasnick, 2000; Li *et al.*, 2000).

In stage one, a carcinogen functions to induce aneuploidy and initiates carcinogenesis by generating a preneoplastic aneuploid cell. The compound achieves this by altering, either physically or chemically, the chromosomes or

the mitotic apparatus. These preneoplastic karyotypes would include aneuploid cells that are immortal but not necessarily tumorigenic. This is followed by stage two where the aneuploidy itself destabilizes the karyoptype and so catalyses karyotypic variation and evolution. The source of the karyotypic instability is the imbalance that aneuploidy imparts on the mitotic apparatus resulting in missegregation of chromosomes. Thus, the initiated cell evolves autocatalytically, generating new lethal, preneoplastic and neoplastic karyotypes; the degree of karyotypic instability would be proportional to the degree of aneuploidy. The heterogenous karyotype and phenotypic variation within a "clonal" cancer, therefore, would be an inevitable consequence of the intrinsic instability of an aneuploid karyotype.

1.5 MECHANISMS UNDERLYING CIN

Two mechanisms frequently reported to lead to numerical chromosomal abnormalities in cancer cells are defects in the mitotic and post-mitotic checkpoints (Hartwell, 1992; Andreassen *et al.*, 2001a) and abnormalities of the centrosomes (Ghadimi *et al.*, 2000). In addition, telomeric attrition, the progressive shortening of telomeres with each cell division, has been suggested to result in some of the structural aberrations of the chromosomes observed in malignant tumours (Gisselsson *et al.*, 2001a).

1.5.1 Mitotic and post-mitotic checkpoints

Gross aneuploidy mediated by defects in cell cycle checkpoints have been suggested to arise through a two-step process. The first step involves an aberrant mitotic exit of cells into G1 with a tetraploid DNA content and, the second is an absence of a G1 surveillance mechanism that would prevent cell

cycle progression of these cells (Margolis *et al.*, 2003). The first could arise from failure of any of the pre-mitotic or mitotic checkpoints and the second, from the suppression of the tetraploidy checkpoint.

1.5.1.1 Mitotic checkpoint

The mitotic checkpoint, also referred to as the spindle checkpoint, monitors the integrity of the random process of kinetochore capture of metaphase chromosomes by spindle microtubules during mitosis, ensuring even segregation of genetic materials to daughter cells.

The molecular components of the mitotic checkpoint are encoded by seven evolutionarily conserved genes (*BUB1-3*, *MAD1-3* and *MPS1*), first identified in budding yeast (Hyot *et al.*, 1991; Li and Murray, 1991; Robert *et al.*, 1994; Hardwich and Murray, 1995; Weiss and Winey, 1996). Homologues of some of these genes have been demonstrated to be essential for establishing the checkpoint response in eukaryotes (Li and Benezra, 1996; Taylor and McKeon, 1997; Abrieu *et al.*, 2001). Preferential binding to unattached kinetochores suggests that these proteins participate in monitoring kinetochore-microtubule interactions (Chen *et al.*, 1996; Chan *et al.*, 1999; Skoufias *et al.*, 2001). Unoccupied kinetochores and lack of tension on mono-orientated chromosomes have been identified as the source of the mitosis inhibitory signal (Reider *et al.*, 1994;1995).

The downstream target proteins of the checkpoint are the anaphase promoting complex/cyclosome (APC/C), a multisubunit E3 ubiquitin ligase that regulates the degradation of specific proteins in order to drive mitosis and Cdc20, a

protein that recruits substrates to APC (Peters, 2002; Yu, 2002). In the event of inappropriate chromosome capture, Cdc20 is inhibited by the mitotic checkpoint complex composed of Mad2, BubR1, Bub3 and Cdc20, preventing ubiquitination of securin by APC. This blocks the enzyme separase from causing proteolysis of cohesin, a multiprotein complex that holds the sister-chromatids together and, therefore, the metaphase to anaphase transition is inhibited (Bharadwaj and Yu, 2004).

1.5.1.2 Tetraploidy checkpoint

The tetraploidy checkpoint is a p53-dependent post-mitotic checkpoint (Lanni and Jacks, 1998) that functions to elicit a G1 arrest in cells that exit mitosis with a tetraploid DNA content (Andreassen *et al.*, 2001a). Tetraploidy could result from insults to the DNA or cellular architecture (Andreassen *et al.*, 1996) but the checkpoint operates regardless of the mechanism by which the cell becomes tetraploid (Andreassen *et al.*, 2001a). Although uncertain, inheritance of double the centrosome number following aberrant mitotic exit or ploidy-specific regulations of gene expression have been suggested to function as the arrest signal (Andreassen *et al.*, 2001a; 2003). In addition to p53, the checkpoint needs intact pRB to function (Borel *et al.*, 2002). p21, a transcriptional target of p53, is the main mediator of G1 arrest in tetraploid cells (Andreassen *et al.*, 2001b) and acts through the inhibition of cyclin E/Cdk2 activity and binding to proliferating-cell nuclear antigen (Stewart *et al.*, 1999).

1.5.1.3 Cell cycle checkpoints and cancer

The mitotic checkpoint has been reported to be defective in a number of human tumours, including hepatocellular, (Saeki *et al.*, 2002), thyroid (Ouyang *et al.*,

2002) and ovarian cancers (Wang *et al.*, 2002). There is some controversy, however, regarding the frequency with which mitotic checkpoint defects occur in cancer because studies using the same colorectal cell lines have produced conflicting results (Cahill *et al.*, 1998; Tighe *et al.*, 2001). Similarly, Yoon *et al.* (2002) reported mitotic spindle checkpoint defects in breast cancer cell lines, data that were contradicted by Blajeski *et al.* (2002) who demonstrated that the same cell lines were able to arrest at lower concentrations of nocodazole. Such discrepancies could be due to differences in experimental design, data interpretation and the characteristics of the drug used.

The infrequent occurrence of mutations in checkpoint genes has further questioned the role of mitotic checkpoint defects in cancer. Somatic mutations in either *BUB1* or *BUBR1* were found in only a small fraction of colorectal cancers (Cahill *et al.*, 1998). Mutational analysis of the *BUB* and *MAD* gene family in lung cancer cell lines (Yamaguchi *et al.*, 1999; Sato *et al.*, 2000; Haruki *et al.*, 2001), breast carcinomas and cell lines (Percy *et al.*, 2000; Langerod *et al.*, 2003), glioblastomas (Reis *et al.*, 2001), colon cancer cell lines (Cahill *et al.*, 1999) and bladder cancer (Hernando *et al.*, 2001) also suggests that these genes are rarely a target for genetic alteration. A more recent study, however, has indicated that nonmutational silencing, such as epigenetic modification of mitotic checkpoint genes, may be more important than mutational inactivation (Shichiri *et al.*, 2002). An intrinsic elevated rate of chromosome misegregation in $BUB3^{+/-}$ mice (Babu *et al.*, 2003) and $MAD2^{+/-}$ human cancer cells (Michel *et al.*, 2001) suggests that haplo-insufficiency of mitotic checkpoint genes could lead to subtle rates of CIN compatible with cell viability. This is consistent with the heterozygous alteration (Tsukasaki *et al.*, 2001; Hempen *et al.*, 2003) and

reduced activity (Ouyang *et al.*, 2002) of mitotic checkpoint genes observed in some cancers. Further, sequestration and mislocalization of checkpoint proteins by viral oncoproteins is another mechanism of checkpoint inactivation (Kasai *et al.*, 2002).

By contrast to the study of the mitotic checkpoint, our understanding of the tetraploidy checkpoint is in its infancy. Tetraploid intermediates appear to be an important mechanism of aneuploidization in carcinogenesis (Shackney *et al.*, 1989) and could act as a direct precursor of aneuploid cells due to their inherent instability (Andreassen *et al.*, 1996). Further, the inheritance of increased numbers of centrosomes could lead to multipolar mitosis, perpetuating the instability caused by the failure of the tetraploid checkpoint (Borel *et al.*, 2002). However, a recent study by Uetake and Sluder (2004) has questioned the existence of the tetraploidy checkpoint in mammalian cells and suggests that the G1 arrest in the tetraploid cells following mitotic exit, described by Andreassen *et al.* (2001a), could be attributed to the subtle disorganization of the actin cytoskeleton by the high concentration of dihydrocytochalasin B (DCB), a cytokinesis inhibitor, which persisted following drug removal.

1.5.2 Centrosomes

The centrosome is the major microtubule-organizing centre (MTOC) of animal cells and is crucial for chromosome segregation (Brinkley, 2001) and cytokinesis (Piel *et al.*, 2001). Through its control of number, polarity and distribution of microtubules, the centrosome coordinates all microtubule-related functions such as cell shape, polarity, adhesion, motility, intracellular transport and organelle positioning (Fry *et al.*, 2000). The centrosome is needed for

progression into S-phase (Hinchcliffe *et al.*, 2001) and has been suggested to function as a scaffold for key cell cycle regulators (Fry *et al.*, 2000). Although mitotic spindles can form in the absence of centrosomes, the MTOC exerts a dominant effect on microtubule organization (Khodjakov *et al.*, 2000).

1.5.2.1 Centrosome physiology

Mammalian centrosomes are small non-membranous organelles, often associated with the nuclear membrane. They consist of a pair of perpendicularly positioned barrel shaped centrioles, surrounded by a mass of amorphous, electron dense matrix, termed the pericentriolar material (PCM), which contains the γ-tubulin ring complexes that nucleate microtubules during interphase and mitosis. Each centriole is cylindrical in shape and is built of nine sets of triplet microtubules (Fukasawa, 2002).

1.5.2.2 Centrosome duplication and regulation

Centrosome duplication is a semi-conservative process, whereby the mother centriole acts as a template for daughter centriole formation, and is unique in its ability to duplicate itself once every cell cycle (Fry *et al.*, 2000). The centrosome duplication cycle in the vertebrate cells consists of several distinct steps (Figure 1.2). Centriole splitting is followed by the formation of a small structure termed the procentriole or daughter centriole at the proximal end, perpendicularly oriented to each parental centriole by early S phase; the parental centriole has been suggested to act as a template for procentriole formation. Elongation of procentrioles occurs throughout S phase and early G2 and centriole maturation is completed by the G2 to M phase transition. Finally, the disjunction of the two sister centrosomes occurs, each containing a pair of mother-daughter

centrioles, signalling the completion of duplication. The physical separation of the sister centrosomes to opposite poles of the cell, mediated by microtubule-based motor proteins, occurs during the mitotic phase (Balczon, 2000; Stearns *et al.*, 2001).

Centrosome duplication is strictly coordinated with DNA replication, mitosis and cell division (Sluder and Hinchcliffe, 2000). Coordination of DNA replication and centrosome duplication is dependent upon the phosphorylation status of the retinoblastoma protein (Rb), which governs the availability of the E2F transcription factor to promote S phase progression, (Meraldi *et al.*, 1999). In mammals, the centrosome duplication event is also dependent upon Cyclin dependent kinase-2 (Cdk) activation (Lacey *et al.*, 1999), with cyclin E as the activating subunit in embryonic cells (Hinchcliffe *et al.*, 1999) and cyclin A in somatic cells (Lacey *et al.*, 1999).

1.5.2.3 Mechanisms of centrosome deregulation

Centrosome deregulation has been suggested to lead to CIN through its ability to mediate abnormal mitosis. There are a number of hypothetical mechanisms through which abnormalities in centrosomes could be generated. Excess centrosomes can be generated through deregulation of centrosome duplication, which could occur either through inappropriate initiation of duplication at late G1 to early S phase or by uncoupling centrosome duplication from DNA replication (Lacey *et al.*, 1999) and by a failure to suppress re-duplication of centrosomes through uncontrolled separation of centriole pairs prior to duplication (Sluder and Hinchcliffe, 2000). Failure of cytokinesis could also result in cells inheriting excess centrosomes (Meraldi *et al.*, 2002) and failure to duplicate or separate

centrosomes in mitosis can result in insufficient centrosomes, resulting in formation of monopolar spindles and segregation of all the chromosomes into a single progeny. Finally, overexpression of PCM components could lead to formation of acentriolar centrosomes capable of ectopic microtubule assembly.

Recent studies strongly suggest that a mechanism centred on mitotic failure leading to tetraploidization and the consequential inheritance of extra centrosomes, could play an important role in mediating CIN (Figure 1.3; Meraldi *et al.*, 2002; Borel *et al.*, 2002). Consistent with this hypothesis, excess centrioles that predispose cells to multipolar mitoses and sequential appearance of tetraploid and aneuploid cell populations have been observed in a mouse model of pancreatic cancer (Levine *et al.*, 1991). This mechanism also provides an explanation as to why alterations of multiple genes acting in pathways unrelated to centrosome duplication can lead to centrosome amplification; co-existence of polyploid cells and centrosome abnormalities, for example, have been observed in association with loss of p53 function (Borel *et al.*, 2002), mutations in BRCA1 (Xu *et al.*, 1999), BRCA2 (Tutt *et al.*, 1999), Skp2 (Nakayama *et al.*, 2000) and overexpression of aurora2 (Meraldi *et al.*, 2002).

1.5.2.4 Centrosome abnormalities and cancer

Centrosome abnormalities are frequently detected in human cancers and tumour derived cell lines (Pihan *et al.*, 1998; Ghadimi *et al.*, 2000). The abnormalities reported include supernumerary centrosomes, centrosomes of different sizes (Sato *et al.*, 2001), physiological abnormalities including disrupted centriole barrel structure, unincorporated microtubule complexes,

centrioles of unusual length, and mispositioned centrosomes (Lingle *et al.*, 1999), increased microtubule nucleating capacity and hyperphosphorylation of centrosome-associated proteins (Lingle *et al.*, 1998). Amongst these, abnormalities in centrosome number and size are the most common. Deregulation of many cellular proteins have been linked to the centrosomal abnormalities observed in cancer, such as loss of p53 activity through mutation or deletion (Ouyang *et al.*, 2001), sequestration (Carrol *et al.*, 1999) and through inactivation of downstream targets, p21/Waf1 (Mantel *et al.*, 1999) and GAAD45 (Hollander and Fornace, 2002), synergistic overexpression of cyclin E and loss of p53 (Kawamura *et al.*, 2004), overexpression of aurora2/STK15/BTAK (Zhou *et al.*, 1998) and mutations in BACR1 (Xu *et al.*, 1999), BACR2 (Tutt *et al.*, 1999) and Skp2 (Nakayama *et al.*, 2000).

The presence of centrosomal abnormalities in precancerous lesions (Pihan *et al.*, 2003), the high frequency of abnormal mitosis in xenograft models of cancer (Shono *et al.*, 2001) and the dynamic karyotypic changes observed in human tumours (Lingle *et al.*, 2002) collectively suggests that abnormal centrosomes could potentially drive CIN and, in turn, carcinogenesis through chromosome misegregation. Consistent with this hypothesis, the coexistence of centrosome defects with aneuploidy has been reported in many tumour types including pancreatic (Sato *et al.*, 2001), bladder (Jiang *et al.*, 2003), prostate (Pihan *et al.*, 2001) and breast cancers (Lingle *et al.*, 2002).

Further, since deregulation of various genes and pathways have been shown to lead to centrosome abnormalities and polyploidy, the centrosome could function as a surrogate marker for genomic instability in cancer. The association of

centrosome amplification with advanced stage malignancies, recurrent tumours, and in cell lines that show more aggressive malignant phenotypes in animal models suggest that centrosome defects may be helpful in predicting patient prognosis (D'Assoro *et al.*, 2002).

1.5.3 Telomeric attrition

Telomeres are specialized DNA-protein structures located at the end of linear chromosomes. In mammalian cells, the telomeric sequence is a repetition of a hexanucleotide motif, TTAGGG, synthesized by the enzyme, telomerase. Telomerase consists of a catalytic reverse transcriptase (TERT) that synthesizes telomeres using an RNA template encoded by the telomerase RNA component (TERC) gene. Telomeric attrition is defined as the shortening of telomeres with each cell division and it occurs due to the inability of DNA polymerases to complete the synthesis of chromosome ends, which in normal cells ultimately leads to senescence and cell death (Campisi *et al.*, 2001). However, in cells with inactivated growth inhibitory pathways, continued proliferation causes further telomere erosion and surviving cells emerge by activating telomere maintenance mechanisms; the most common being the reactivation of telomerase (Artandi and DePinho, 2000; Maser and DePinho, 2002).

Telomere length abnormalities detected in precursor lesions of a variety of cancers suggests that telomere dysfunction is an early event in carcinogenesis (Meeker *et al.*, 2004). Loss of telomere capping proteins forces the telomere to become a substrate for end-to-end chromosome fusion and exonucleolytic degradation leading to formation of dicentric chromosomes and breakage-

fusion-bridge cycles (de Lange, 2002). Furthermore, the high level of anaphase bridges (Rudolph *et al.*, 2001), nuclear blebs, chromatin strings and micronuclei (Gisselsson *et al.*, 2001b), dicentric chromosomes (Gisselsson *et al.*, 2001a; 2002) and chromosomal amplification and deletions (O'Hagan *et al.*, 2002) observed in tumours and cell lines with dysfunctional telomeres suggests that telomere dysfunction may play a part in CIN.

1.6 *IN VITRO* MODELS OF CIN

Although CIN is prevalent in cancers, the lack of an *in vitro* model to study CIN and its contribution to cancer hinders our understanding of the underlying mechanisms involved. Since CIN has been postulated to be induced by chemical carcinogens, many studies have used chemicals such as nitrosomethylurea (Fabarius *et al.*, 2002), aromatic polycyclic hydrocarbons (Li *et al.*, 1997) and bulky adduct forming agents (Bardelli *et al.*, 2001) to induce aneuploidy and neoplastic transformation *in vitro*. However, these studies were invariably carried out using rodent and/or carcinoma cell lines that are naturally more unstable and prone to transformation. Recently, Bardelli *et al.* (2001) induced CIN in a colorectal cancer cell line using the bulky adduct forming agent, 2-amino-1-methyl-6-phenylimidazo[4,5-b]pyridine (PhIP). The presence of CIN was detected after 25-50 populations doubling by FISH analysis, using a combination of centromeric and telomeric probes to chromosome 12. However, the CIN status was estimated at a static time point, which may not reflect the presence of the dynamic karyotypic changes associated with CIN and again the experiment was carried out using carcinoma cells. The use of normal cells in similar experiments might more accurately represent the induction of CIN in normal or preneoplastic cells.

1.7 ORAL CANCER

1.7.1 Pathology

The term oral cancer, according to the International Classification of Disease (ICD), version 9, encompasses lip, tongue, mouth, oropharynx, hypopharynx and ill-defined sites within lip, oral cavity and pharynx but excludes nasopharynx and salivary glands (Cancer Research Campaign, 2000). The majority of oral malignancies (>90%) are squamous cell carcinomas of the lining mucosa.

Oral cancer is an important disease of the developing world with the highest rates being reported in South Asia (Parkin *et al.*, 1999). For example, in India, oral cancer is the most common cancer and may cause up to 50% of all new cases of cancer. By contrast, in Europe and the United States, oral cancer is less prevalent and accounts for only 1%-9% of all new cases of cancer (Cancer Research Campaign, 2000). Significantly, the disease is associated with high rates of morbidity and mortality; typically only 50% of those diagnosed with oral cancer will be alive after a period of five years. The mortality rates associated with oral cancer have not improved in the last 20 years (Lippman and Hong, 2001).

Oral cancer is associated with multiple risk factors, the two most important being tobacco usage and alcohol consumption, which are thought to be responsible for 75%-95% of all oral cancer cases. Worldwide, the most common form of tobacco use is smoking, however, tobacco chewed in the form of betel-quid is an important aetiological factor in South East Asia. Alcohol is often regarded as a co-carcinogen and is known to act synergistically with concurrent tobacco use. Other risk factors include dietary deficiencies, viral infections of

the oral cavity (Cancer Research Campaign, 2000) and the differing capacity of individuals to metabolise the carcinogens found in tobacco and alcohol (Harty *et al.*, 1997; Schwartz *et al.*, 2001; Buch *et al.*, 2002).

1.7.2 Oral premalignant lesions

In oral cancer, the initial presence of a premalignant lesion subsequently developing into cancer is well recognised. The two major types of oral premalignant lesions are erythroplakia and leukoplakia. Erythroplakia is defined as "a fiery red patch that cannot be characterised clinically or pathologically as any other definable disease" and leukoplakia as "a predominantly white lesion of the oral mucosa that cannot be characterised as any other definable lesion" (Crissman and Sakr, 2001). Leukoplakias can be further divided into homogeneous, predominantly white lesions and non-homogeneous or speckled lesions, which contain a mixture of white and red areas (Crissman and Sakr, 2001).

Erythroplakia is a rare lesion and is usually the clinical manifestation of either severe dysplasia or carcinoma. Leukoplakias are more common lesions and have variable rates of malignant transformation; the estimated rate of transformation is approximately 6% over a 10-year period. When histologically dysplastic lesions are considered as a group, the estimated rate of transformation, however, increases to between 16-36% (Warnakulasuriya, 2000). Furthermore, there is evidence that some white patches can develop cancer in the absence of pre-existing epithelial dysplasia and some with dysplasia may even regress (Mao, 1997, Reibel, 2003).

In the West, only a loose association exists between oral premalignant lesions and subsequent carcinoma development. However, in South East Asia, premalignant lesions commonly precede oral carcinomas. Currently, the limited ability to identify lesions that have the greatest malignant potential poses a great challenge in targeting patients for treatment (Reibel, 2003).

1.7.3 Molecular pathology of oral cancer

Frequent genetic alterations of genes in oral cancer suggest that these events are important in the development of oral cancer. Some of the most commonly altered chromosomal regions in oral cancer includes 3p, 9p21-22, 11q13 and 17p13 (Scully *et al.*, 2000; Kim and Califano, 2004)

Loss of heterozygosity (LOH) at chromosome 3p has been identified in approximately 60% of oral carcinomas (Califano *et al.*, 1996). Some of the putative tumour suppressor genes identified at 3q include the fragile histidine triad (*FHIT*) gene and *RASSF1A*. Hypermethylation of these genes have been reported in a variety of cancers but their involvement and their role in oral cancer, however, is unclear (Scully *et al.*, 2000; Kim and Califano, 2004).

Amongst the various putative tumour-suppressors located at 9p21-22, alteration of the CDKN2A locus that encodes for $p16^{INK4A}$ and $p14^{ARF}$ has assumed considerable importance. Genetic alteration of $p16^{INK4A}$ is the most common abnormality in oral cancer (Kim and Califano, 2004) and approximately 90% of OSCCs exhibit lack of $p16^{INK4A}$ expression (Wu *et al.*, 1999). $p16^{INK4A}$ is a Cdk inhibitor, which functions in the retinoblastoma (Rb)/E2F pathway. Inactivation of $p16^{INK4A}$ results in deregulation of the Rb pathway and inappropriate cell

cycling. Alteration of *p14^{ARF}* has also been reported to occur concomitant with *p16^{INK4A}* inactivation in oral cancer (Shintani *et al.*, 2001). p14^{ARF} functions to modulate MDM2-mediated degradation of p53 (Nevins, 2001), loss of which might result in deregulated cell cycle arrest and apoptosis.

Amongst the many genes harboured within the 11q13 region, *Cyclin D1* is frequently altered in oral cancer. *Cyclin D1* amplification and protein overexpression has been shown to occur in oral cancer (Rousseau *et al.*, 2001). Cyclin D1 regulates the phosphorylation of Rb through binding with Cdk4 or Cdk 6 of the Rb pathway. Concomitant amplification of *Cyclin D1* with inactivation of p16^{INK4A} has been suggested to confer additional advantage to tumour cells (Okami *et al.*, 1999).

The p53 gene, which is located at 17p13 is one of the most frequently mutated gene in all human malignancies and is mutated in up to 50% of oral cancers (Paterson *et al.*, 1996). p53 is a critical modulator of the cellular response to various stresses. Loss of p53 is thought to occur late in oral cancer (Murti *et al.*, 1998) and is associated with transformation to the invasive phenotype (Shanavaz *et al.*, 2000). Mutations within the DNA binding surface region of p53 have been reported to be associated with aggressive tendency within tumours and worsened clinical outcome (Yamazaki *et al.*, 2003).

1.7.4 Markers of malignant development in oral precursor lesions

The estimation of the malignant potential of oral precursor lesions is currently based on histologic assessment of the presence and degree of epithelial dysplasia, which is graded as mild, moderate or severe. This technique is,

however, highly subjective and frequently lacks agreement between observers (Sudbo *et al.*, 2001c). Consequently, reliable biomarkers of malignant transformation are actively being sought. For example, loss of heterozygosity (LOH) at selected chromosome regions, defects in p53 and aneuploid status have been evaluated for their ability to predict malignant change in oral premalignant lesions.

1.7.4.1 Loss of heterozygosity (LOH)

LOH resulting from loss of genomic material from one of a pair of chromosomes, assessed using microsatellite markers to short tandem repeats of DNA sequences, has frequently been used to predict malignant development.

For example, the presence of LOH at 3p14 and/or 9p21 in oral leukoplakias was shown to carry a higher risk of malignant progression (Mao *et al.*, 1996). Later, based on identical allelic loss between premalignant lesions and cancer and additional LOH analysis, a linear progression model was developed for oral cancer, whereby retention of 3p and/or 9p is associated with low risk of progression, LOH at 3p and/or 9p is associated with intermediate risk of progression and LOH at 3p and 9p accompanied by additional LOH at 4q, 8p, 11q, 13q or 17p have a high risk of malignant progression (Califano *et al.*, 1996; Rosin *et al.*, 2000). The overall accumulation of genetic defects rather than the order in which they occur has been suggested to be critical for oral cancer development (Califano *et al.*, 1996; Partridge *et al.*, 1998; Jiang *et al.*, 2001)

The use of LOH to predict malignant progression, however, is limited because only selected microsatellite loci are examined, which might be unsuitable for

analysis of lesions with LOH at different sites. Further, the assessment of multiple markers is both time consuming and expensive. In addition, evidence of the polyclonal nature of cancer, possibly due to the field cancerization effect of the oral mucosa (Jang *et al.*, 2001; Ai *et al.*, 2001; Partridge *et al.*, 1997), suggests that malignant progression might not occur in a linear fashion as previously suggested (Shahnavaz *et al.*, 2001). A long-term study of cancer risk assessment in oral premalignant lesions, however, indicates that LOH at chromosome 3p or 9p is predictive when used in conjunction with other biomarkers such as chromosome polysomy and p53 expression along with histopathological parameters and the prior cancer history of the patient (Lee *et al.*, 2000)

1.7.4.2 p53

p53 protein is activated and stabilized in response to cellular stress and then functions as a transcription factor for genes involved in inducing either cell cycle arrest or cell death (Vogelstein *et al.*, 2001). p53 is usually not detected in normal cells, whilst mutant p53 protein has a prolonged half-life and, therefore, can be detected by immuno-staining techniques.

Recent evidence suggests that suprabasal expression of p53 in dysplastic lesions (Cruz *et al.*, 1998) and non-malignant mucosa at the resection margin of carcinomas (Cruz *et al.*, 2000) could predict carcinoma development and recurrence, respectively. However, other studies have indicated that mutation of p53 is a late event in oral carcinogenesis (Murti *et al.*, 1998; Shanavaz *et al.*, 2000) and, therefore, may be unsuitable as a marker of malignant progression. Furthermore, inconsistencies between mutations in p53 and

immunohistochemical detection of the mutant protein (Shanavaz *et al.*, 2000; Kuo *et al.*, 1999), and involvement of other p53 inactivating mechanisms such as overexpression of MDM2 (Carroll *et al.*, 1999), loss of $p14^{ARF}$ (Bradley *et al.*, 2001) and interaction with viral proteins (Gasco and Crook, 2003), could result in false interpretation of results. p53 status, therefore, is unlikely to be a reliable predictor of malignant transformation (Warnakulasuriya, 2000).

1.7.4.3 Aneuploid status

Genomic instability reflects the propensity and susceptibility of the genome to acquire multiple alterations resulting in an altered DNA content or aneuploidy. Chromosomal abnormalities are frequently encountered in both premalignant and malignant lesions of the oral cavity (Weber *et al.*, 1998) and have been demonstrated in oral carcinoma cell lines (Okafuji *et al.*, 1999, Hermsen *et al.*, 1997). One study has showed that aneuploidy can occur even in morphologically normal oral mucosa suggesting that genomic instability occurs early in oral cancer and precedes morphological changes (Ai *et al.*, 2001). Furthermore, genomic instability could potentially provide the tumour cells with a significant growth advantage through incidental alterations of bystander genes that might not be related to malignant progression (Masayesva *et al.*, 2004).

The hallmark study by Sudbo and colleagues (Sudbo *et al.*, 2001a) showed the importance of genomic instability in the pathogenesis of oral cancer by demonstrating the diagnostic potential of altered DNA content in oral premalignant lesions. This study used the DNA ploidy status of oral dysplasias to predict malignant progression. A total of 150 oral dysplastic leukoplakias, from patients who were followed for a mean of 8.6 years, were investigated with

respect to DNA content. Only 3/105 diploid cases (3%) as opposed to 21/25 aneuploid (84%) progressed to carcinoma during follow-up. The cumulative disease free survival rates of diploid, tetraploid and aneuploid groups were 97%, 40% and 16%, respectively. The reliability of DNA ploidy assessment in predicting malignant progression was further strengthened following the successful prediction of oral erythroplakias in a majority of patients (92%), which is consistent with the high tendency of these lesions to progress. Most significantly, aneuploidy was also shown to reliably predict malignant progression of non-dysplastic lesions (Sudbo *et al.*, 2001b). Subsequently, Sudbo *et al.* (2004) reviewed their original 150 patients over a 3-year period and demonstrated that complete resection of oral leukoplakia does not prevent progression to carcinoma and further, oral carcinoma arising from aneuploid leukoplakia demonstrates aggressive clinical behaviour associated with advanced stage and poor survival in comparison to tetraploid or diploid lesions.

Taken together, these studies suggest that aneuploidy is an excellent marker of malignant progression in oral premalignant disease. Little is known, however, about the mechanisms responsible for aneuploidy in oral cancer. Knowledge of these mechanisms would greatly enhance our understanding of the molecular biology of the disease and might identify specific genetic markers of malignant progression.

1.8 GENERAL AIMS

CIN or aneuploidy, characterised by an altered DNA content and the presence of structural and numerical chromosomal aberrations, has been suggested to drive cancer progression by unbalancing the gene dosage of tumour suppressor

genes and oncogenes. Aneuploidy has been shown to occur early in oral cancer and is a reliable predictor of malignant progression in a variety of oral premalignant lesions. There is a paucity of information, however, regarding the mechanisms underlying CIN in oral cancer.

Previous cytogenetic characterization of a series of human oral squamous cell carcinoma (OSCC)-derived cell lines established in the Experimental Pathology Group at the University of Bristol revealed that the cells exhibited consistent chromosomal rearrangements and altered chromosome numbers, indicating that the cell lines were aneuploid (Patel *et al.*, 1993). These cell lines, therefore, represent valuable tools to investigate the underlying mechanisms of CIN in oral cancer. The MIN status of these cell lines has not been examined and, therefore, the present study first examined the expression of the *hMLH1* and *hMSH2* genes to confirm that that cell lines did not exhibit MIN. Due to the chromosome alterations in the OSCC-derived cell lines, defects in the chromosome segregation machineries such as the mitotic and tetraploidy checkpoints and the centrosomes were investigated.

During the course of this work, it was determined that centrosomal abnormalities occur frequently in OSCC-derived cell lines suggesting that centrosome defects may underlie CIN in oral cancer. The study was extended to analyse the status of the centrosomes in oral tissues with a view to determining whether centrosome abnormalities were associated with a malignant phenotype and progression.

In a parallel investigation, immortalised human normal oral keratinocyte cells were treated with the carcinogen PhIP in an attempt to develop an *in vitro* model of CIN. Having determined that induction of PhIP resistance resulted in consistent chromosomal abnormalities only and not a dynamic CIN, we aimed to determine if the induction of PhIP resistance could have produced cells that were resistant to other forms of DNA damage.

1.9 HYPOTHESIS

This study tested the hypothesis that defects in the chromosome segregation machinery are responsible for the CIN observed in oral cancer and that this process can be recapitulated in human immortalised normal oral keratinocytes *in vitro*.

1.10 OBJECTIVES

1. To analyse the fidelity of the mitotic checkpoint in a series of human oral-SCC cell lines.
2. To analyse centrosome physiology and function in a series of human oral-SCC cell lines.
3. To analyse centrosome abnormalities in archival paraffin-embedded oral dysplasias and SCCs
4. To develop an *in vitro* model of CIN using an immortalised human normal oral keratinocyte treated with the carcinogen PhIP.

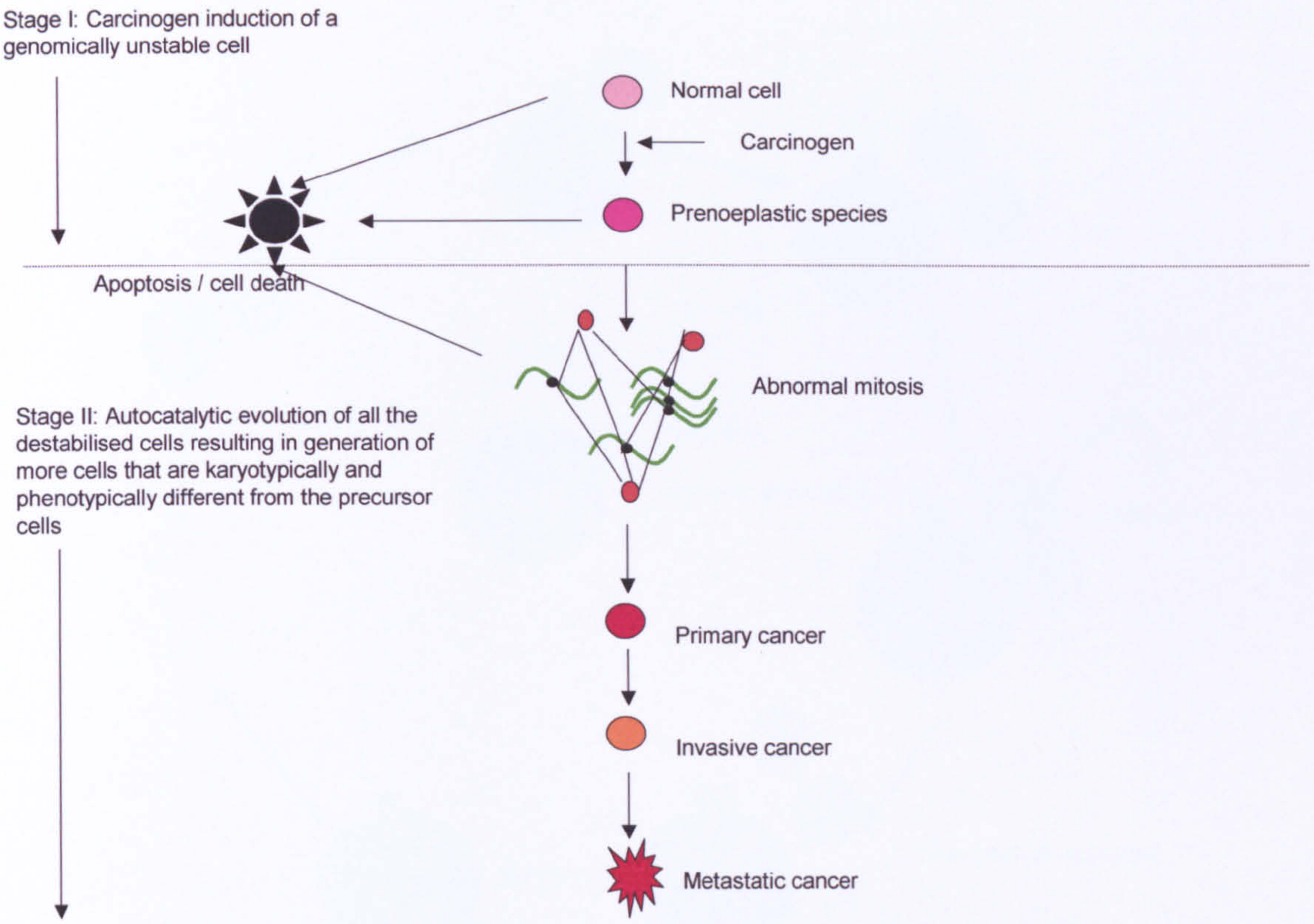

Figure 1.1 A two-stage model for how carcinogens may cause cancer via aneuploidy.

In the first stage, a carcinogen "initiates" carcinogenesis by generating an aneuploid, preneoplastic cell. The process will also generate cells with nonviable chromosome combinations. In the second stage, the destabilization of the karyotype and the chromosome segregation machineries by the induction of aneuploidy, in turn, drives the autocatalytic evolution of the preneoplastic and its progeny cells to generate cells with new karyotypes capable of tumour progression. The autocatalytic karyotype evolution and the low probability of generating a viable karyotype by chance that can outperform normal cells would also explain the previously unresolved, carcinogen-independent transformation of a preneoplastic into a neoplastic cell and the notorious long latent periods from initiation to cancer.

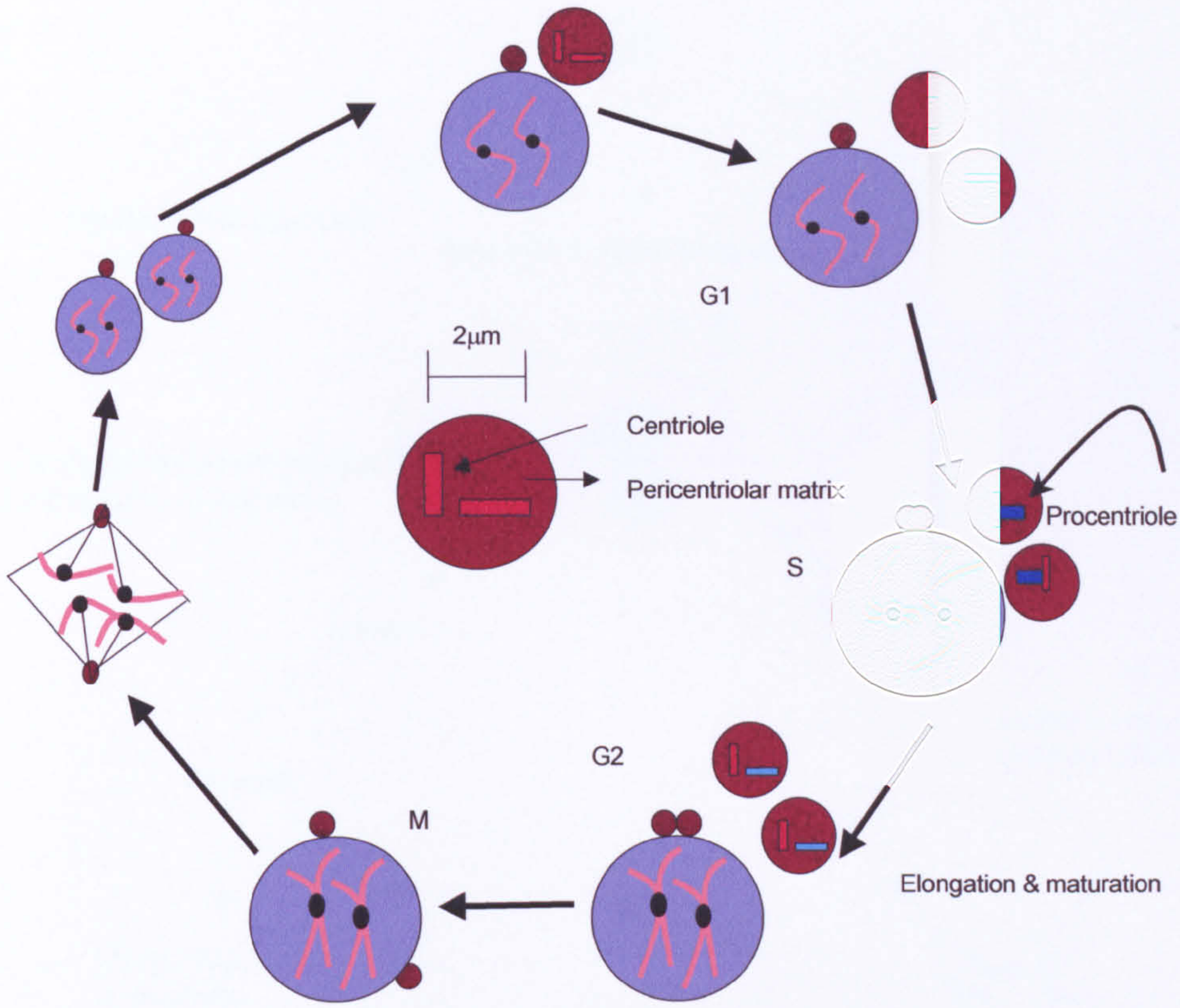

Figure 1.2 The centrosome duplication cycle in animal cells.

The centrosome is composed of a pair of perpendicularly oriented centrioles. (~0.2μm in diameter and 0.2-0.5μm in length) composed of nine identical and equally spaced microtubule arrays. Centrosome duplication is initiated at the late G1/early S phase of the cell cycle by the splitting of the centriolar pair. This is followed by the formation of procentrioles (blue) in the vicinity of the parental centrioles (red); the procentrioles continue to elongate during S and G2. At the end of G2, the new pair of mature centrosomes migrate to opposite poles of the cell to form bipolar spindles.

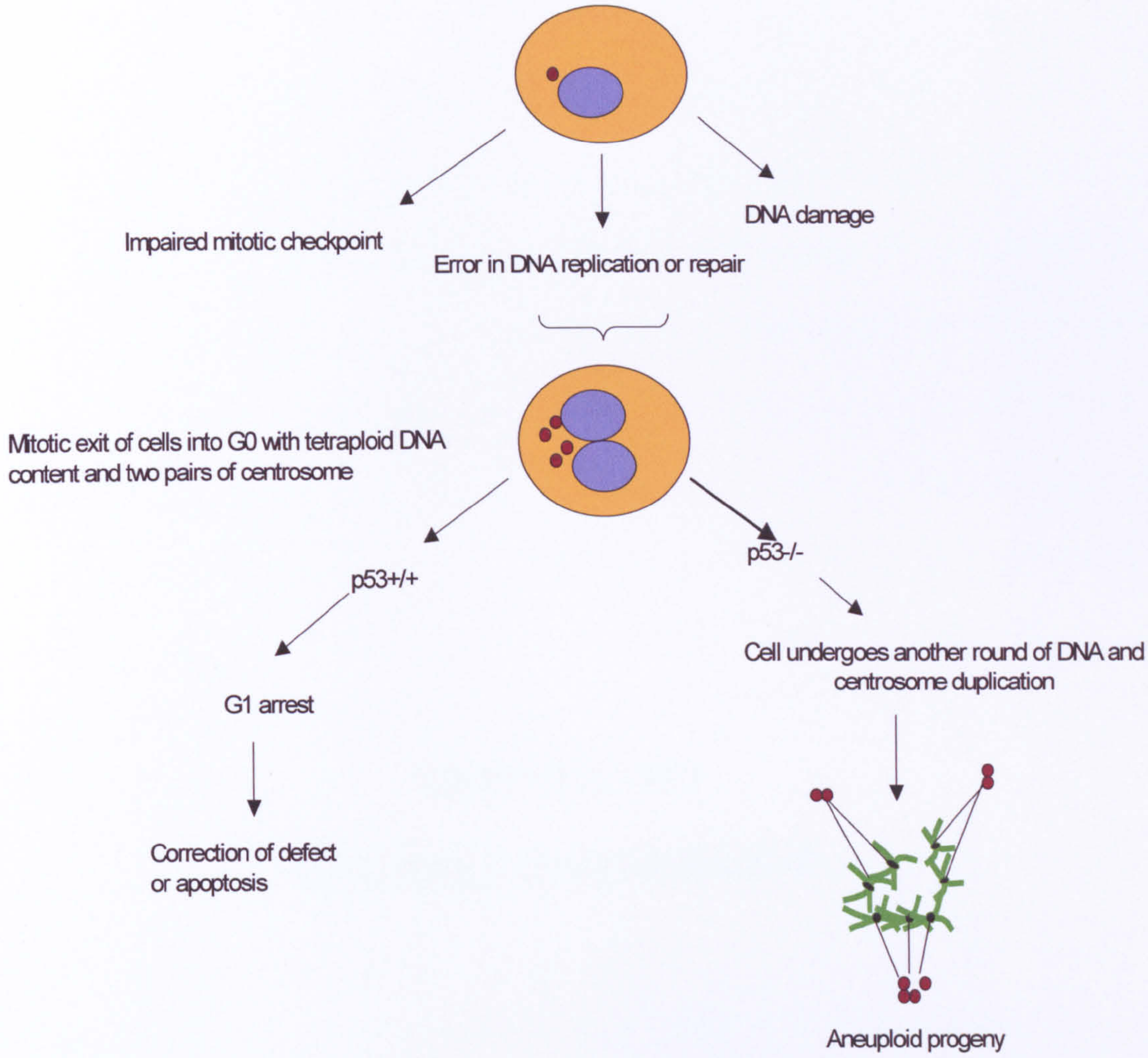

Figure 1.3 Defects in cell division as a major route to numerical centrosome aberrations and aneuploidy.

According to this model, tetraploidization (rather than enhanced centrosome duplication) is a prevalent cause for numerical centrosome aberrations. A number of errors could lead to an abortive mitotic exit, generating cells with tetraploid DNA and two pairs of centrosomes. A p53 wild type cell will be arrested in G_1 and/or eliminated. In the absence of a functional p53, however, cells will progress through an extra round of DNA replication and centrosome duplication, giving rise to cells with four pairs of centrosome, which during subsequent mitosis, mediate multipolar mitosis and generate aneuploid progeny.

CHAPTER TWO

MATERIALS AND METHODS

2.1 CELL LINES

2.1.1 OSCC-derived cell lines

Seven human oral squamous cell carcinoma (SCC) cell lines (H103, H157, H314, H357, H376, H400, H413) established in the Division of Oral Medicine, Pathology and Microbiology, University of Bristol, were used in the present study. Details of the methods by which the tumour-derived cell lines were established, including the prevention of infection and 3T3 fibroblast support, have been described previously (Prime *et al.*, 1990). Briefly, tissues were collected from fresh surgical biopsies of untreated human oral squamous cell carcinomas. The tissues were divided and half was used for cell culture and the remaining half was fixed in 10% (v/v) formol saline prior to histological examination. Tumours were classified clinically with regard to the site (S), tumour size (T), lymph node involvement (N), metastatic spread (M) and pathological grade of the tumour (P). The tumours were staged according to the STNMP system (Langdon, 1995; Table 2.1).

The cells have been characterised with regard to chromosomal anomalies (Patel *et al.*, 1993), Ha-*ras*, p53 and p16 mutations (Yeudall *et al.*, 1993; 1995, Wu *et al.*, 1999) and tumorigenicity following orthotopic transplantation to the floor of the mouth in athymic (Balb/C; nu/nu) mice (Prime *et al.*, 2004). The characteristics of the human oral carcinoma cell lines are summarised in Table 2.2.

2.1.2 Normal and immortalised human oral keratinocytes

Normal human oral keratinocyte cultures were established from excess tissue originating from routine oral surgical procedures. Although different primary cultures of normal keratinocytes were used in individual experiments they were assumed to behave similarly. The Swiss mouse embryo fibroblast cell line 3T3 (European Collection of Animal Cell Cultures, UK) was used in the culture of normal oral keratinocytes in order to assist their growth and to limit host fibroblast contamination

OKF6/TERT-1, an oral mucosal keratinocyte cell line immortalised via the retroviral transduction of the human telomerase reverse transcriptase (hTERT), was obtained from Dr J. Rheinwald. (Harvard Institute of Medicine, Boston, USA). OKF6/TERT-1 has a heterozygous deletion involving all three exons of p16INK4a and has a wild type p53 (Dickson *et al.*, 2000).

2.1.3 Control cell lines

Two colorectal cell lines, HCT116 and CaCo2, were used as controls in this study. HCT116, a mismatch repair deficient (Bardelli *et al.*, 2001), diploid human colorectal carcinoma cell line carrying wild type p53, was obtained from Dr. B. Vogelstein (School of Medicine, John Hopkins University; Chan *et al.*, 2000). Caco2, which contains hyperamplified centrosomes, was obtained from Dr. C. Paraskeva (Department of Microbiology and Pathology, University of Bristol; Ghadimi *et al.*, 2000).

2.2 TISSUES

Formalin-fixed paraffin embedded tissues were obtained from the Department of Histopathology, Bristol Royal Infirmary of the United Bristol Healthcare Trust (UBHT). Approval from the UBHT Research Ethics Committee was obtained prior to commencing the study.

2.3 MATERIALS

For all techniques, unless otherwise stated, chemicals were of molecular biology or Analar grade and were obtained from Sigma (UK), BDH (UK), Difco, Merck or ICN. Restriction enzymes were obtained from Promega (UK). All cell culture and associated procedures were carried out in a MDH laminar flow cabinet (Microflow Ltd., UK) and cell culture medium and supplements were obtained from Invitrogen (UK). Cell culture plastics were obtained from Iwaki (UK), while plastics for other purposes, such as molecular biology, were obtained from Greiner (UK) and Corning (UK). The commercial suppliers are listed in Appendix 1.

2.4 CELL CULTURE TECHNIQUES

2.4.1 3T3 feeder cells

$1x10^5$ 3T3 fibroblasts were cultured in 90 mm culture dishes containing 10 ml Dulbecco's modified Eagle's medium (DMEM) containing 10% (v/v) foetal bovine serum (FBS) and 0.6 µg/ml L-glutamine (fibroblast medium). Cells were incubated for 7 days in a humidified atmosphere of 95% air/5% CO_2 at 37°C. Confluent cultures of 3T3 fibroblasts were used as feeder cells for normal keratinocyte cultures (Rheinwald and Beckett, 1981). Prior to use, 3T3s were

treated with a final concentration of 10 µg/ml mitomycin C for 2 hours at 37^{0}C and, after cell number determination, 2x10^5 cells were seeded into 25 cm^2 flask containing normal human oral keratinocytes.

2.4.2 Primary culture of normal oral keratinocytes

Primary cultures of human normal oral keratinocytes were established by single cell suspension. Excess tissue originating from routine oral surgical procedures was transported to the laboratory in Dulbecco's modified Eagle's medium (DMEM)/F12 (1:1) containing 10% (v/v) foetal bovine serum (FBS), 0.6 µg/ml L-glutamine, 0.5 µg/ml hydrocortisone (epithelial medium) supplemented with 10 ng/ml cholera toxin, 200 IU/ml penicillin, 200 µg/ml streptomycin and 5 µg/ml fungizone. The tissues were washed twice in sterile PBS containing 200 IU/ml penicillin and 200 µg/ml streptomycin, immersed briefly in absolute ethanol and rinsed thoroughly in PBS to remove surface contaminants. The tissue was then cut into fine pieces and incubated in 2 ml of 0.025% (w/v) type III trypsin containing 200 IU/ml penicillin, 200 µg/ml streptomycin and 5 µg/ml fungizone, at 4°C for 12 hours. Following overnight incubation, most of the trypsin was discarded and the tissues incubated in the residual trypsin solution at 37°C for 1 hour. The trypsin was then neutralised by the addition of 5 ml of epithelial medium, containing antibiotics and anti-fungals, and the epithelial cells were detached by vigorous pipetting. The supernatant containing the epithelial cells was centrifuged (60*g*, 10 minutes) and the pellet resuspended in epithelial medium containing 10 ng/ml cholera toxin, 0.04 IU/ml insulin, 1 µg/ml transferrin. 5x10^5 keratinocytes were seeded together with 2x10^5 of mitomycin

C treated mouse 3T3 fibroblast (Section 2.4.1) into a 25 cm^2 flask and incubated at 37°C in a humidified atmosphere of 95% air/5% CO_2.

Primary oral keratinocytes were also grown in keratinocyte serum free medium (KSFM; Section 2.4.3.3). Normal keratinocytes grown in KSFM medium do not require mitomycin C treated 3T3 fibroblast cells to support growth.

2.4.3 Maintenance of cultured cells

2.4.3.1 Normal oral keratinocytes

Newly established primary cultures of normal oral keratinocytes were left undisturbed for 4 days to allow cell attachment to the culture flask. Subsequently, the culture medium was replaced every 2-4 days depending upon the growth rate of the cells. The fresh epithelial medium was supplemented with 5 ng/ml epidermal growth factor (EGF) to stimulate growth. Host fibroblasts and 3T3 fibroblasts were removed from keratinocyte cultures prior to experiments by washing the cells with PBS and incubating them in 0.02% (w/v) ethylene diamine tetra-acetic acid (EDTA) solution in PBS for 30-60 seconds at room temperature. An equal volume of PBS was added and the solution was pipetted over the cells for 60 seconds. The solution was removed and the cells were washed with PBS. Complete removal of host fibroblast was determined microscopically. Cells were normally discarded after the second or third passage when they showed signs of senescence.

2.4.3.2 Tumour-derived epithelial cell lines

Tumour-derived epithelial cell lines were cultured in Dulbecco's modified Eagle's medium (DMEM)/F12 (1:1) containing 10% (v/v) foetal bovine serum (FBS), 0.6 µg/ml L-glutamine, 0.5 µg/ml hydrocortisone and 1 mg/ml cholera toxin (epithelial medium) and were grown in a humidified atmosphere of 95% air/5% CO_2 at 37°C. The culture medium was replaced every 3-4 days. CaCo2 cells were cultured in DMEM medium containing 10% FBS, 0.6 µg/ml L-Glutamine and 0.5 µg/ml hydrocortisone.

2.4.3.3 Immortalised normal oral cells

The OKF6-TERT/1 cell line was grown in keratinocyte serum-free medium (KSFM; Invitrogen) containing 25 µg/ml bovine pituitary extract, 0.4 ng/ml epidermal growth factor (EGF) [diluted in 20 mM HEPES-buffered Earle's salt, 0.1% bovine serum albumin (BSA)] and the calcium chloride ($CaCl_2$) concentration increased to 0.4 mM (Dickson *et al.*, 2000). The culture medium was replaced every 2 days.

2.4.4 Sub-culture and cell number determination

Cells were sub-cultured every 7-10 days when ~90% confluent. The culture medium was discarded and the cultures were washed with PBS. The cells were enzymatically detached by incubating in 0.025% (v/v) trypsin / 0.01% (w/v) EDTA solution in PBS for 5-30 minutes at 37°C. The trysin/EDTA solution was neutralised by the addition of an equal volume of epithelial medium and the cell suspension was centrifuged (60*g*, 10 minutes). The cell pellet was resuspended in 5 ml of culture medium. Cell number was determined using Coulter counter

(Coulter Z Series, Coulter Corporation, USA). Cells were re-seeded at $5x10^5$ cells per 75 cm^2 flask in epithelial medium and maintained in culture, as previously described.

For the immortalised normal oral keratinocyte cell line, OKF6/TERT-1, cells were sub-cultured every 5 days, when about 30% confluent. The KSFM medium has been designed to support low density and clonal growth of cells and does not contain levels of nutrients and growth factors that are required to maintain keratinocytes in a healthy proliferative state at high densities. Cells were harvested as described above for the tumour-derived oral cell lines. The cell pellet was resuspended in KSFM medium and the cells re-seeded at $1x10^5$ cells per 75 cm^2 flask and maintained in culture as previously described.

2.4.5 Storage and retrieval of cell

Stocks of epithelial cells were maintained in liquid N_2. After determination of the cell number, $5x10^5$ – $1x10^6$ cells were re-suspended in epithelial medium with 20% (v/v) FBS and 10% (v/v) dimethylsulphoxide (DMSO) and then transferred into cryovials. The cells were placed in a –70°C freezer for 12-24 hours before being transferred to liquid N_2 at –196°C for long-term storage.

To cryopreserve OKF6-TERT/1 cells, an equal volume of chilled epithelial medium containing 20% (v/v) FBS and 20% (v/v) DMSO was added to cells suspended in KSFM medium, prior to freezing as described above.

Cells were recovered from storage in liquid N_2 by rapid thawing of the cryovials in a water bath at 37°C. The cells were then transferred into 10 ml of epithelial

medium and centrifuged (60*g*, 10 minutes). The supernatant was discarded, the cell pellet resuspended in epithelial medium for tumour-derived cell lines or KSFM medium for the OKF6/TERT-1 cell line and the suspension transferred to a 75 cm^2 tissue culture flask. The cells were maintained in culture, as previously described (Section 2.4.3).

2.4.6 Microscopy

Cell cultures were examined with an Olympus IMT-2 (UK) inverted phase contrast microscope. Photomicrographs of the cultured cells were taken with an Orthomat camera attached to the inverted phase contrast microscope. Photomicrographs were printed on Kodak polycontrast paper (Kodak, UK).

2.4.7 Mycoplasma testing and treatment

Cell cultures were examined routinely for mycoplasma contamination using the Hoescht fluorescent staining technique (Chen, 1977). The cells were grown on sterile glass coverslips in 60 mm dishes with culture medium lacking antibiotics and G418. After 10 days without a change of medium, the cells were fixed by the addition of glacial acetic acid/methanol fixative (1:1) for 2 minutes. The fixative was removed and replaced with another 5 ml fixative for 5 minutes and this step was repeated. Following aspiration of the fixative, the cells were air dried for 10 minutes at room temperature. The Hoescht No 33258 stain (Sigma, UK) stock solution [0.05% (w/v) in ddH_2O] was diluted 1:500 in PBS and added to the cells for 10 minutes at room temperature. After removal of the stain, the cells were washed twice with PBS and the coverslips mounted in PBS/glycerol (1:9). Stained cells were examined under ultraviolet light at 340nm using a Leitz

Ortholux microscope (Leica, UK) with a UGI filter, a BG38 suppression filter, a blue filter and a x40 objective. Mycoplasma contamination was indicated by the presence of speckled perinuclear fluorescence. Cells, which were found to be myocoplasma positive by Hoescht staining, were treated with mycoplasma removal agent (MRA; ICN Pharmaceuticals, UK). Cells were incubated with 10 μl MRA per ml culture medium for 7 days at 37°C and then re-tested using the Hoescht stain.

2.4.8 Transfection of cell lines

Cells were transfected using the Fugene 6 Reagent (Roche, UK). To prepare the transfection mixture, 30 μl Fugene 6 was added to 100 μl of epithelial medium without FBS (serum-free medium) in an eppendorf tube and mixed. The mixture was left for 5 minutes at room temperature. The Fugene-medium mixture was then transferred into an eppendorf tube containing 10 μg plasmid DNA, mixed and left for 15 minutes at room temperature.

For transfection, cells were grown to 30-50% confluence in 60mm dishes. The culture medium was removed and the cells were washed twice in serum-free medium and 100 μl of Fugene/DNA mixture was added to each culture dish containing 1.8 ml epithelial medium. The cells were incubated in a humidified atmosphere of 95% air/5% CO_2 at 37°C overnight, after which the culture medium was replaced with 5 ml epithelial medium and the cells were cultured for a further 48 hours. The cells were then harvested through trypsinization as previously described (Section 2.4.4) and sub-cultured into 75 cm^2 flasks in

epithelial medium containing 600 μg/ml geneticin sulphate (G418) in order to select for stable transfectants.

2.4.9 Cell cloning of transfectants

1 x 10^3 cells per dish were seeded into 100 mm dishes and cultured until islands of approximately 1000 cells per colony were observed. Small islands of cells were selected which had proliferated from single cells and which were at a distance from other cells. The medium was aspirated and the cells were washed with PBS. Cloning rings were coated on their base with sterile Vaseline and were placed over the chosen cell islands; the placement of the rings was checked microscopically before selective enzymatic detachment of the cells within the rings. Trypsin/EDTA was pipetted into the rings and incubated for 20 minutes at 37°C. The cells were then removed to 6-well plates containing medium supplemented with G418. Cells were grown to confluence before transfer to 75 cm^2 tissue culture flasks.

2.4.10 Irradiation of cell cultures

Cells were grown to approximately 40% confluence in a 25 cm^2 flask. Prior to irradiation, the medium was replaced with fresh medium containing 4.5 mM Hepes buffer. The cells were irradiated using a RX30/55 irradiator (Gravatom Industries) with a total dose of 5Gy using a Caesium 137 source (Amersham). Following irradiation, the medium was replaced and the cells incubated at 37°C as required.

2.4.11 MTT assay

3-[4,5-Dimethylthiazol-2yl]-2,5-diphenyltetrazolium bromide; thiazolyl blue (MTT) (Sigma) was made up as a 5 mg/ml stock in warm serum free medium and left in the dark for 20 minutes to dissolve. The solution was filter sterilised using a 0.2 μm filter and diluted in KSFM medium to give a 1 mg/ml solution. The medium was aspirated from the wells and 1 ml of the MTT solution added to each well and incubated for 1 hour. The MTT solution was removed, the cells rinsed with PBS and the resulting water-insoluble formazan salt, created by the metabolic activity of viable cells, was dissolved using 1 ml/well DMSO. The absorbance of the salt solution at 520 nm was determined with DMSO as a blank.

2.4.12 Assessment of apoptosis

Cells were harvested using accutase (PAA Laboratories) in place of trypsin, as described in section 2.4.4. Accutase combines protease and collagenolytic activities for gentle detachment of adherent cells for the study of cell surface markers via FACS. The cell pellet obtained following centrifugation was resuspended in 200 μl cold binding buffer (10 mM Hepes [pH 7.4], 140 mM $NaCl_2$, 5 mM $CaCl_2$) containing 4 μl Annexin V-FITC (Alexis) for every $1x10^6$ cells. Cells were incubated in the dark at room temperature for 10 minutes. Additional binding buffer was added to the cells and centrifuged (60*g*, 10 minutes, room temperature). The cell pellet was resuspended in 400 μl binding buffer containing 2 μg/ml propidium iodide and FACS analysis was performed on a FACScan (Becton Dickinson) within an hour of processing the cells.

Controls included unstained cells and cells stained individually with annexin V-FITC or PI.

2.5 FLUORESCENCE ACTIVATED CELL SORTING (FACS)

Following cell number determination, cells were centrifuged (60*g*, 10 minutes, room temperature), washed with PBS and resuspended in fresh ice cold 70% ethanol to yield a final concentration of $1x10^6$ cells /ml. The fixed cells were stored at –20°C in 1ml aliquots until needed for FACS analysis.

Prior to FACS analysis, ethanol fixed cells were centrifuged (60*g*, 10 minutes, room temperature) and resuspended in 1 ml PBS containing 15 μg/ml RNAse A and 20 μg/ml propidium iodide and incubated at 37°C in the dark for 30 minutes and stored at 4°C for 24 hours. The cells were syringed to create a single cell suspension prior to analysis and $1x10^4$ cells were analysed per sample using FACScan (Becton Dickinson) and the data were analysed using the ModFit LT, version 2 (Becton Dickinson).

2.6 CELL CYCLE CHECKPOINT ANALYSES

2.6.1 Mitotic checkpoint analysis

Cells were seeded at a density of $1x10^6$ cell per 75 cm^2 flask and incubated for 24 hours. Cells were then incubated in fresh epithelial medium containing 0.2 μg/ml nocodazole for 18 hours; cells treated with epithelial medium containing DMSO were used as controls. Loosely attached cells were first isolated through gentle agitation and adherent cells were harvested by trypsinization, as previously described (Section 2.4.4). The cells were pooled, centrifuged (60*g*,

10 minutes, room temperature) and the pellet resuspended in epithelial medium and the cells counted. Cell cycle analysis of the harvested cells was performed, as previously described (Section 2.5).

2.6.2 Tetraploidy checkpoint analysis

Cells were grown to ~70% confluence and then treated with 0.04 μg/ml nocodazole for 18 hours. Arrested mitotic cells were harvested through 'mitotic shakeoff' (i.e. gentle knocking of the flask), centrifuged (60*g*, 10 minutes, room temperature) and washed in serum free medium to remove any traces of nocodazole. The cells were then incubated in epithelial medium containing 10 μM dihydrocytochalasin B (DCB; Sigma) for 5 hours. Following DCB treatment, the cells were washed in serum free medium to remove traces of DCB and incubated in drug free epithelial medium for 18 or 36 hours. Cells were harvested, counted (Section 2.4.4) and cell cycle analysis was performed as previously described (Section 2.5).

2.7 IMMUNOFLUORESCENCE

2.7.1 Centrosome abnormalities in OSCC-derived cell lines

Cells were seeded at a density of $3x10^5$ cells/coverslip (22 mm), in a 6-well plate and allowed to adhere overnight at 37°C. Attached cells were treated with permeabilization buffer (45 mM Pipes (pH6.9), 45 mM Hepes, 10 mM EGTA, 0.1% TritonX-100/PBS) for 5 minutes and fixed in methanol (-20°C) for 10 minutes, air dried briefly and washed in 0.1% tritonX-100/PBS (pH7.2; PBST). Cells were blocked in blocking buffer (1% normal goat serum, 3% bovine serum albumin in PBST) for 30 minutes followed by incubation in primary monoclonal

mouse anti gamma-tubulin (T6557; Sigma) and polyclonal rabbit anti-pericentrin [PRB-432C; Berkley Antibody Company (BabCo, USA)] antibodies at 1:300 dilution in blocking buffer, for 1 hour at room temperature in a humidified chamber. Cells were washed in PBST and incubated in secondary Cyc 3 conjugated anti-mouse (1:500; Jacksons Laboratories) and FITC conjugated anti-rabbit antibody (1:100; Sigma) in PBS (pH7.2), for 1 hour at room temperature in a dark humidified chamber. Cells were washed in PBST, air-dried and mounted in Vectashield mounting medium with DAPI (Vector Laboratories) and stored at 4°C until analysis.

A minimum of 200 cells was counted for each cell line under a fluorescence microscope to determine the percentage of cells with centrosomal abnormalities. Images of centrosomes were obtained using the Inverted Leica Confocal Imaging Spectrophotometer System (TCS-SP2) attached to a Leica DMIRBE inverted microscope. The microscope was equipped with a five laser configuration, which included an Argon laser (458, 476, 488, 514 nm lines), a Green HeNe laser (543 nm lines), a Red HeNe laser (633 nm lines), a UV laser (351, 364 nm lines) and a 430 nm laser.

2.7.2 Centrosome abnormalities in paraffin embedded oral archival material

5 µm thick sections were cut from paraffin-embedded archival tissues, mounted on polylysine-coated slides (Shandon) and incubated at 37°C overnight. Sections were dewaxed in xylene (3 x 5 minutes), rehydrated through 100% ethanol (3 x 2 minutes) and finally in running tap water. Antigen retrieval was achieved by microwaving; sections were immersed in 1 litre of 0.1 M citrate

buffer (pH 6.0) and microwaved at 960W for 30 minutes. The sections were cooled to room temperature with running tap water and washed in PBS (pH7.2). The sections were then incubated with mouse monoclonal anti-gamma tubulin antibody (Sigma) and polyclonal rabbit anti-cytokeratin at dilutions of 1:200 and 1:70 respectively, in blocking solution [10% normal goat serum in PBS (pH7.2)] for 1 hour at room temperature. The sections were then washed in PBS (pH7.2), incubated with secondary Cyc 3 conjugated anti-mouse (Jacksons Laboratories) and FITC conjugated anti-rabbit antibodies (Sigma) at dilutions of 1:250 and 1:80 respectively, in PBS (pH7.2), for 1 hour at room temperature in a dark humidified chamber. The sections were again washed in PBS, air dried and mounted in Vectashield mounting medium containing DAPI. Stained sections were stored at 4°C.

2.7.3 Microtubule nucleation assay

Cells were seeded at a density of $3x10^5$ cells/coverslip (22 mm) in a 6-well plate and allowed to adhere for 24 hours. Cells were then incubated in epithelial medium containing 10 μg/ml nocodazole (stock: 5 mg/ml in DMSO) for 2 hours. The medium was discarded; the cells washed in PBS and allowed to nucleate microtubules for 2 minutes. The cells were then fixed and stained, as described in Section 2.7.1, to observe microtubule nucleation by the centrosome. The mouse anti-alpha tubulin (Sigma) and rabbit anti-pericentrin primary antibodies were used at dilutions 1:200 and 1:300, respectively.

2.7.4 Mitotic index

Cells were seeded at a density of $3x10^5$ cells/coverslip (22 mm) in a 6-well plate and allowed to adhere for 24 hours. Cells were then incubated in epithelial medium containing 0.2 µg/ml nocodazole at 37°C for 6-42 hours. The cells were then stained immunocytochemically using anti-phospho histone H3 antibody (1:200; Upstate Biotech), as described (Section 2.7.1).

2.8 CLONING OF CETN2

2.8.1 Transformation of competent *E.coli* with plasmid DNA

One Shot TOP10 competent *E.coli* cells (Invitrogen, UK) were used for transformation of plasmid DNA. A 50 µl aliquot of One Shot cells was used for each ligation. Cells were thawed on ice and 1 µg plasmid DNA or 10 µl ligation mixture (Section 2.8.8) was added and the vial was tapped gently to mix. The *E. coli*/DNA mix was incubated on ice for 30 minutes, heat shocked in a water bath at 42°C for exactly 30 seconds and promptly placed on ice for 2 minutes. 250 µl room temperature S.O.C medium (supplied with the cells) or LB medium was added to the cells and the mixture was incubated for 1 hour at 37°C, with constant agitation. 20 µl-200 µl of each transformation were plated on LB/agar (1.5%, w/v) plates containing 100 µg/ml ampicillin and incubated overnight at 37°C. Glycerol stocks of clones containing the correct plasmid construct were prepared by adding sterile glycerol to overnight bacterial cultures to a final concentration of 20% and stored at –70°C.

2.8.2 Purification of plasmid DNA

2.8.2.1 Small-scale

Transformed *E.coli* cells were grown on LB agar [1.5% (w/v)] plates containing ampicillin (100 μg/ml). Single colonies were isolated and inoculated into 5 ml LB medium containing 100 μg/ml ampicillin and incubated on an orbital shaker overnight at 37°C. Preparations of plasmids were obtained by the alkaline lysis of cells derived from overnight cultures (Sambrook *et al.*, 1989). For small-scale preparation of DNA, 1.5 ml of overnight culture was centrifuged in an eppendorf tube at 12,000*g* for 30 seconds. Following removal of the supernatant, the pellet was evenly resuspended in 100 μl of Solution I (50 mM glucose; 25 mM Tris-HCl, 10 mM EDTA; pH 8.0). 200 μl of freshly prepared Solution II (0.2 M NaOH; 1% (w/v) SDS) was added and mixed rapidly by inverting the tube and the tube placed on ice. Then 150 μl of ice cold Solution III (3 M potassium acetate; 5 M glacial acetic acid) was added, vortexed and stored on ice for 3-5 minutes. The solution was centrifuged (12,000*g*, 5 minutes, 4°C) and the supernatant transferred to a fresh tube. An equal volume of phenol/chloroform/isoamyl alcohol (25:24:1) was added, mixed by vortexing and centrifuged (12,000*g*, 5 minutes, 4°C). The top phase was transferred into a fresh eppendorf tube. The plasmid DNA was precipitated by adding 2 volumes of ethanol at room temperature, the tube vortexed and left at room temperature for 2 minutes and centrifuged (12,000*g*, 5 minutes, 4°C). The pellet was rinsed with 1 ml 70% ethanol and the supernatant removed following brief centrifugation. The pellet was allowed to air dry at room temperature for 10 minutes and dissolved in 50 μl TE (pH8.0) containing 20 μg/ml RNAase A. DNA was stored at –20°C until needed.

2.8.2.2 Large scale

For large-scale preparation of plasmid DNA, 500 ml sterile LB medium containing 100 μg/ml ampicillin was inoculated with 200 μl from a previously prepared 10 ml culture of *E.coli* and incubated, with agitation, overnight at 37°C. The resultant cell suspension was centrifuged (4,000*g*, 20 minutes, 4°C), the supernatant discarded and the pellet re-suspended in 100 ml ice cold STE (0.1 M NaCl; 10 mM Tris-HCl (pH8.0); 1 mM EDTA (pH 8.0)). After further centrifugation (4,000*g*, 20 minutes, 4°C), the pellet was re-suspended in 18 ml Solution I followed by the addition of 2 ml of freshly prepared lysozyme solution (10 mg/ml in 10 mM Tris-HCl (pH 8.0)). 40 ml freshly made Solution II was added to lyse the cells and the solution was mixed by inversion and at room temperature for 10 minutes. 20 ml Solution III was added and mixed by inversion and incubated on ice for 10 minutes to precipitate the protein. The protein was removed by centrifugation (4,000*g*, 20 minutes, 4°C) and the supernatant filtered through cheesecloth and transferred to a 50 ml polypropylene tube. 0.6 volumes isopropanol was added to the supernatant and the mixture was incubated for 10 minutes at room temperature to precipitate the DNA, which was recovered by further centrifugation (4,500*g*, 15 minutes, room temperature). The pellet was washed with 70% (v/v) ethanol at room temperature, air dried for 10 minutes at room temperature and then re-suspended in 3 ml TE buffer (10 mM Tris-HCL; 1 mM EDTA; pH 8.0).

The maxipreped DNA was purified by equilibrium centrifugation in Caesium chloride (CsCl) - ethidium bromide continuous gradient. 1 g of CsCl (ultrapure) for every ml of DNA solution was added and mixed gently until the salt is

dissolved. 0.8 mg/ml ethidium bromide (EtBr) was added for every 10 ml of CsCl/DNA solution and mixed. The solution was centrifuged (4500*g*, 5 minutes, room temperature) and the clear red solution transferred into a Beckman (UK) tube and the DNA was purified by centrifugation for 16-22 hours at 65,000 rpm in a Beckman Ultracentrifuge (NVT 65 rotor, UK) at 20°C. Under ultraviolet (U.V.) light, two bands were visible within the tube: the higher band was contained linear bacterial chromosomal DNA and nicked circular plasmid DNA; the lower band contained the closed circular plasmid DNA. The plasmid DNA was removed into another Beckman tube using a 19G needle and syringe and the CsCl gradient centrifugation was repeated.

The extracted plasmid DNA was transferred into a 15 ml polypropylene tube, and the EtBr removed from the DNA by adding equal volume of CsCl-saturated isopropanol. The solution was vortexed, centrifuged (1500*g*, 3 minutes, room temperature) and the upper pink isopropanol phase was removed and the process repeated until there were no traces of the pink EtBr. Finally, the lower aqueous phase containing plasmid DNA was transferred into a clean tube and diluted with 3 volumes of ddH_2O followed by 2 volumes of 100% (v/v) ethanol and then incubated for 10 minutes at 4°C in order to precipitate the DNA. The DNA was collected by centrifugation (4,500*g*, 15 minutes, room temperature), washed with 70% (v/v) ethanol and re-centrifuged (4,500*g*, 15 minutes, room temperature). After centrifugation, the pellet was air-dried (20 minutes, room temperature) and re-suspended in 1 ml TE buffer (pH8.0). The maxi preparation was stored at –20°C until required.

2.8.3 RNA extraction

Total RNA was prepared from cell pellets of the cell lines using the RNeasy total RNA kit (Qiagen, UK). Cells were lysed with 350 µl RLT lysis buffer containing 3.5 µl ß-mercaptoethanol and then placed in a QIA shredder column and homogenised by centrifugation (13,000*g*, 1 minute, room temperature). 350 µl 70% (v/v) ethanol was added to the homogenised lysate and placed in an RNeasy spin column and centrifuged (8,000*g* 15 seconds, room temperature). The flow-through was discarded and the spin column was washed with 700 µl RW1 buffer and re-centrifuged (8,000*g*, 15 seconds, room temperature). Following further washing with 500 µl RPE buffer, the spin column was centrifuged (13,000*g*, 2 minutes, room temperature) to ensure complete drying of the RNeasy spin column membrane. The RNA was eluted by the addition of 35 µl RNase-free H_2O to the column membrane, followed by incubation (30 minutes, on ice) and centrifugation (8,000*g*, 1 minute, room temperature). The concentration of the RNA was calculated from its optical density at a wavelength of 260 nm using a UVmini 1240 spectrophotometer (Shimadzu, Japan). The eluted DNA can be stored at –20°C until needed.

2.8.4 Reverse transcriptase - Polymerase Chain Reaction (RT-PCR)

RT-PCR was performed using the TITANIUM One-Step RT-PCR Kit (Clontech: PT3397-2) to amplify the CETN2 gene from mRNA extracted from H413 cells. Primers that incorporated XhoI and XmaI restriction enzyme sites into the 5' and 3' ends, respectively, were used. The primer sequences were:

Forward primer: 5'**CTCGAGTG**ATGGCCTCCAACTTTAAGAAGGC3'

(coding strand, nucleotides 48-67; an additional **TG** was added to the primer sequence in order to ensure that the CETN2 gene sequence was cloned 'in frame')

Reverse primer: 5'**CCCGGG**ATAGAGGCTGGTCTTTTTCATGATGCGCAG3'

(non-coding strand, nucleotides 534-563, which produced a 430 base pair fragment)

RT-PCR was carried out using the following reaction mixture at final concentrations of 1X One-Step buffer, 1X dNTP mix, 20 units recombinant RNase Inhibitor, 25 μl thermostabilizing reagent, 10 μl GC-melt, 1 μl oligo(dT) primer, 1X RT-Titanium *Taq* enzyme mix, 1μg RNA sample, 0.5 μl of each forward and reverse primer (1μg/μl). The final volume was made up to 50 μl using RNase-free H_2O. RT-PCR was carried out using a Gene Amp PCR System 2400 thermal cycler (Perkin-Elmer, UK). The initial synthesis of the cDNA strand was performed at 50°C for 1 hour. The mRNA-cDNA template was then denatured at 94°C for 5 minutes followed by 35 cycles of denaturation at 94°C for 30 seconds, primer annealing at 65°C for 30 seconds, primer extension at 68°C for 1 minute and a final extension at 68°C for 7 minutes. The PCR products were visualised by agarose gel electrophoresis, as described (Section 2.8.6). The PCR product was cloned into the pCR4-TOPO vector, a commercially available kit for direct cloning of PCR products (TOPO TA Cloning Kit for Sequencing; Invitrogen), according to manufacturers instructions. A small-scale preparation of the pCR4-TOPO vector containing the PCR insert

was performed following transformation into competent *E.coli* cells, as described (Section 2.8.1), and stored at –20°C until required.

2.8.5 Expression vector: pEGFP-C1

The mammalian expression vector pEGFP-C1 (Clontech, UK) encodes a red-shifted variant of wild-type GFP (1–3), which has been optimised for brighter fluorescence and higher expression in mammalian cells. Genes cloned into the multiple cloning sites between the EGFP coding sequences and the SV40 poly A, will be expressed as fusions to the C-terminus of EGFP if they are in the same reading frame as EGFP. SV40 polyadenylation signals downstream of the EGFP gene direct proper processing of the 3' end of the EGFP mRNA. A neomycin resistance cassette (neo), consisting of the SV40 early promoter, the neomycin/kanamycin resistance gene, and polyadenylation signals from the Herpes simplex thymidine kinase (HSV TK) gene, allows stably transfected eukaryotic cells to be selected using G418. A bacterial promoter upstream of this cassette expresses kanamycin resistance in *E. coli*. The pEGFP-C1 backbone also provides a pUC origin of replication for propagation in *E. coli* and an f1 origin for single-stranded DNA production. A map of pEGFP-C1 is shown in Figure 2.1.

2.8.6 Restriction digestion and agarose gel electrophoresis

Restriction enzyme digests were used to release the CETN2 cDNA from the pCR4-TOPO vector and to linearise the pEGFP-C1 vector for the purpose of sub-cloning the CETN2 gene into pEGFP-C1. 1-5 μg plasmid DNA was digested with 5 units of XhoI, 5 units of XmaI, 3 μl 10X restriction enzyme buffer

D (Promega) and H_2O added to a final volume of 30 μl. The plasmid was digested for 2 hours at 37°C and the reaction was terminated by the addition of 3 μl of 10X nucleic acid loading buffer (0.025% (w/v) bromophenol blue; 50% (v/v) glycerol; 1 mM EDTA; pH 8.0). The DNA fragments were separated on 1% (w/v) agarose gels containing 0.5X TBE buffer (0.089 M Tris-Borate (pH 8.3), 2 mM EDTA) and 0.5 μg/ml EtBr (stock: 10 mg/ml). DNA markers of known molecular weight (Sigma: λDNA HindIII or φX174 HaeIII digest) were run in parallel. The DNA was visualised using a U.V. transilluminator with a wavelength of 254 nm.

2.8.7 Purification of DNA from agarose gels

The Sephaglas BandPrep Kit (Amersham Pharmacia Biotech, UK) was used to purify DNA from agarose gels. The DNA band of the correct molecular weight was excised from the agarose gel and placed in a 1.5 ml eppendorf. To a gel slice weighing less than 250 mg, 250 μl of gel solubiliser was added and the mixture incubated at 60°C for 10 minutes with intermittent vortexing until the agarose slice was dissolved. 5 μl Sephaglas BP suspension was added to the solution, incubated at room temperature and vortexed gently every minute for 5 minutes. The Sephaglas pellet was collected by centrifugation (13,000*g*, 1 minute, room temperature) and the supernatant discarded. Centrifugation was repeated and any residual liquid was removed. The pellet was resuspended in 80 μl wash buffer and collected by centrifugation (13,000*g*, 1 minute, room temperature). The wash step was repeated twice and supernatant discarded. The tube was tapped to disperse the Sephaglas pellet and air dried for 10 minutes at room temperature. The pellet was re-suspended in 20 μl elution

buffer (1 mM EDTA; 10 mM Tris-HCl; pH 8.0) and incubated for 5 minutes at room temperature with periodic agitation. The solution was centrifuged (13,000*g*, 1 minute, room temperature) and the supernatant containing the purified DNA was used in ligation reactions in order to create plasmid constructs.

2.8.8 Ligation

A 2:1 molar ratio of vector to insert was used for ligation. Ligation was carried out in solution containing, vector, insert, 1X ligation buffer, 100 U T4 DNA ligase (New England Biolabs, UK) and H_2O added to the reaction mixture to make a final volume of 20 μl. Ligation was carried out overnight at 4°C and heat inactivated at 65°C for 10 minutes.

2.8.9 Sequencing

1 μg of DNA was precipitated using 1/10-volume 3 M sodium acetate and 2.5-volumes of ethanol at –20°C for 1hour. The DNA was centrifuged (13,000*g*, 10 minutes, 4°C) and the DNA pellet was washed with 70% ethanol. The pellet was air-dried and the sequencing reaction performed commercially by MWG (Germany). The sequence of the CETN2 gene is listed in Appendix II

2.9 WESTERN BLOTTING

2.9.1 Preparation of protein samples

Cells were cultured until 70-80% confluent, harvested, counted (Section 2.4.4) and resuspended in sufficient PBS to yield $1x10^6$ cell/ml. 1 ml aliquot of the cell suspension was transferred into sterile 1.5 ml eppendorf tubes, centrifuged

(13,000*g*, 3 minutes, room temperature), the supernatant aspirated and the cell pellet stored at –70°C until needed.

Prior to western blot analysis, the cell pellets were lysed in 50 µl of ice-cold RIPA buffer [0.15 M NaCl, 1% (v/v) Nonidet P40, 0.5% (v/v) sodium deoxycholate, 0.1% (w/v) SDS, 50 mM Tris-HCl (pH8.0)] containing 5µl protease inhibitor [cocktail set III (Calbiochem)], 1 mM sodium orthovanadate, 2 mM sodium pyrophosphate, 5 mM β-glycerophosphate and 49.5 mM sodium fluoride. The lysates were vortexed and incubated on ice for 15 minutes and centrifuged (13,000*g*, 20 minutes, 4°C). The supernatant was collected and an equal volume of 2x gel sample buffer [100 mM Tris-HCl (pH6.8), 20% (v/v) glycerol, 200 mM dithiothreitol, 4% (w/v) bromophenol blue] was added. The samples were boiled for 5 minutes and used immediately or stored at –20°C until required.

2.9.2 Polyacrylamide gel electrophoresis

For resolution of proteins, the resolving gel consisted of 8% Protogel [30% (w/v) acrylamide, 0.8% (w/v) bisacrylamide)], 0.38 M Tris pH8.8, 0.1% SDS, 0.1% ammonium persulphate (APS) and 0.06% N,N,N',N'-tetramethylethylenediamine (TEMED). The stacking gel consisted of 4.98% Protogel, 0.14 M Tris pH6.8, 0.1% sodium dodecyl sulphate, 0.1% APS and 0.1% TEMED. The samples were electrophoresed in running buffer [0.38 M glycine, 49 mM Tris and 0.2 % SDS] (pH8.3), together with stained protein markers (Bio-Rad Precision Protein Standards), for 1½ hours at 30mAmp/gel. The separated proteins were transferred to a polyvinylidene difluoride (PVDF) membrane (Immobilon-P, pore

size; 0.45 µm, Millipore, UK). Prior to protein transfer, the PVDF membrane was soaked in methanol for 5 minutes and washed in Hoeffer buffer [0.19 M Glycine, 0.02 M Tris, 0.04% SDS, 20% Methanol; (pH8.3). Proteins were transferred using a dry blotter, Semiphor Transfer Unit TE70 (Hoefer Scientific Instruments, USA) for 2 hours at 0.8 mAmp/cm^2.

Electroblotted membranes were blocked in milk block buffer [10 mM Tris-HCl pH8.0, 150 mM NaCl, 4% non-fat dried milk, pH 7.4] for 1 hour to block non-specific binding of proteins. Membranes were incubated with primary antibodies in milk buffer, overnight on a rotator at 4^{0}C. The membranes were then rinsed in ddH_2O and washed twice in milk buffer, twice in Tween buffer [10 mM Tris/HCl, pH8, 150 mM NaCl, 0.2% Tween-20 (w/v) (Sigma), pH 7.4] and finally in milk buffer, for 10 minutes each. The membranes were then incubated in horse-radish peroxidase (HRP)-conjugated secondary goat anti-mouse antibody (Sigma), at 1:1000 dilution, in milk buffer for 1 hour on a rotator at room temperature. The membranes were then washed for 20 minutes in milk buffer on a rocking platform at room temperature, followed by a 10 minute wash in Tween buffer and then rinsed in ddH_2O. The peroxidase activity was detected using an Enhanced Chemiluminescence (ECL) detection kit (Amersham), following the manufacturer's instructions and developed on Kodak X Omat film. Equal loading of proteins was confirmed by incubating the blot in the primary antibody alpha-tubulin (Sigma) at dilution 1:10, 000 in milk block buffer and detected as described above.

For the detection human MLH1 and MSH2 proteins, primary mouse monoclonal anti-human MLH1 and MSH2 (BD Pharmingen) antibodies were used at a dilution of 1:250.

For detection of p21 and MDM2 proteins, primary mouse monoclonal anti-$p21^{Waf1}$ (Oncogene: OP64) and MDM2 (Oncogene: OP46T) antibodies were used at 1:100 dilutions. Primary mouse monoclonal anti-p53 antibody was provided by Dr. Chris Paraskeva and was used at a dilution of 1:100.

2.10 TREATMENT OF CELLS WITH THE CHEMICAL CARCINOGEN PHIP

OKF6/TERT-1 cells were grown to 50% confluence and harvested as described previously. $1x10^6$ cells were incubated in suspension with 50 μM PhIP [stock: 50 mM in DMSO (ICN)], 0.4 mg/ml Aroclor 1254-induced S9 rat liver extracts (Moltox Boone, NC), 0.23 mM NADP, 0.28 mM glucose 6-phosphate, 0.45 mM $MgCl_2$, 0.45 mM KCl and 200 mM Tris.HCl (pH7.5) in KSFM medium at 37°C, for 3 hours with intermittent shaking. Controls included cells treated with an equal volume of DMSO. Following PhIP treatment, cells were centrifuged (60*g*, 10 minutes, room temperature), washed in serum free epithelial medium and re-seeded in KSFM medium. The PhIP treated cells were allowed to recover exponential growth, harvested and re-treated as above and seeded in 90 mm dishes. Cells were allowed to grow until they formed colonies of approximately 1000 cells and single cell clones were obtained using cloning rings as described previously (Section 2.4.9).

To identify PhIP resistant clones, $1x10^6$ cells of PhIP clones were treated with 50 μM of PhIP, as described above and seeded in $25cm^2$ flasks and allowed to grow for 14 days until colonies were visible. $1x10^6$ parental OKF6/TERT-1 cells were treated in parallel as controls. Cells were then washed with PBS (pH7.2) and fixed in 10% formol saline (36g NaCl in 10% formaldehyde) for 10 minutes and stained with 0.5% methylene blue/PBS (pH7.2) solution. The relative resistance of PhIP clones was normalised to the plating efficiency of untreated controls. Clones that formed more or bigger colonies in comparison to PhIP treated parental cells were, therefore, considered PhIP resistant.

2.11 COMPARATIVE GENOMIC HYBRIDISATION (CGH)

The Qiagen Blood and Cell Culture DNA Kit (Cat. no. 13323) was used to extract genomic DNA from cell lines. Cells were harvested through trysinization as described (Section 2.4.4) and genomic DNA was extracted according to the manufacturers instructions. Briefly, cells were resuspended in PBS to a final concentration of 10^7 cells/ml and 0.5 ml ($5x10^6$) was used per reaction. The cell suspension was transferred to a 15 ml falcon tube and 1x volume of ice-cold buffer C1 and 3x volume ice-cold ddH_2O were added. The solution was mixed by inverting the tube, incubated on ice for 10 minutes and centrifuged (4000*g*, 15 minutes, 4C). The supernatant was discarded and the process repeated. Following centrifugation, the pellet was resuspended in 1 ml buffer G2 and treated with 25 μl proteinase K solution at 50°C for 60 minutes. Before harvesting the genomic DNA, the QIAGEN tip with was equilibrated with 2 ml buffer QBT and the proteinase K treated sample was applied to the equilibrated tip. The tip was washed 3x with 1 ml of buffer QC and the genomic DNA eluted

2 x with 1 ml buffer QF, prewarmed to 50°C. 0.7x volume of room temperature isopropanol was added and the precipitated DNA harvested by centrifugation (4,500*g* for 15 minutes, 4°C). The DNA pellet was washed with 1ml of cold 70% ethanol and centrifuged (4,500*g* for 15 minutes, 4°C). The DNA pellet was air dried for 5-10 minutes at room temperature, resuspended in 0.1 ml TE (pH8) and left at room temperature to dissolve and stored at –20°C.

CGH was carried out in collaboration with Dr. P. Murray (Division of Cancer Studies, University of Birmingham) using a previously described method (Dyer *et al.*, 2002). Briefly, tumour and reference DNA were nick-translated and directly labelled with Spectrum Green-2'-deoxyuridine-5'-triphosphate and Spectrum Red-2'-deoxyuridine-5'-triphosphate (Vysis, Downers Grove, IL), respectively. The volume of enzyme mix and incubation period were varied to give fragment sizes of 200 to 5000 bp as determined by gel electrophoresis. 800 ng of tumor DNA, 400 ng of reference DNA, and 30 µg of Cot-1 DNA (Invitrogen, UK) were co-precipitated and resuspended in 3 µl of nuclease-free H_2O and 7 µl of CGH hybridization buffer (Vysis). The probe mixture was denatured (75°C, 5 minutes) and hybridized to denatured, dehydrated male metaphase slides (Vysis) at 37°C for 72 hours. Slides were washed in 0.4x standard saline citrate/0.3% Nonidet P-40 (75°C, 2 minutes) and 2x standard saline citrate/0.1% Nonidet P-40 (room temperature, 30 seconds) and counterstained with 4,6-diamino-2-phenylindole (125 ng/ml) in anti-fade solution. Red, green, and blue images from representative metaphase spreads were digitized using a Cytovision (Applied Imaging, Santa Clara, CA) imaging system. Karyotypes from 15 metaphases were combined to produce a mean CGH ratio profile for each hybridization. Detection of imbalances was performed using

Applied Imaging CytoVision High-Resolution CGH (HRCGH) software, which allows direct comparison of a mean CGH profile from a test hybridization with standard reference intervals produced from a series of CGHs using normal test DNA. Regions where the mean CGH ratio profile, confidence limits, and standard reference intervals deviate from each other represent areas of genomic imbalance in the test specimen. A test:reference fluorescence ratio >1.5 was classified as a high-level gain, whilst a ratio of < 0.5 was classified as a loss.

2.12 DNA PLOIDY ANALYSIS OF ARCHIVAL ORAL TISSUES

Ploidy analysis of oral archival material was carried out in collaboration with Dr. J. Sudbo (Norwegian Radium Hospital, University of Oslo, Norway) using a previously described method (Sudbo *et al.*, 2001a). Two 50 µm sections of paraffin-embedded blocks of biopsy specimens were deparaffinized, rehydrated and enzymatically digested (type XXIV protease, Sigma) to yield a suspension of nuclei. The suspension was centrifuged, and the pellet was resuspended and placed on a slide to form a monolayer. The monolayer was the stained with Feulgen's and periodic acid–Schiff stain in order to assess the DNA content of the nuclear DNA

The DNA content of nuclei stained with Feulgen's stain and periodic acid–Schiff stain was measured and analyzed using the Fairfield ploidy system (Fairfield Imaging, Kent, United Kingdom). The nuclei of at least 300 cells were measured, and the information was stored in a computerized folder, or "gallery," for each patient, and lymphocytes were included as internal controls.

Table 2.1 Clinical features of human oral squamous cell carcinomas from which the cell lines were derived [1]

Cell line	Age	Sex	Site[2]	Size	Nodal spread	Metastases	Pathology[3]	STNMP Grade[4]
H103	32	M	T	<20	-	-	W	I
H157	84	M	BM	20 – 40	+	-	W	II
H314	82	M	FOM	20 – 40	+	-	M	II
H357	74	M	T	<20	-	-	W	I
H376	40	F	FOM	20 – 40	+	-	W	III
H400	55	F	AP	20 – 40	-	-	M	II
H413	53	F	BM	20 – 40	-	-	M	II

[1] Prime *et al.* (1990)

[2] Tongue (T), Buccal mucosa (BM), Floor of the mouth (FOM), Alveolar process (AP)

[3] Well differentiated (W), Moderately differentiated (M)

[4] STNMP grading is a prognostic indicator for oral squamous cell carcinoma with 51.5%, 40.7%, 21.6% and 8.3% 5 year survival for patients with a stage I, II, III or IV tumours, respectively (Langdon, 1995)

Table 2.2 Characteristics of the human oral squamous cell carcinoma cell lines

Cell line	Differentiation[1]	Tumorigenicity (orthotopic)[2]	p53 mutation [3]	CDKN2A[4]		Modal chromosome number[5]
				Mutation	Methylation	
H103	M	T	244 (7) G –T	p16 R58X(nonsense)	-	41
H157	M	NT	306 (8) G – A	p16 R80X(nonsense)	-	88
H314	P	T	176 (5) G –T, 373 (11) A – G	p16 205delG (premature stop codon downstream)	-	72
H357	W	NT	110 (4) G – A	p16R58X(nonsense), 3' UTR base 500 C> G	-	83
H376	M	NT	266 (8) G –T	wt	+	75
H400	M	T	283 (8) C – G	wt	+	82-91
H413	W	T	68 (4) G –T	wt	+	76

[1] Sugiyama *et al.*, 1993; Prime *et al.*, 1994; Well differentiated (W), moderately differentiated (M), poorly differentiated (P).

[2] Prime *et al.*, 2004; tumorigenic (T), non-tumorigenic (NT).

[3]Yeudall *et al.*, 1995.

[4] Wu *et al.*,1999.; wild type (wt)

[5] Patel *et al.*, 1993.

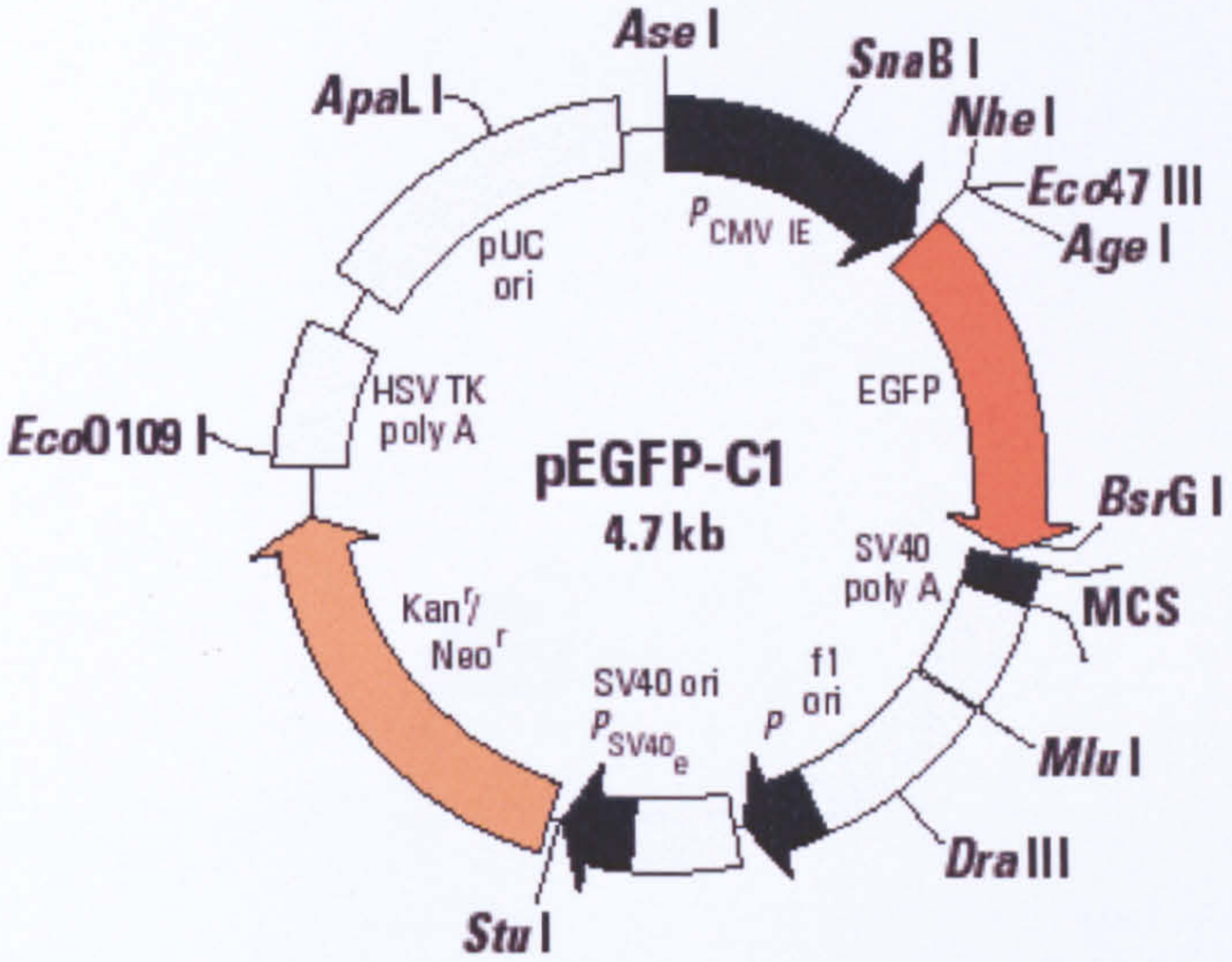

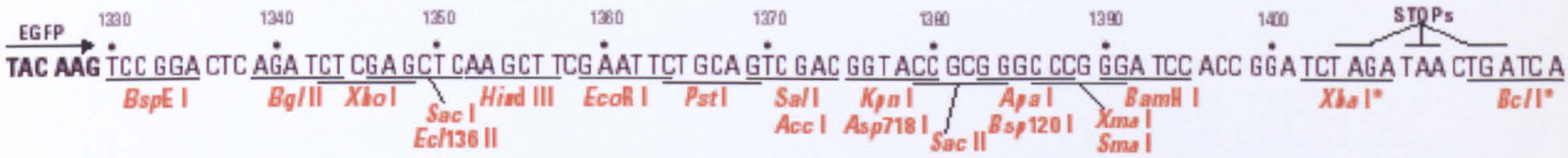

Figure 2.1 Mammalian expression vector pEGFP-C1

The CETN2 gene was inserted between the XhoI and XmaI site within the multiple cloning site of the plasmid.

CHAPTER THREE

THE ANALYSIS OF THE MITOTIC AND TETRAPLOIDY CHECKPOINTS IN HUMAN OSCC-DERIVED CELL LINES

3.1 INTRODUCTION

CIN and MIN are two mutually exclusive types of genetic instability, such that a tumour would have one abnormality or the other, but rarely both together (Lengaur *et al.*, 1997; 1998). CIN is characterised by an abnormal number of chromosomes, termed aneuploidy (Rajagopalan *et al.*, 2004), whilst MIN is characterised by a widespread alteration of microsatellite sequences (Yamasaki and Mironov, 2000) due to mutations in mismatch repair (MMR) genes (Buermeyer *et al.*, 1999). At least five human genes (hMSH2, hMSH6, hMLH1, hPMS1 and hPMS2) are known to participate in the MMR pathway but mutations in the hMLH1 and hMSH2 genes have been shown to account for the majority of mismatch repair defects (Jiricny and Lahti, 2000).

Previous work has showed that the H-series of OSCC-derived cell lines (H103, H157, H314, H357, H376, H400, H413; Prime *et al.*, 1990) exhibited alterations in chromosome numbers (Patel *et al.*, 1993), indicating that these cells were aneuploid and exhibit CIN. Therefore, these cell lines represent a unique model to determine whether defects in the chromosome segregation machinery could be the underlying cause of CIN in oral cancer. The MIN status of these cell lines, however, is not known.

Accumulating evidence suggests that defects in the chromosome segregation machinery such as the mitotic (Saeki *et al.*, 2002, Ouyang *et al.*, 2002, Wang *et al.*, 2002) and tetraploidy checkpoints (Andreassen *et al.*, 2001a) could play an important role in the development of aneuploidy and CIN. The mitotic checkpoint ensures the fidelity of chromosome segregation during cell division, whilst the tetraploidy checkpoint functions downstream of the mitotic checkpoint

and acts by recognising and inducing a cell cycle arrest in cells exiting mitosis with a tetraploid DNA content. There is a paucity of information, however, regarding the integrity of these checkpoints in oral cancer.

The aim of the present study, therefore, was to confirm that the H-series of the OSCC-derived cell lines express the hMLH1 and hMSH2 proteins and then to examine the fidelity of the mitotic checkpoint in the same series of cell lines. The study was extended to analyse the integrity of the tetraploidy checkpoint in those cell lines that exhibited an aberrant G2/M arrest during prolonged nocodazole treatment.

3.2 RESULTS

3.2.1 Basal expression of hMLH1 and hMSH2 proteins in human OSCC-derived cell lines

To analyse the status of the MMR pathway, the basal expression of the hMLH1 and hMSH2 proteins was analysed in the H-series of OSCC-derived cell lines.

Western blot analysis showed that all cell lines expressed both hMLH1 and hMSH2 (Figure 3.1). HCT116, a colorectal cancer cell line, was used as a control because it fails to express the hMLH1 protein, rendering it MMR deficient (Bardelli *et al.*, 2001).

3.2.2 Analysis of the mitotic checkpoint

3.2.2.1 Cell cycle analysis

To determine the status of the mitotic checkpoint in the OSCC-derived cell lines, the response of the cell lines following activation of the mitotic checkpoint was assessed by FACS. A human colorectal cancer cell line, HCT116, shown previously to have an intact mitotic checkpoint (Tighe *et al.*, 2001) was used as a control.

The mitotic checkpoint was activated by treating the cells with 0.2 μg/ml nocodazole. FACS analysis performed after 18 hours of nocodazole treatment examined the ability of the cells to arrest at G2/M and analysis after 36 hours of treatment showed whether the cells were able to maintain the G2/M arrest or if they proceeded to reduplicate their DNA following prolonged perturbation of the microtubule network

The FACS profile of diluent (DMSO) treated asynchronous control HCT116 cells exhibiting G0/G1 (diploid; 2N) and G2/M (tetraploid; 4N) peaks is shown in Figure 3.2A; a similar profile was observed in diluent treated cultures of all the other cell lines (data not shown). Treatment of the OSCC-derived cell lines and HCT116 with nocodazole for 18 hours resulted in the majority of cells (62%-100%) arresting at G2/M, indicating an intact mitotic checkpoint (Figure 3.2B, Figure 3.3). An additional G0/G1 arrest was also seen in H157 (24.5%) and H413 (6.3%).

Following 36 hours of nocodazole treatment, the majority of cells (48%-85%) in the H103, H157, H314, H400, H413 and HCT116 cell lines were arrested at

G2/M with a tetraploid DNA content (Figure 3.2C, Figure 3.4). H157 also continued to maintain a high proportion of cells at G0/G1 (25%) after 36 hours of treatment (data not shown). By contrast, H357 and H376 exhibited only a low percentage (19%-34%) of cells arrested at G2/M.

Whilst only a small subpopulation (1.4%-7%) of H103, H157, H314, H400, H413 and HCT116 cells went on to reduplicate their DNA in the presence of nocodazole (Figure 3.2C, Figure 3.4), a substantial number of H357 and H376 cells (20% and 63%, respectively) showed evidence of DNA reduplication (Figure 3.4). The cell cycle analysis of H376 cells treated for 36 hours with nocodazole is shown in Figure 3.5.

3.2.2.2 Mitotic indices

To confirm the status of the mitotic checkpoint in the OSCC-derived cell lines, the mitotic index (percentage of cells in mitosis) of cells treated with nocodazole for 12–42 hours was determined by immunofluorescence analysis using an anti-phospho-histone H3 antibody. The majority of the diluent treated asynchronous control HCT116 cells lacked phospho-histone H3 staining (Figure 3.6A), whilst the majority of nocodazole treated cells had condensed chromatin positive for phospho-histone H3, indicating cells in mitosis (Figure 3.6B). Similar staining patterns for phospho-histone H3 were seen in all the OSCC-derived cell lines before and after treatment with nocodazole (data not shown).

With the exception of H376, the greatest number of mitotic cells was observed between 18-24 hours in all cell lines following nocodazole treatment (Figure 3.7). The number of mitotic cells fell to basal levels after 36-42 hours. The drop

in the percentage of cells in mitosis after 24 hours indicates the exit of the mitotic cells to G0/G1. H376 exhibited a similar trend, albeit at a faster rate.

The increase in the percentage of mitotic cells observed between 18-24 hours of nocodazole treatment suggests a transient mitotic arrest, indicating a functional mitotic checkpoint. H357 and H400 cells behaved in a similar way to HCT116 controls with approximately 70% of cells in mitosis after 18 hours treatment with nocodazole, indicating an intact mitotic checkpoint. By contrast, only 37%-55% of H103, H157, H314 and H413 cells and 51.4% of H376 cells were in mitosis after 18 and 12 hours of incubation, respectively, suggesting that the mitotic checkpoint might be compromised in these cell lines.

3.2.3 Tetraploidy checkpoint analysis

The high level of DNA reduplication observed in H357 and H376 following 36 hours of nocodazole treatment suggests a defective post-mitotic or tetraploidy checkpoint. To test this hypothesis, the ability of H357 and H376 cells to arrest with a tetraploid DNA content following transient exposure to dihydrocytochalasin B (DCB), an agent known to inhibit cytokinesis, was analysed by FACS. H400, which exhibited a minimal amount of reduplication, was used as a control.

Asynchronous cultures of H400 exhibited a cell cycle profile corresponding to the G0/G1, S and G2/M phases of the cell cycle (Figure 3.8A). The cells were first pre-synchronized with 0.04 μg/ml nocodazole for 18 hours prior to treatment with DCB. Nocodazole treated cells accumulated at the G2/M phase with a 4N DNA content and were able to exit the arrest and begin cycling within

5 hours of release into drug free medium (Figure 3.8B). The nocodazole pre-synchronised cells were harvested through 'mitotic shakeoff' and replated in 10 μM DCB for 5 hours. A G2/M arrest was seen following DCB treatment of nocodazole pre-synchronised cells, which taken together with the observation that the nocodazole pre-synchronised cells began cycling following release into drug free medium, shows that the DCB treatment is responsible for the arrest (Figure 3.8C). After 5 hours exposure to DCB, the cells were then released into drug free medium and harvested after 18 hours for FACS analysis. H400 was able to maintain the arrest induced by DCB after 18 hours of release into drug free medium (Figure 3.8D).

By contrast, although H357 and H376 exhibited a G2/M arrest following treatment with DCB, within 18 hours of release into drug free medium, H357 cells exhibited a tendency towards emergence of a polyploidy cell population as seen through the progression of cells arrested at G2/M into S-phase (Figure 3.9A) whilst H376 already exhibited an 8N population resulting from DNA reduplication (Figure 3.9B). However, a polyploid population of cells was observed in H357, H376 and H400, 36 hours after release into drug free medium (data not shown).

3.3 SUMMARY

This study initially examined the expression of the hMLH1 and hMSH2 proteins in the H-series of OSCC-derived cell lines in order to determine the status of the MMR pathway and to exclude the presence of MIN in these cell lines. All of the cell lines expressed both hMLH1 and hMSH2 proteins indicating that they have an intact MMR pathway and, therefore, are likely to be microsatellite stable.

Taken together with the previously reported chromosome number alterations in the H-series (Patel *et al.*, 1993), the results show that the cell lines used in the present study exhibit CIN and not MIN.

The study was then extended to examine the status of the mitotic checkpoint in the same series of cell lines. A G2/M arrest was observed in all cell lines following 18 hours of nocodazole treatment, as assessed by FACS, indicating an intact mitotic checkpoint. Examination of the mitotic indices after 18 hours of nocodazole treatment showed that H357 and H400 behaved in a similar way to control HCT116 cells with approximately 70% of cells in mitosis, whilst a lower percentage of cells in mitosis (37%-55%) was seen in the remaining cell lines. Taken together, the results indicate that the mitotic checkpoint is intact in all the cell lines but it is possible that the function of the checkpoint is attenuated in five of seven cell lines.

Examination of the cell cycle after 18 hours release from DCB treatment revealed a G2/M arrest in H400 cells indicating that the tetraploidy checkpoint was intact. By contrast, the S-phase progression observed in H357 and the emergence of a polyploid cell population in H376 suggests that the tetraploidy checkpoint was defective in these cell lines. However, the fact that polyploid cell populations emerged in all cell lines after 36 hours release from DCB treatment suggests that the checkpoint could be defective in all cell lines. This may be due to the mutations in the p53 gene harboured by these cells and it has been suggested that wild-type p53 is important for maintenance of the tetraploidy checkpoint.

A: hMLH1

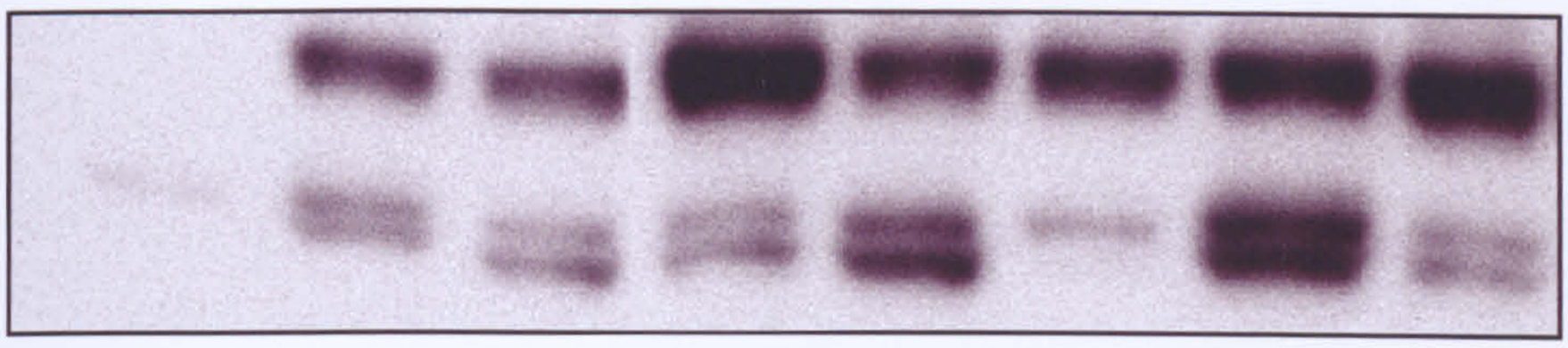

HCT116 H103 H157 H314 H357 H376 H400 H413

B: hMSH2

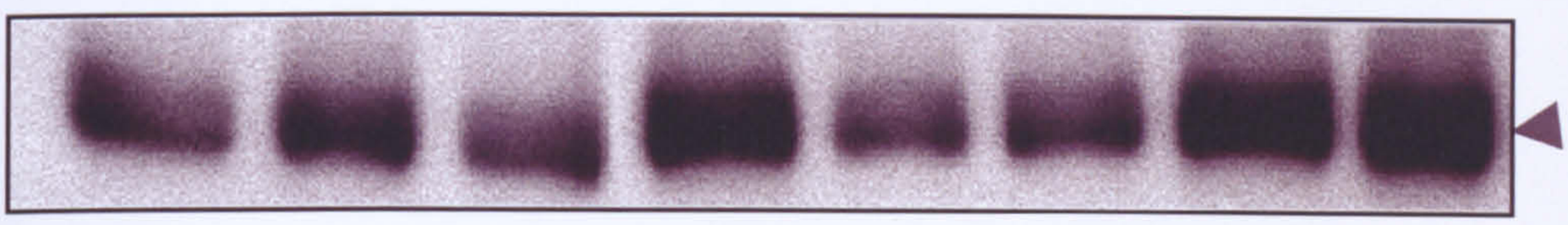

HCT116 H103 H157 H314 H357 H376 H400 H413

Figure 3.1 Western blot analysis of the expression of hMLH1 and hMSH2 proteins

Expression of both hMLH1 and hMSH2 proteins in all cell lines of the H-series indicates an intact MMR pathway. Proteins were detected using anti-hMLH1 and anti-hMSH2 antibodies. The additional bands on the hMLH1 blot are non-specific and were normally present during the analyses. HCT116, which fails to express the hMLH1 was used as a control.

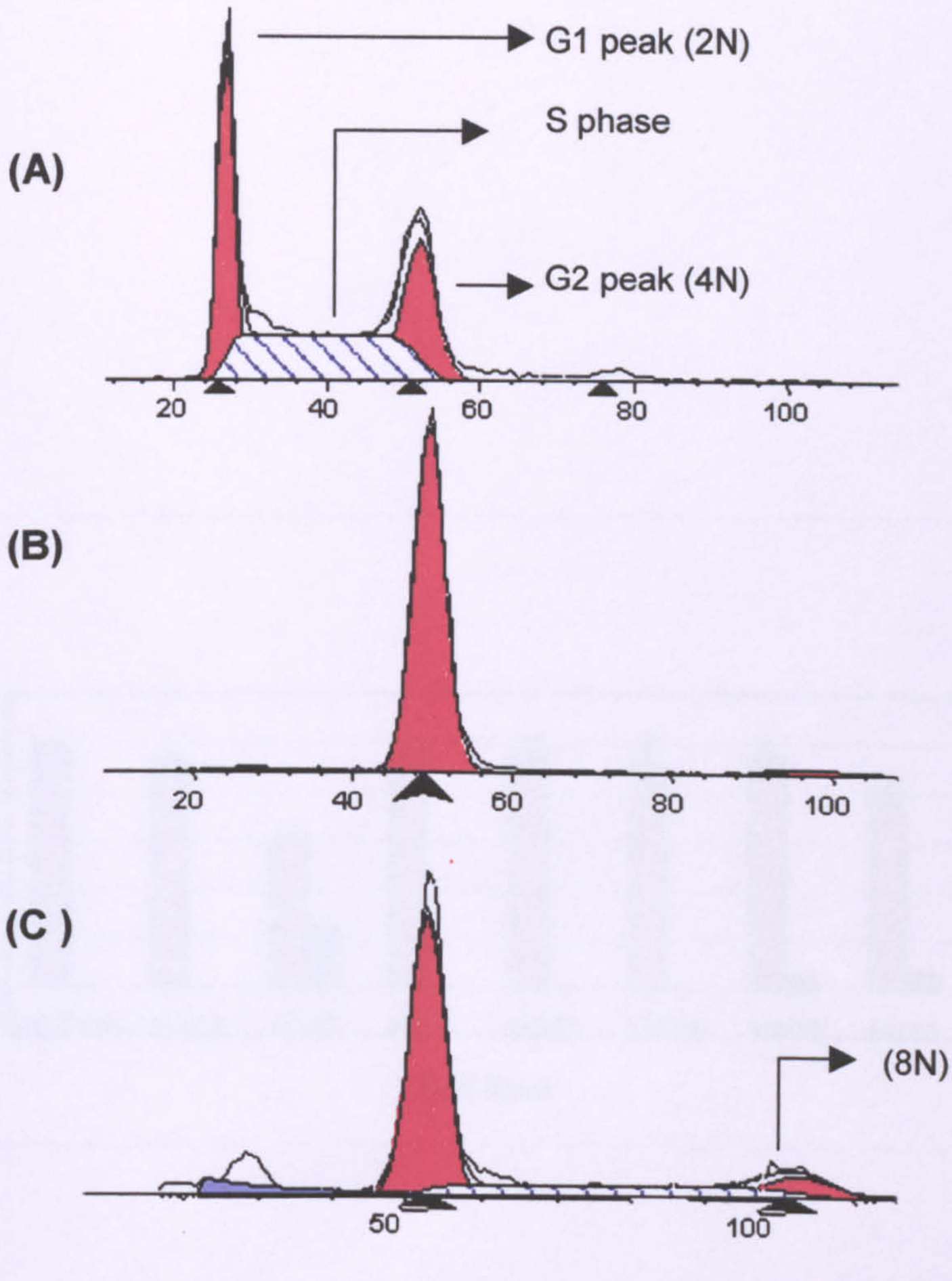

Figure 3.2 Cell cycle analysis of HCT116 cells indicating an intact mitotic checkpoint

(A) Diluent (DMSO) treated control HCT116 cells exhibited G0/G1, G2 and S phase peaks, indicating an asynchronous replicating population of cells. (B) Cells treated in 0.2 μg/ml nocodazole for 18 hours arrested at the mitotic phase with a large G2/M peak, indicating an intact mitotic checkpoint. (C) G2/M phase arrest was maintained after 36 hours in nocodazole with a small population of cells (~5%) reduplicating their DNA.

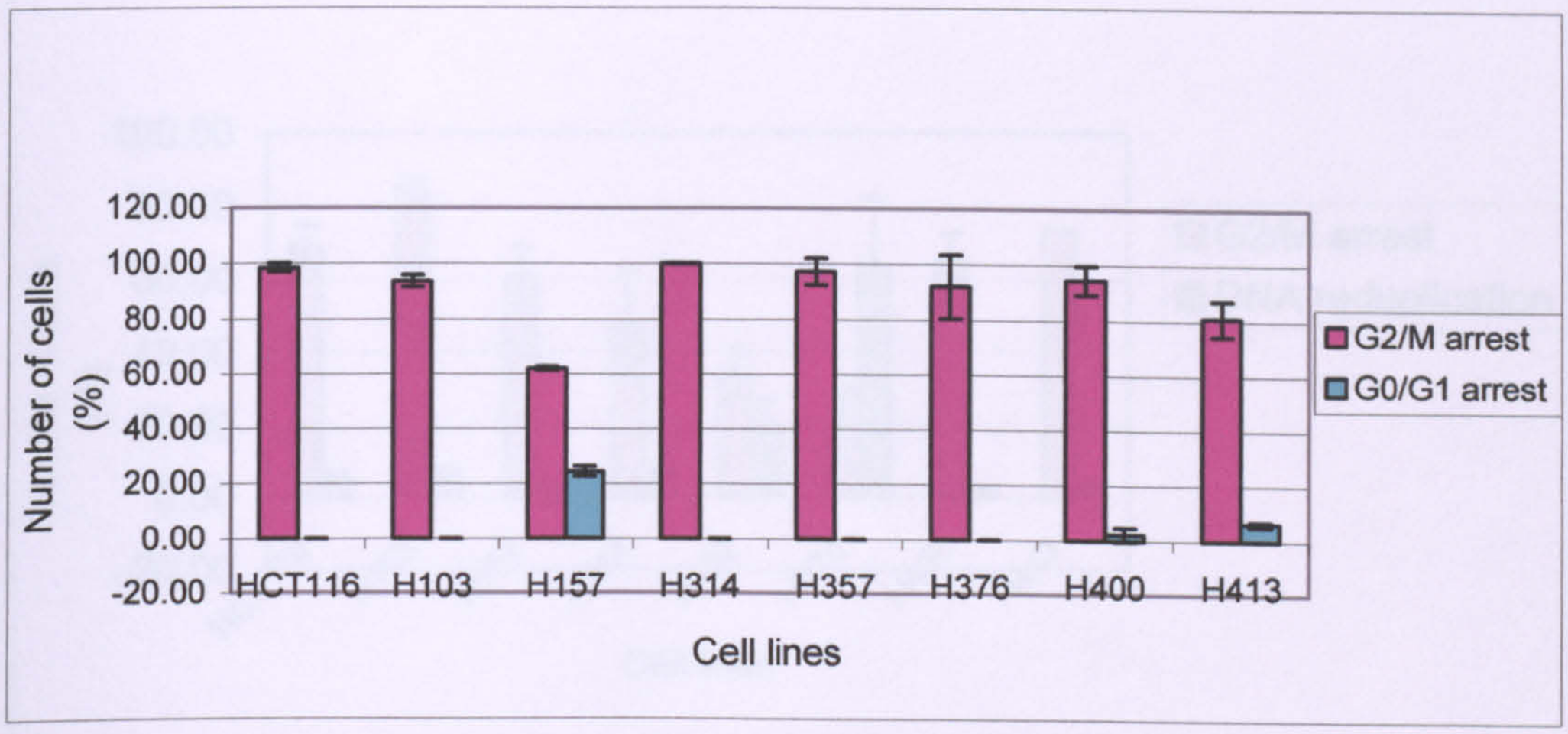

Figure 3.3 Cell cycle analysis of the H-series of OSCC-derived cell lines exhibiting G0/G1 and G2/M arrest following 18 hours incubation in 0.2 μg/ml nocodazole.

HCT116, known to have an intact mitotic checkpoint was used as a positive control. All cell lines of the H-series, and the HCT116 control cells exhibited a high percentage of G2/M arrest, indicating an intact mitotic checkpoint. Data points reflect the means (± standard deviation) of two separate experiments.

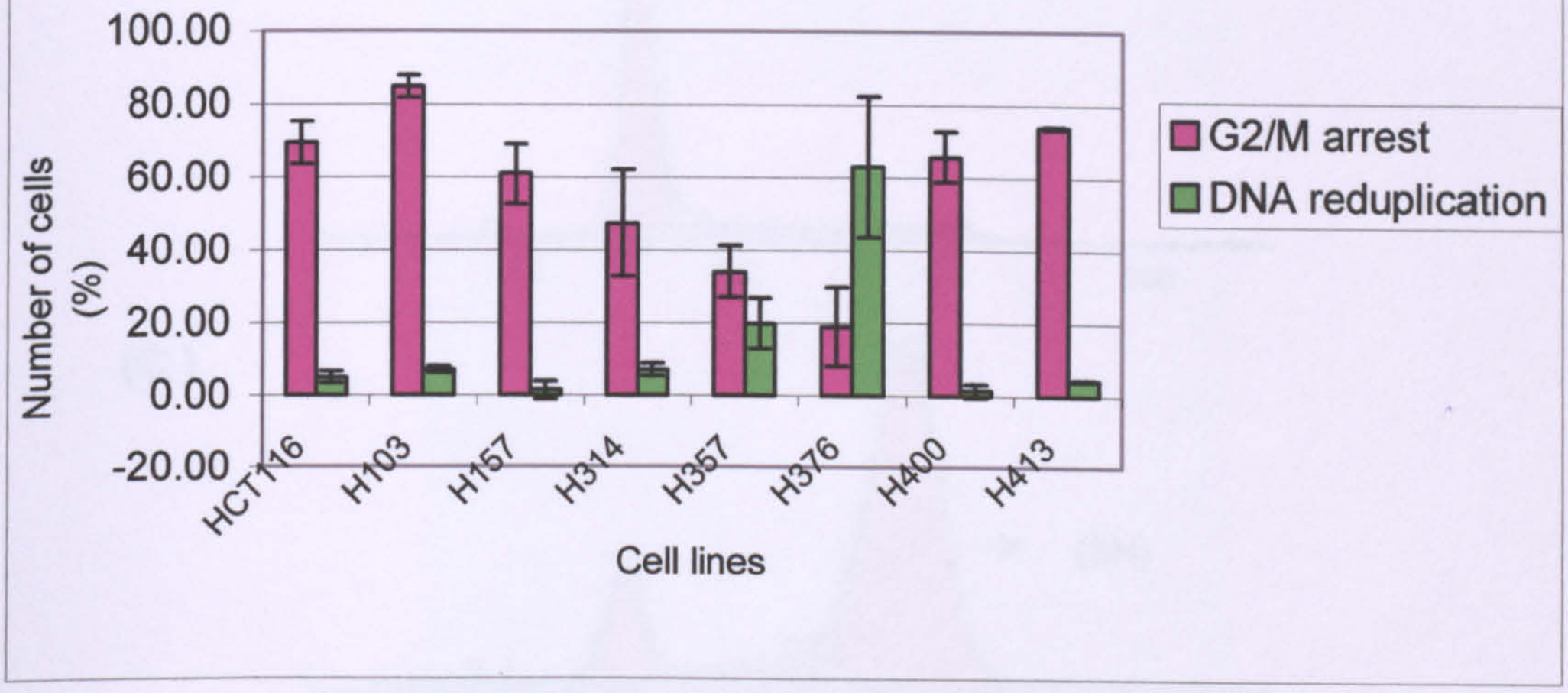

Figure 3.4 Cell cycle analysis of the H-series of OSCC-derived cell lines exhibiting G2/M arrest and DNA reduplication following 36 hours incubation in 0.2 μg/ml nocodazole.

All OSCC-derived cell lines and HCT116 exhibited a G2/M arrest and showed evidence of DNA reduplication in a varying proportion of cells. H357 and H376 exhibited DNA reduplication in a high percentage of cells relative to the other cell lines, indicating an inability to maintain arrest following prolonged nocodazole treatment. Data points reflect the means (± standard deviation) of two separate experiments.

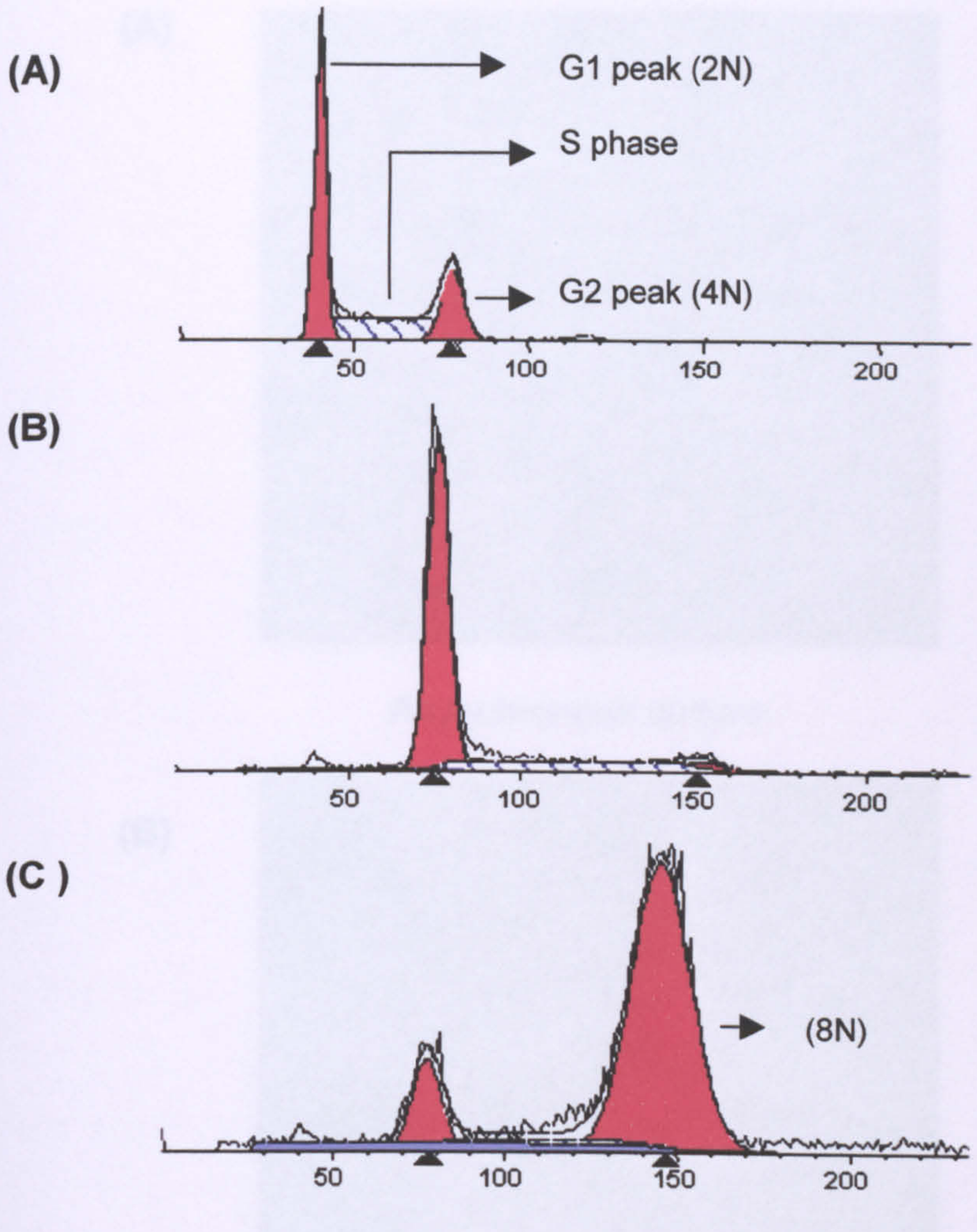

Figure 3.5 Cell cycle analysis of H376 cells exhibiting DNA reduplication following 36 hours incubation in 0.2 μg/ml nocodazole

(A) Diluent (DMSO) treated control cells exhibited G0/G1, G2 and S phase peaks, indicating an asynchronous replicating population of cells. (B) Following 18 hours of nocodazole treatment, the majority of cells arrested at G2/M, indicating an intact mitotic checkpoint. (C)The majority of the 4N cells have reduplicated their DNA, resulting in an 8N peak after 36 hours in nocodazole, indicating an inability to maintain prolonged arrest in nocodazole.

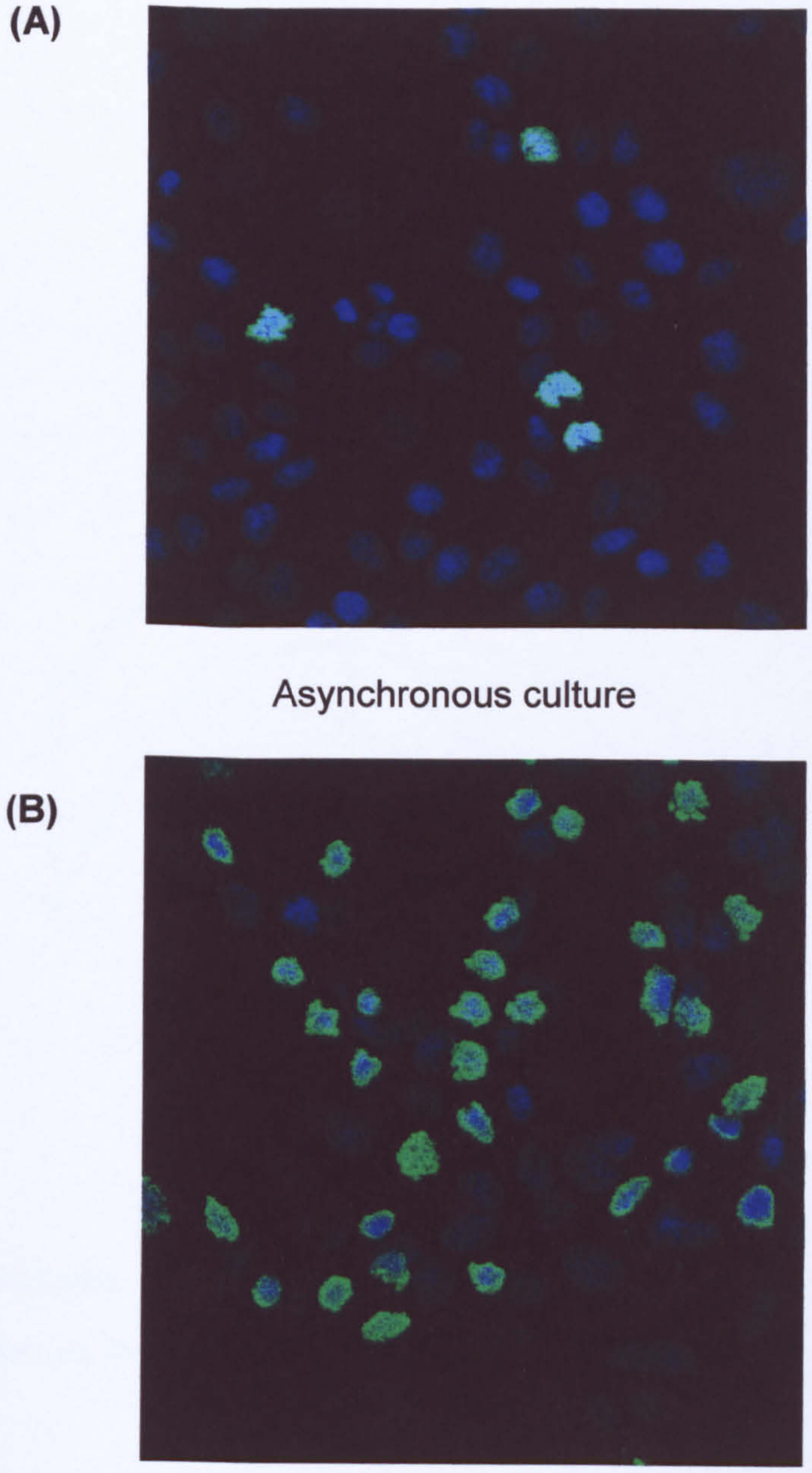

Figure 3.6 Immunofluorescence image of anti-phospho histone H3 stained HCT116 cells.

Cells were stained with anti-phospho histone H3 primary and FITC conjugated secondary antibodies, which detected cells with condensed chromatin (green) characteristic of cells in the mitotic phase. The nuclei were counterstained with DAPI (blue). An increase in the number of mitotic cells with condensed chromatin was observed in (B) nocodazole treated cells compared to (A) diluent treated control cells.

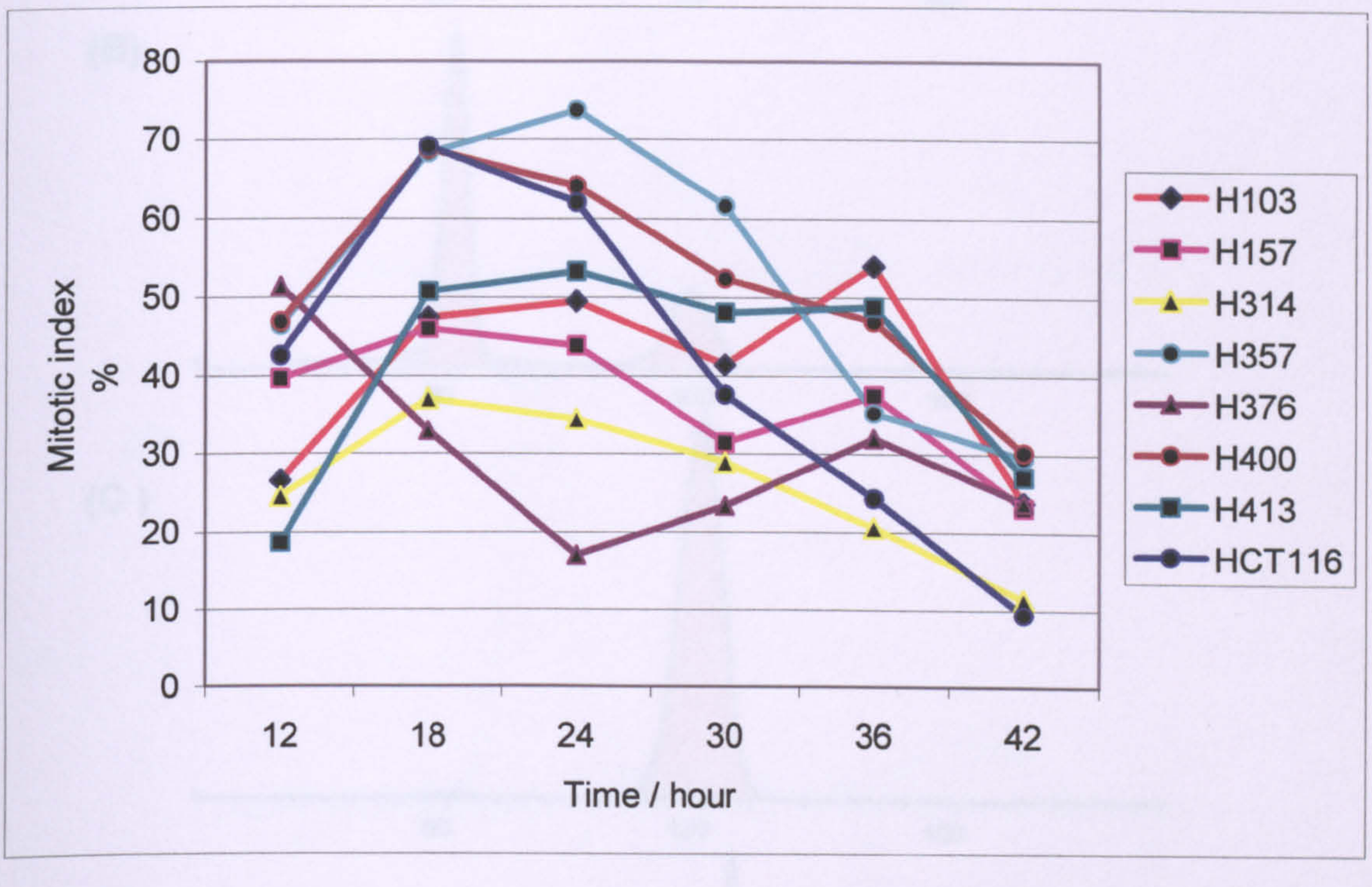

Figure 3.7 Mitotic index of the H-series of OSCC-derived cell lines during incubation in 0.2 μg/ml nocodazole.

Similar to HCT116, H357 and H400 exhibited a peak in the percentage of mitotic cells between 18-24 hours of incubation in 0.2 μg/ml nocodazole, demonstrating a transient cell cycle arrest following microtubule perturbation. A similar peak with lower percentage of cells in H103, H157, H314, H376 and H413 suggests a compromised mitotic checkpoint in these cell lines. H376 exhibited a similar trend, at a faster rate. The decline in the percentage of mitotic cells after 24 hours indicates exit of cells from mitosis into the G0/G1 phase.

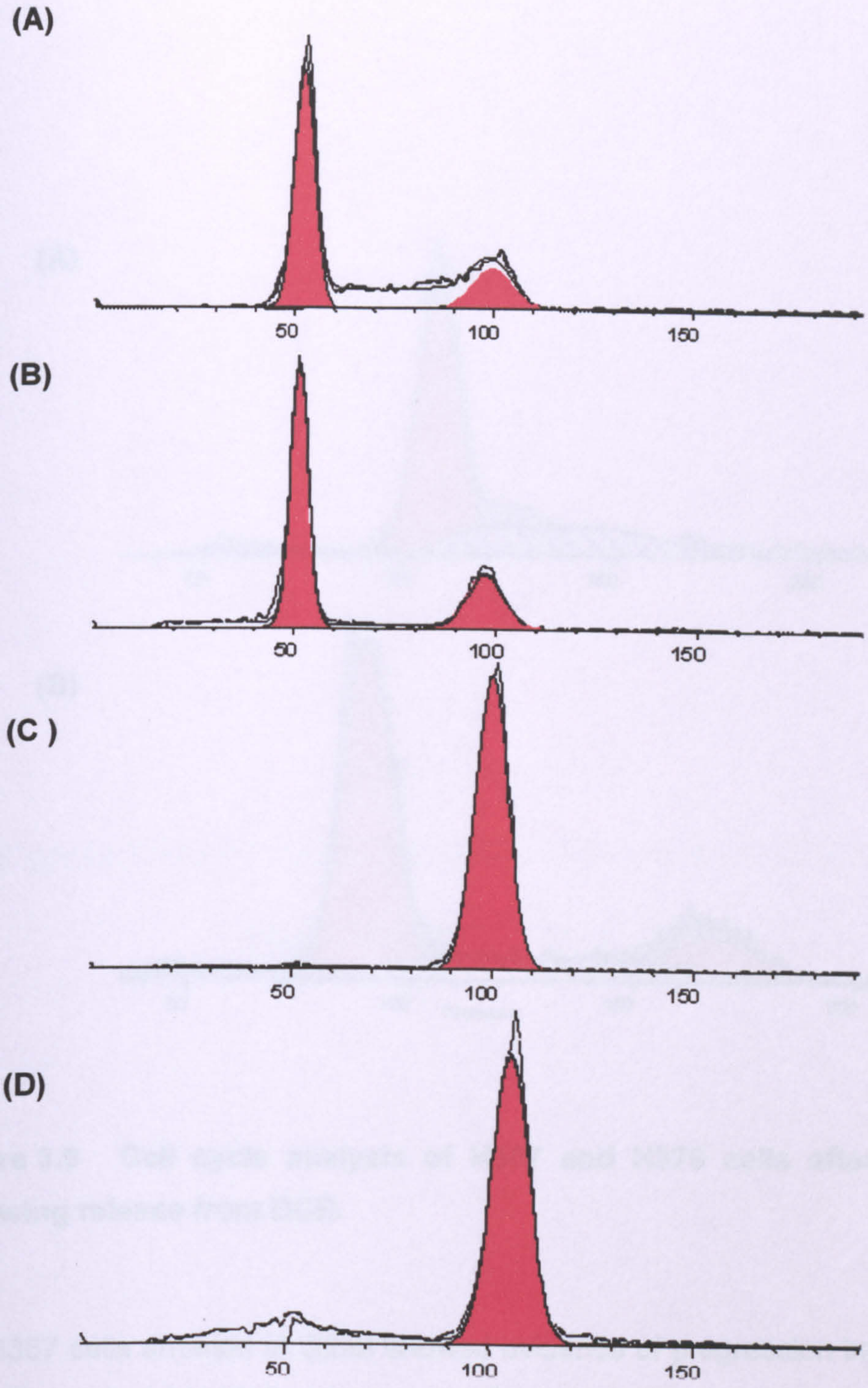

Figure 3.8 Cell cycle analysis of H400 cells following pre-synchronization with nocodazole and DCB treatment

(A) Asynchronous H400 cells exhibited 2N, 4N and S-phase peaks. (B) Nocodazole pre-synchronised cells were able to exit G2/M arrest within 5 hours of release into drug free medium. (C) Transient 5 hours incubation of nocodazole pre-synchronised cells in 10 μM DCB induced a G2/M arrest. (D) Cells maintained G2/M arrest 18 hours after release from DCB into drug free medium.

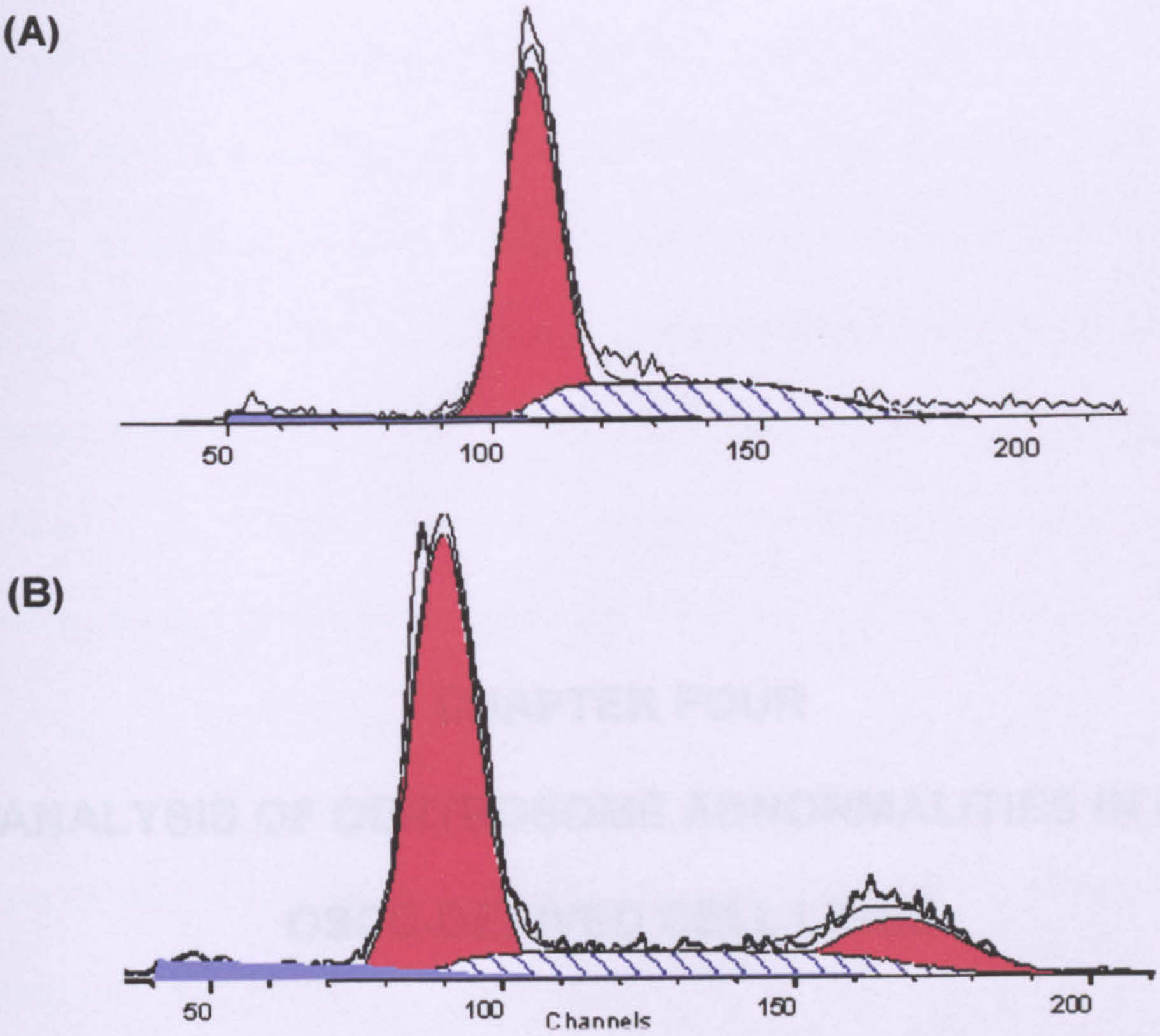

Figure 3.9 Cell cycle analysis of H357 and H376 cells after 18 hours following release from DCB.

(A) H357 cells arrested at G2/M showed evidence of progression into S-phase, exhibiting a trend towards emergence of a polyploid population of cells (B) 8N cells emerged in the H376 cell line within 18 hours of release from DCB into drug free medium.

CHAPTER FOUR

THE ANALYSIS OF CENTROSOME ABNORMALITIES IN HUMAN OSCC-DERIVED CELL LINES

4.1 *INTRODUCTION*

The result of Chapter 3 demonstrated that the H-series of human OSCC-derived cell lines expressed hMLH1 and hMSH2, which confirmed earlier cytogenetic data to indicate that the cells exhibited CIN. Analysis of the mitotic checkpoint revealed that this checkpoint was functional in all cell lines although its function may be attenuated in five of seven cell lines. A compromised mitotic checkpoint could allow low levels of chromosome missegregation, but is unlikely to be responsible for the marked cytogenetic abnormalities seen in these cell lines (Patel *et al.*, 1993). It is likely, therefore, that alternative mechanisms are responsible for the CIN in these cell lines.

The centrosome is a part of the chromosome segregation machinery which functions to nucleate and organise the mitotic spindle for equal segregation of chromosomes during mitosis. Centrosome abnormalities have been reported in cell lines derived from pancreatic (Sato *et al.*, 2001), colon (Ghadimi *et al.*, 2000) and breast cancers (D'Assoro *et al.*, 2002). The common centrosome abnormalities observed in these cells include supernumerary centrioles, centrosome of larger diameter, mislocalised centrosomes and compromised function. These abnormalities are suggested to predispose cells to multipolar mitosis, resulting in erroneous chromosome segregation and CIN (Sato *et al.*, 2001) and interestingly, centrosomal abnormalities have been observed exclusively in aneuploid cell lines but not in chromosomally stable MIN lines (Ghadimi *et al.*, 2000). There is a paucity of information, however, on the occurrence of centrosomal abnormalities in oral cancer.

The purpose of the present study was to i) determine if defects of the centrosome, in terms of number, size and localization, occurred in the H-series of OSCC-derived cell lines and ii) to evaluate centrosome function in these cell lines by examining the capacity of the centrosomes to nucleate microtubules following microtubule depolymerization. The study was then extended to examine the stability of centrosomes in a cloned population of H413 cells because parental H413 cells exhibited a high level of centrosome abnormalities.

4.2 RESULTS

4.2.1 Centrosome identification and evaluation criteria

Centrosomes were visualised through co-localization of immunofluorescence staining of two different antibodies directed against intrinsic components of the centrosome, namely γ-tubulin and pericentrin. Both pericentrin and γ-tubulin are located within the pericentriolar material (PCM) surrounding the centrosome; in normal human oral keratinocytes, centrosomes appeared as one or two punctate structures adjacent to the nucleus (Figure 4.1).

When analysing the cell lines, cells exhibiting one or two centrosomes were considered to be normal, whilst cells exhibiting more than two centrosomes were considered to have centrosome hyperamplification. The presence of abnormalities in centrosome morphology and localization were qualitatively determined through comparison between centrosomes of normal human oral keratinocytes and the tumour cells or with populations of cells within the tumour cell lines exhibiting normal centrosome morphology and number.

4.2.2 Analysis of centrosome abnormalities in human OSCC-derived cell lines

The percentage of cells exhibiting more than two centrosomes in the human OSCC-derived cell lines, human normal oral keratinocytes and the control MIN (HCT116) and CIN (CaCo2) cell lines is shown in Table 4.1.

Centrosome analysis of the chromosomally stable control cell line, HCT116 (MIN and near diploid), revealed a pattern indistinguishable from normal human oral keratinocytes. By contrast, CaCo2, the aneuploid control CIN cell line, exhibited centrosome hyperamplification in a high percentage of cells (23.81%). Similarly, five of the seven OSCC-derived CIN lines (H103, H157, H314, H400 and H413) exhibited alterations in centrosome number, with H103 and H413 showing the highest levels of centrosome hyperamplification (12.5% and 18.8%, respectively. 3-14 centrosomes per nuclei were observed in a subpopulation of cells in each cell line and up to 22 centrosomes per nuclei were observed in a subpopulation of H103 cells (Figure 4.2A,B). Some of the supernumerary centrosomes were detached from the nucleus and many of the supernumerary centrosomes were heterogeneous in size (Figure 4.2C). Further, dispersed pericentrin staining that did not co-localise with γ-tubulin was observed in some cells with centrosome hyperamplification (data not shown). Multipolar mitoses were frequently observed in H103 and H413, cell lines with a high degree of centrosome hyperamplification. Although infrequent, multiple centrosomes were seen to cluster at the spindle poles in an attempt to create a bipolar spindle (data not shown). The centrosome profile of the remaining OSCC-derived cell lines, H357 and H376, was similar to that of normal human oral keratinocytes.

4.2.3 Analysis of centrosome function in human OSCC-derived cell lines

To examine centrosome function in the cell lines, the microtubule nucleation capacity of the centrosomes was evaluated in terms of their ability to nucleate microtubules from the endogenous pool of cytoplasmic α and β tubulin, following nocodazole induced microtubule depolymerization. Microtubule nucleation was observed as aster formation at the nuclear periphery after release from nocodazole. The nucleation capacity of the centrosomes in the H-series of OSCC-derived and the control cell lines is shown in Table 4.1.

The nucleation capacity of the control cell lines HCT116 and CaCo2 was similar, as demonstrated by aster formation in the majority of their cells (95.28% and 76.36%, respectively) by 2 minutes after release from nocodazole (Figure 4.3, Table 4.1). A varied response was observed amongst the OSCC-derived CIN lines, with 18.45% - 82.35% of cells nucleating microtubules.

No clear association was observed between the centrosome hyperamplification status and the ability of the centrosomes to nucleate microtubules after 2 minutes release from nocodazole. For example, H413 and H376 exhibiting high (18.8 %) and low (0.4%) centrosome hyperamplification showed aster formation in the majority of cells (82.35% and 75.23%, respectively), whilst the remaining cell lines exhibited asters formation in only 18.45%-60.4% cells by 2 minutes following release from nocodazole (Figure 4.4A-C). Excessive microtubule nucleation in H413 cells (Figure 4.4D) and unorganised microtubule network formation in H357 cells were observed following 2 minutes release from nocodazole.

Dual staining of the microtubule-organizing centres with antibodies against α-tubulin and pericentrin showed that microtubule nucleation was invariably initiated from one or two centrosomes, suggesting that not all of the numerous centrosomes in cells with centrosomal hyperamplification are functional (data not shown). All cell lines fully recovered their tubulin network after 30 minutes release from nocodazole (Figure 4.3C, Figure 4.4C).

4.2.4 Analysis of centrosome stability in the H413 OSCC-derived cell line exhibiting high centrosome abnormalities.

To examine the stability of centrosome abnormalities, the ability of a cloned population of cells from a cell line exhibiting centrosome hyperamplification, to maintain a stable centrosome number was investigated. The H413 cell line exhibiting the highest percentage of centrosomal hyperamplification was selected. Briefly, the centrosome was labelled with EGFP following transfection of cells with human centrin-2 (CETN2) cDNA, cloned in-frame into the C-terminal enhanced green fluorescent protein vector (EGFP). Stable clones were obtained and the localization of CETN2 to the centrosome was confirmed by co-localization of γ-tubulin staining through immunofluorescence, as both CETN2 and γ-tubulin are intrinsic components of the centrosome (Figure 4.5). A total of three H413 clones expressing CETN2-EGFP and three untransfected H413 clones were analysed. Centrosomes in the untransfected clones were visualised by staining with antibodies against γ-tubulin and pericentrin (data not shown). Centrosomes were designated as stable if the expanded culture of the cloned population of cells maintained normal centrosome number and unstable if a mixture of cells with normal and multiple centrosomes were seen.

The majority of cells in both CETN2-EGFP tagged and untransfected H413 clones maintained normal centrosome number. However, a small sub-population of cells in all six clones, exhibited abnormalities in centrosome numbers and size. This suggests that centrosome duplication might have been uncoupled from the cell cycle in the H413 cells, thus giving rise to progenies with numerous centrosomes. A CETN2-EGFP tagged clone exhibiting the normal two (Figure 4.5A) and multiple centrioles (Figure 4.5B) is shown in Figure 4.5.

4.3 SUMMARY

This study examined centrosomal abnormalities in human OSCC-derived cell lines. By contrast to the control diploid and chromosomally stable MIN HCT116 cell line, centrosome number abnormalities were observed in five of seven OSCC-derived cell lines. Alterations in centrosome size, localization and overexpression of pericentriolar matrix protein were also detected. The prevalence of centrosome abnormalities in the cell lines suggests that it may be a widespread phenomenon in oral cancer.

Analysis of the capacity of cells to nucleate microtubules revealed that despite an initial delay in microtubule nucleation, the full recovery of the tubulin network after 30 minutes of release from nocodazole suggests that the centrosomes in all the OSCC-derived cell lines are fully functional. However, a possible impairment of other aspects of the centrosome was suggested by the excessive and unorganised microtubule nucleation observed in H413 and H357.

The analysis of cloned population of H413 cells transfected with CETN-EGFP showed that they are unable to maintain a stable centrosome number because a subpopulation of cells exhibited numerous centrosomes. This suggests that the morphologically normal centrosomes within cell lines exhibiting centrosome abnormalities might have an intrinsic centrosome instability that could result in further centrosome abnormalities with every cell division.

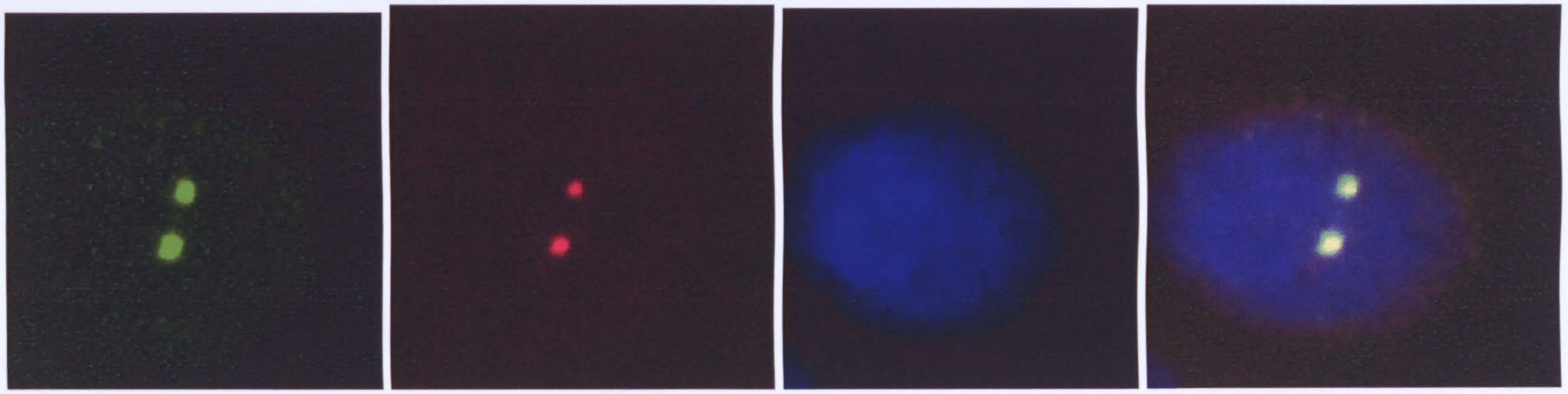

(A) (B) (C) (D)

Figure 4.1 Immunofluorescence detection of centrosomes in normal human oral keratinocytes

Centrosomes were detected after staining with (A) primary polyclonal rabbit anti-pericentrin antibody, (B) monoclonal mouse anti-gamma-tubulin antibodies and FITC and Cyc3 conjugated secondary antibody, respectively. (C) The nucleus was stained with DAPI. (D) An overlay of all staining resulted in co-localization of signals, confirming the specificity of centrosome staining. In normal oral keratinocytes, centrosomes appeared as point like structures and never exceeded two copies per cell. (x4000 magnification).

(A)

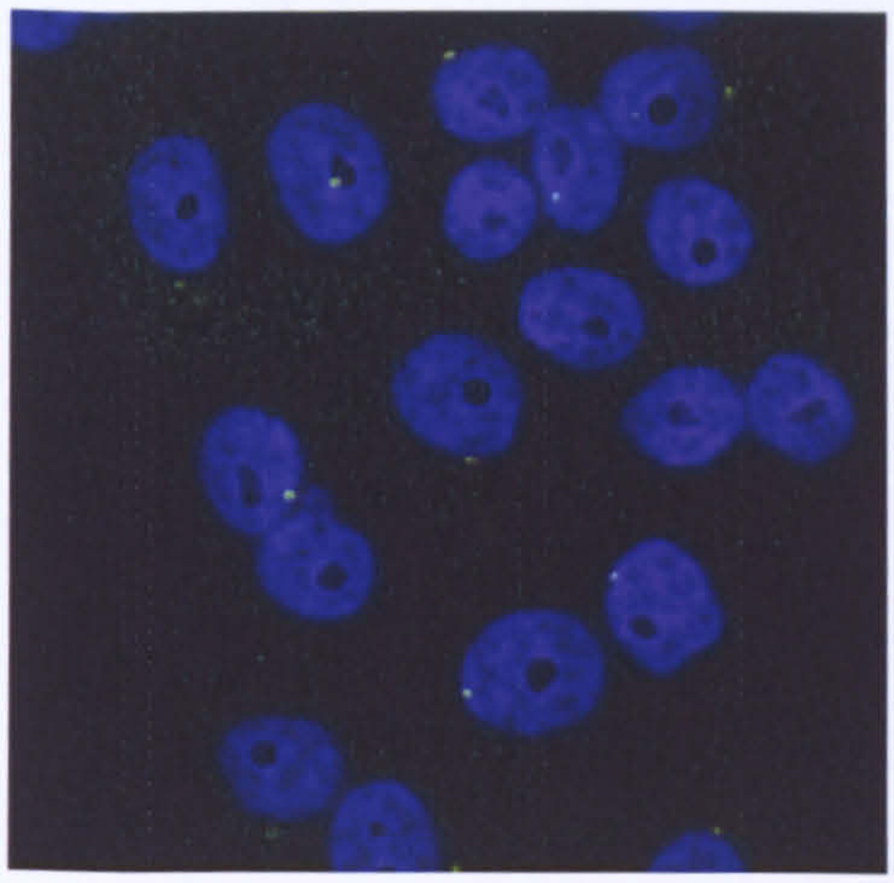

A subpopulation of H103 cells exhibiting normal numbers of centrosomes (one or two)

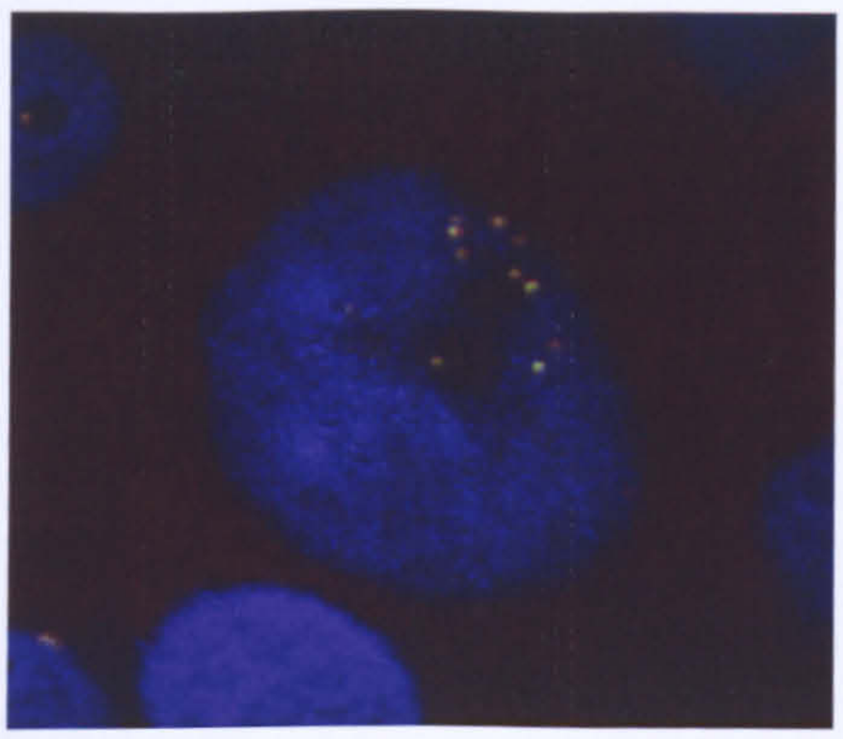

B

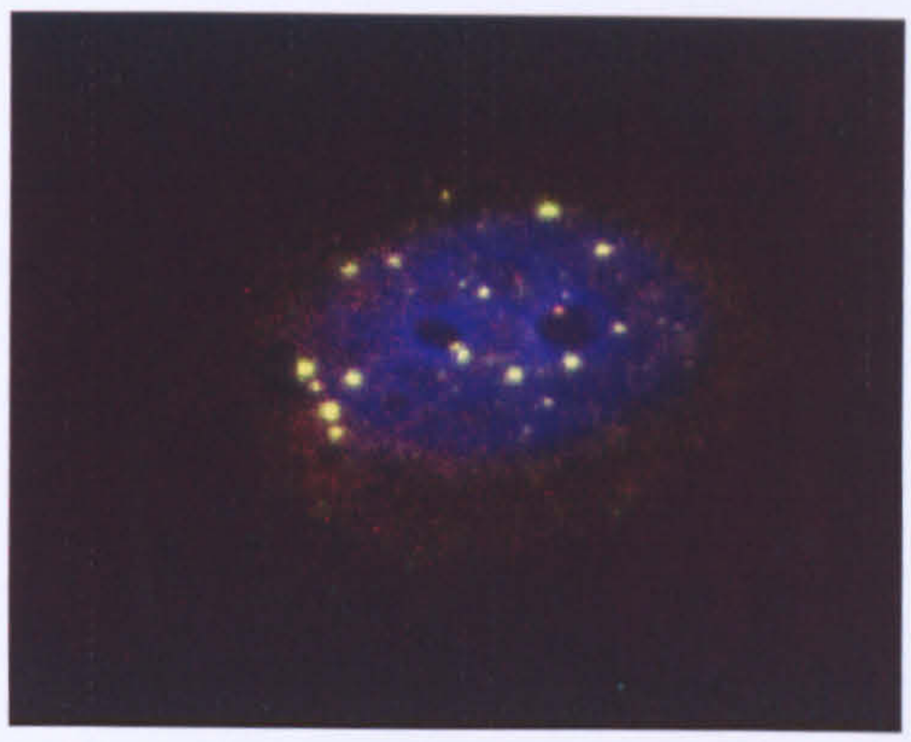

C

Numerical and morphological centrosomal aberrations in H103

Figure 4.2 Types of centrosome abnormalities observed in the aneuploid H103 cell line.

The cells of the H103 cell line exhibited various degree of centrosomal abnormalities. (A) A subpopulation of cells maintained normal centrosome numbers (x400), (B) while some cells exhibited up to 12 centrosomes per nuclei (x2000). (C) The excess centrosomes also exhibited heterogeneity in size.

Table 4.1 Degree of hyperamplification and microtubule nucleation function of the centrosomes in human OSCC-derived and control cell lines

Cell line	Hyperamplification [1]	Nucleation [2]
Normal keratinocytes	1.9	ND
HCT116	1.4	95.28
CaCo2	23.81	76.36
H103	12.5	51.96
H157	6.9	18.45
H314	3.2	60.40
H357	0	37.50
H376	0.4	75.23
H400	5.5	25.38
H413	18.8	82.35

[1]Hyperamplification is expressed as the percentage of cells with more than 2 centrosomes per cell in a minimum of 200 cells counted.

[2] Nucleation is expressed as percentage of cells capable of nucleating microtubule after 2 minutes release from 10 μg/ml nocodazole. A minimum of 200 cells was scored.

ND; not done

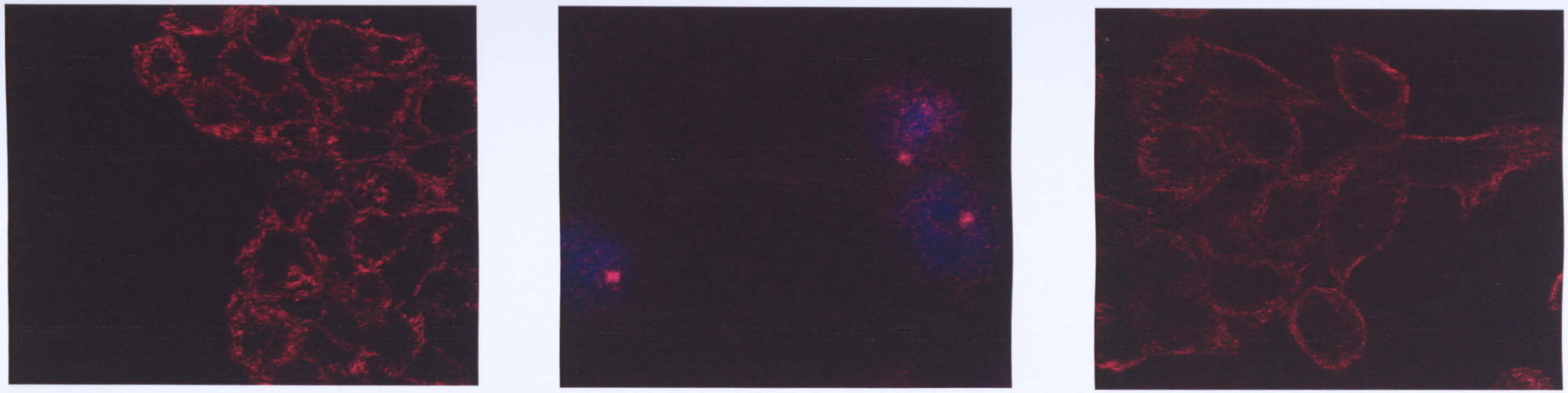

A B C

Figure 4.3 Time course of microtubule nucleation in HCT116 cells showing centrosomes nucleating microtubules after 2 minutes release from nocodazole induced microtubule depolymerization.

Microtubules were stained with primary anti-α tubulin and Cy3 conjugated secondary antibodies. (A) Homogeneous cytoplasmic tubulin network of untreated cells. (B) Cells nucleating microtubules after 2 minutes of release from nocodazole. The bright spots are the microtubule organizing centres or centrosomes showing aster formation. (C) Cells with fully recovered tubulin network within 30 minutes of release as indicated by the lack of aster formation and similar homogeneous staining as the untreated cells. (1000X magnification).

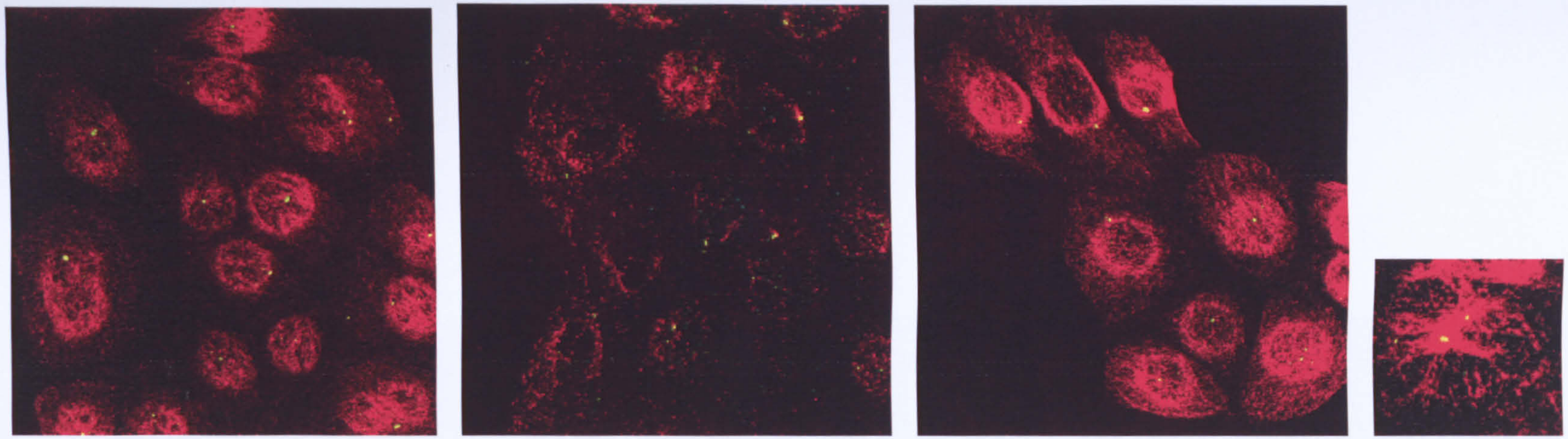

Figure 4.4 Time course of microtubule nucleation in H157 cells showing centrosomes lacking microtubule nucleation and a H413 cell showing excessive microtubule nucleation after 2 minutes release from nocodazole-induced microtubule depolymerization.

Microtubules were stained with primary anti-α tubulin and Cy3 conjugated secondary antibodies while the centrosome was stained with primary anti-pericentrin and FITC conjugated secondary antibodies. (A) Untreated cells exhibit evenly stained cytoplasmic microtubules (B) Cells with centrosomes lacking microtubule nucleation after 2 minutes of release from nocodazole. (C) Cells with fully recovered tubulin network within 30 minutes of release, as indicated by the lack of aster formation and similar homogeneous staining as the untreated cells. (1000x magnification). (D) Excessive microtubule nucleation in nucleation competent centrosomes observed in H413 cells after 2 minutes of release from nocodazole. (2000X magnification)

A

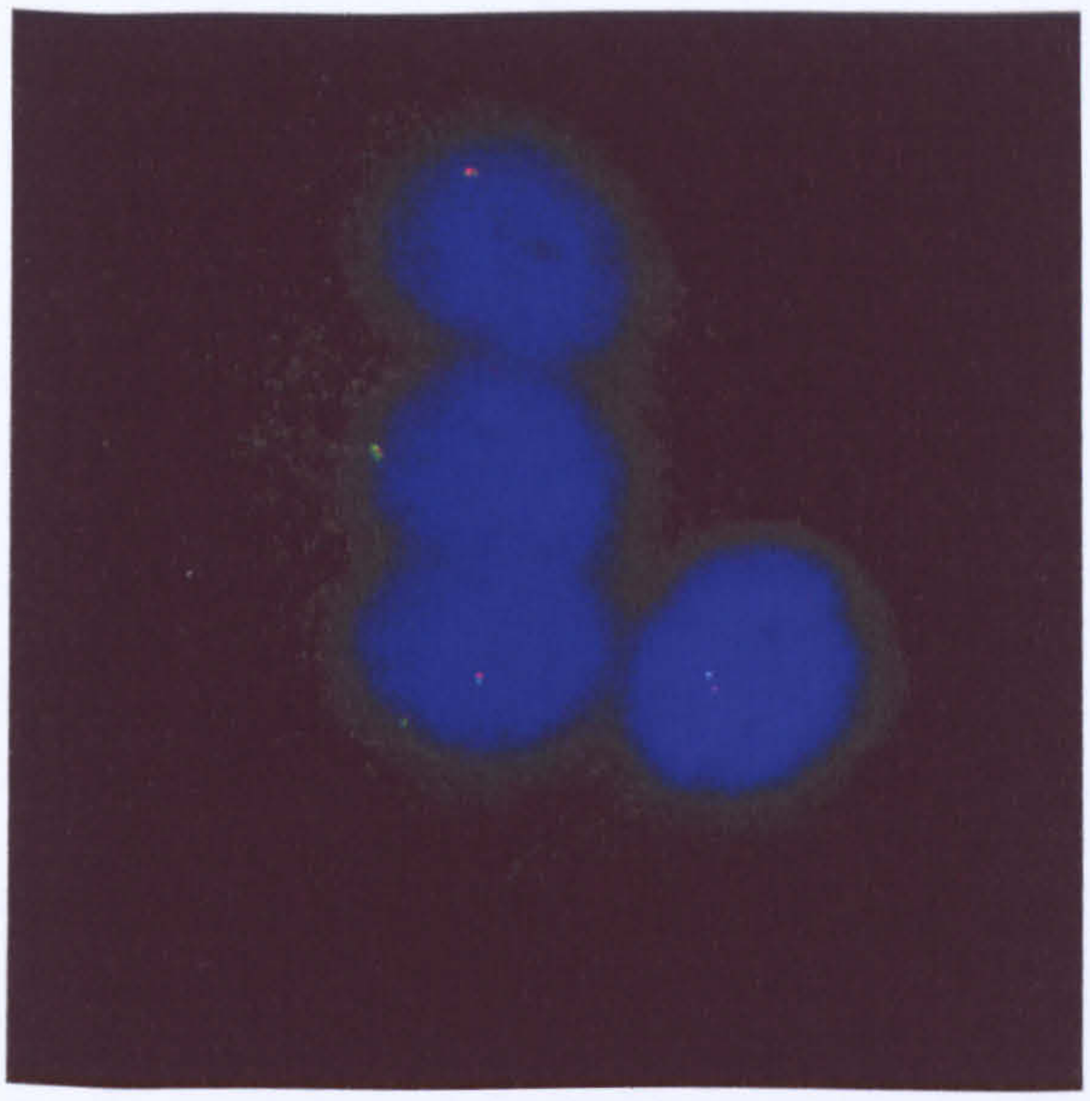

B

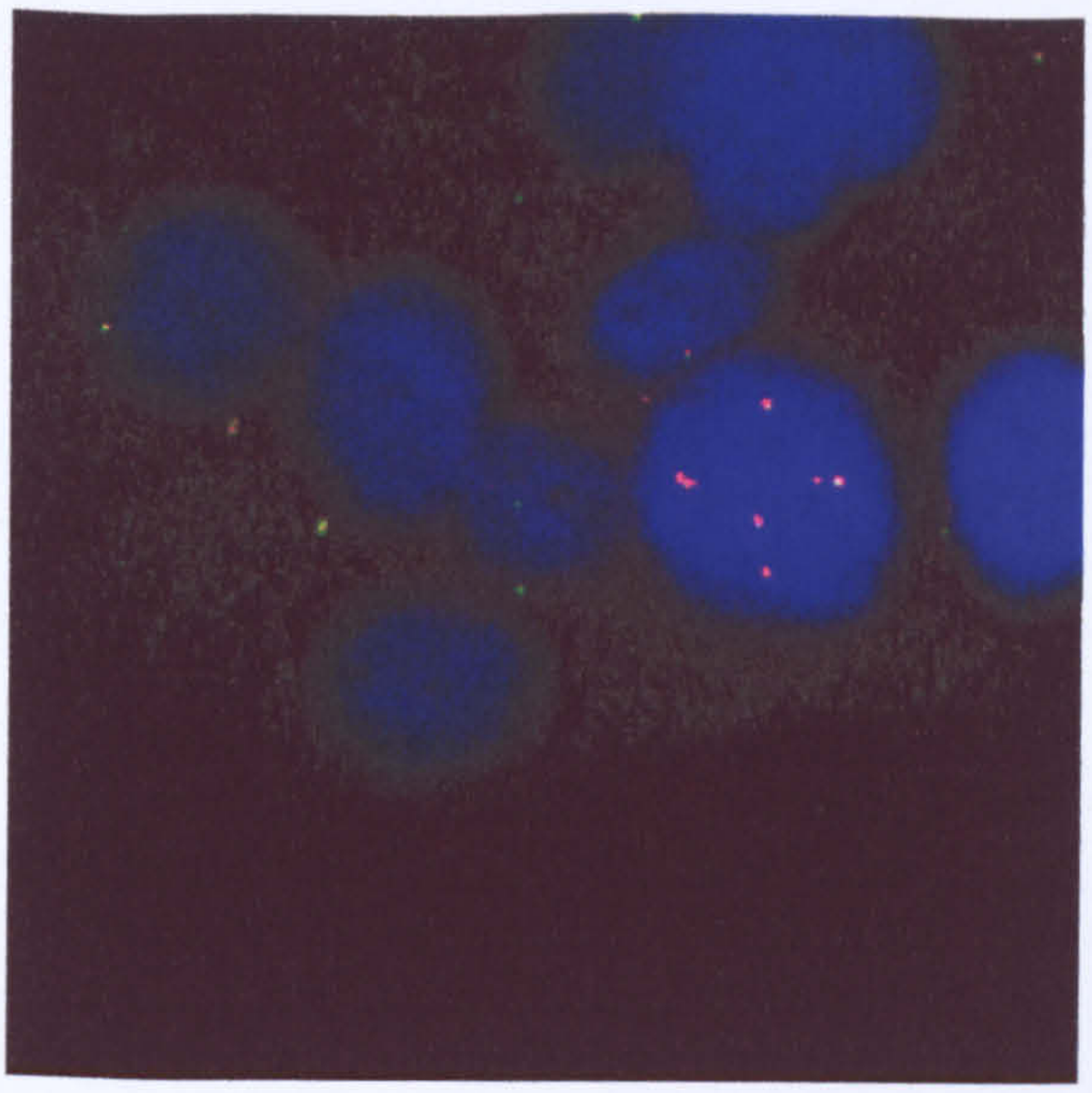

Figure 4.5 Immunofluorescence co-localization of CETN2-EGFP signals with antibody against γ-tubulin of the centrosome to authenticate CETN2 targeting to the centrosome in a clonal population of transfected H413 cells.

The centrosomes were observed as green fluorescent dots due to localization of the EGFP tagged CETN2 protein to the centrosome, whilst the staining of the centrosome by the primary γ-tubulin antibody was detected using secondary Cyc 3 antibody (red). The CETN2-EGFP transfected H413 clones exhibited (A) a population of cells showing normal number of centrosomes, with centrioles at close proximity to each other, near the nucleus and (B) a mixed population of cells with normal and abnormal centrosome numbers within the same clone. (1000X).

CHAPTER FIVE

CENTROSOME ABNORMALITIES AND DNA PLOIDY IN ORAL PREMALIGNANT LESIONS AND CARCINOMAS

5.1 INTRODUCTION

Recent studies have demonstrated the importance of aneuploidy as a marker of malignant progression and patient prognosis in oral cancer. DNA ploidy analysis in non-dysplastic oral lesions demonstrated that aneuploidy can occur very early in oral cancer (Sudbo *et al.*, 2001b) and that aneuploid lesions have a higher and faster rate of malignant progression in contrast to diploid and tetraploid lesions (Sudbo *et al.*, 2001a). Furthermore, the presence of aneuploidy associated strongly with poor survival (Sudbo *et al.*, 2004).

The presence of centrosome abnormalities is a feature common to many human tumours (Pihan *et al.*, 1998). Centrosomal defects appear early in cancer (Pihan *et al.*, 2003) and are frequently associated with loss of tissue architecture (Pihan *et al.*, 2001) and tumour aggressiveness (D'Assoro *et al.*, 2002). Centrosome abnormalities have been suggested to drive CIN and, in turn, cancer by their ability to cause chromosome missegregation through abnormal mitosis. (Shono *et al.*, 2001). Consistently, coexistence of centrosome defects with aneuploidy has been reported in pre-invasive lesions (Pihan *et al.*, 2003) and carcinomas of a variety of cancers (Gustafson *et al.*, 2000, Sato *et al.*, 2001, Jiang *et al.*, 2003), suggesting that centrosome defects may contribute to the earliest stages of cancer development through the generation of chromosome instability.

There is currently a lack of information about the centrosomes status in oral cancer and the contribution of such abnormalities to oral tumour progression is unknown. The results of Chapter Four demonstrated that centrosome abnormalities are common in OSCC-derived CIN cell lines. These data suggest

that defects in the centrosome could be the underlying mechanism of CIN in oral cancer. The aim of this study, therefore, was to establish if centrosome abnormalities occurred in oral cancer. Centrosome abnormalities were first investigated in OSCCs and the study was then extended to examine oral dysplasias to determine if such defects occurred early during the genesis of oral cancer. Centrosome abnormalities in dysplasias were then examined in the context of DNA ploidy to determine if these defects were associated with the potential of the lesions to undergo malignant progression.

5.2 RESULTS

5.2.1 Centrosome identification and evaluation criteria in paraffin embedded archival oral tissue.

Centrosomes in paraffin embedded oral tissues were visualised through immunofluorescence staining using a primary antibody against γ-tubulin. A second primary anti-cytokeratin antibody was used to demarcate the basal and tumour areas from the stromal area, as the architecture of the tissue is less obvious when examined under high magnification. The anti-cytokeratin antibody also assisted in distinguishing areas of invasive tumour within the stromal area under high magnification.

Similar parameters to those used in Chapter Four were used to evaluate centrosomal abnormalities, namely, increase in centrosome number, size and abnormal structure. Abnormal mitotic figures were also scored during the analysis as they reflect functional supernumerary centrosomes. A minimum of 200 cells exhibiting stained centrosomes under a high-powered field were evaluated per sample.

5.2.2 Centrosome defects in oral dysplasias and carcinomas

A total of twenty-eight oral dysplasias, consisting of nine moderate and twenty severe dysplasias and a total of seventeen OSCCs, consisting of five well, six moderate and six poorly differentiated SCCs were analysed for centrosome defects. Paraffin embedded normal oral mucosa and breast ductal carcinoma *in situ* were used as negative and positive controls, respectively. Breast ductal carcinoma was chosen as a positive control because centrosomal abnormalities in this tumour have been well documented previously (Lingle *et al.*, 2002, Pihan *et al.*, 1998),

In normal tissues, interphase cells exhibited a single or a pair of centrosomes at close proximity to each other (Figure 5.1), whilst a normal mitotic cell exhibited brightly stained bipolar centrosomes nucleating mitotic spindles (Figure 5.2A). By contrast, a variety of centrosome abnormalities were observed in the oral lesions, including centrosomes of larger diameter (Figure 5.3A), elongated centrosomes (Figure 5.3B) and supernumerary centrosomes (Figure 5.3C). Abnormal mitoses were observed in both dysplasias and SCCs (Figure 5.2B). Similar defects were observed in breast ductal carcinoma tissues, thus validating the results for the oral lesions. The frequency of centrosome defects in breast ductal carcinoma tissues were similar to that observed in the SCCs (data not shown). Normal oral tissues did not exhibit any centrosomal defects, indicating that centrosomal abnormalities are rare events in normal oral tissue.

The percentage of tumour cells showing centrosomal abnormalities was low (2.5%-4.5%) but defects were observed in all the carcinomas analysed. Similarly, all twenty-eight oral dysplasias exhibited centrosomal abnormalities

albeit at a lower frequency (1.7%-2.3%). Amongst the different types of centrosomal abnormalities, alterations in centrosome size and structure were dominant, whilst numerical abnormalities were the least common within the lesions analysed in this study.

The number of centrosome abnormalities correlated with a loss of tumour cell differentiation (non-parametric Kruskal-Wallis test, $P<0.03$; Figure 5.4), with the highest percentage of centrosomal abnormalities observed in poorly differentiated SCCs and the lowest in well-differentiated SCCs. Centrosomal abnormalities were significantly less common in oral dysplasias than carcinomas (1.8% vs 3.4%; Unpaired T-test: $P<0.0001$). Centrosome abnormalities were restricted to the dysplastic areas of the lesion and none were observed in the surrounding normal epithelial or stromal area.

5.2.3 Ploidy status of oral premalignant lesions

The results of the present study showed that there was a low level of centrosome abnormalities in all oral dysplasias examined. To examine whether these defects were associated with malignant progression, centrosome abnormalities were examined in the context of DNA ploidy because an abnormal DNA content has been shown to be a marker of malignant progression in oral dysplasias (Sudbo *et al.*, 2001a).

The ploidy status of the oral dysplastic lesions was determined in collaboration with Dr. J. Sudbo and Dr. A. Reith (Norwegian Radium Hospital, University of Oslo, Norway), as described previously (Sudbo *et al.*, 2001a). Briefly, a nuclear monolayer was prepared on a glass slide following trpysin digestion of two 50

μm sections of paraffin-embedded oral tissues. The nucleus was stained with Feulgen's and periodic acid-Schiff stain and the density of the stained DNA was measured using high resolution image cytometry to determine the ploidy status of the lesion. All specimens were coded, and DNA histograms were classified in a blinded manner by two observers (Dr. J. Sudbo and Dr. A. Reith). A lesion was classified as diploid if there was only one peak (which was 2c) during the G0 or G1 phase, if the number of 4c nuclei during the peak of the G2 phase did not exceed 10 percent of the total, or if the number of nuclei with a DNA content of more than 5c did not exceed 1 percent of the total. A lesion was defined as tetraploid when there was a 4c peak during the G0 or G1 phase together with an 8c peak during the G2 phase or when the number of 4c nuclei during the peak of the G2 phase exceeded 10 percent of the total. A lesion was defined as aneuploid if there were aneuploid peaks (3c, 5c, 7c, or 9c) or if the number of nuclei with a DNA content of more than 5c or 9c exceeded 1 percent of the total.

The ploidy status was determined in a total of seven moderate and eighteen severe oral dysplasias (Table 5.1). The moderate dysplasias were predominantly diploid (71.4%; 5/7), whereas only 55.6% (10/18) of severe dysplasias were classified as being diploid. Aneuploidy was more common in the severe dysplasia compared to moderate dysplasia (44.4% vs. 28.6%).

Although a slight increase in the prevalence of centrosome abnormalities was seen in the aneuploid lesions compared to the diploid lesions (2% vs 1.7%), the difference was not statistically significant.

5.3 SUMMARY

This study examined centrosome abnormalities in SCCs and dysplastic lesions of the oral cavity. Centrosome abnormalities in terms of size, structure and number were seen in both SCCs and dysplasias with defects in size and structure being the most common. The existence of centrosome abnormalities in both the dysplasias and SCCs shows that defects in the centrosome are common in oral cancer and occur early in the disease process. Centrosome abnormalities appeared to be associated with disease progression because the percentage of cells containing abnormal centrosomes was greater in the tumours than in the dysplasias. Further, the percentage of centrosome abnormalities in SCCs correlated with a loss of tumour cell differentiation.

DNA ploidy was used as a marker of malignant progression and was detected in ten of twenty-five dysplasias. In this study, aneuploidy associated strongly with the degree of dysplasias but there was no correlation between centrosome abnormalities and ploidy. A small increase in centrosome abnormalities was seen in the aneuploid vs diploid lesions (2% vs 1.7%) but the increase was not statistically significant.

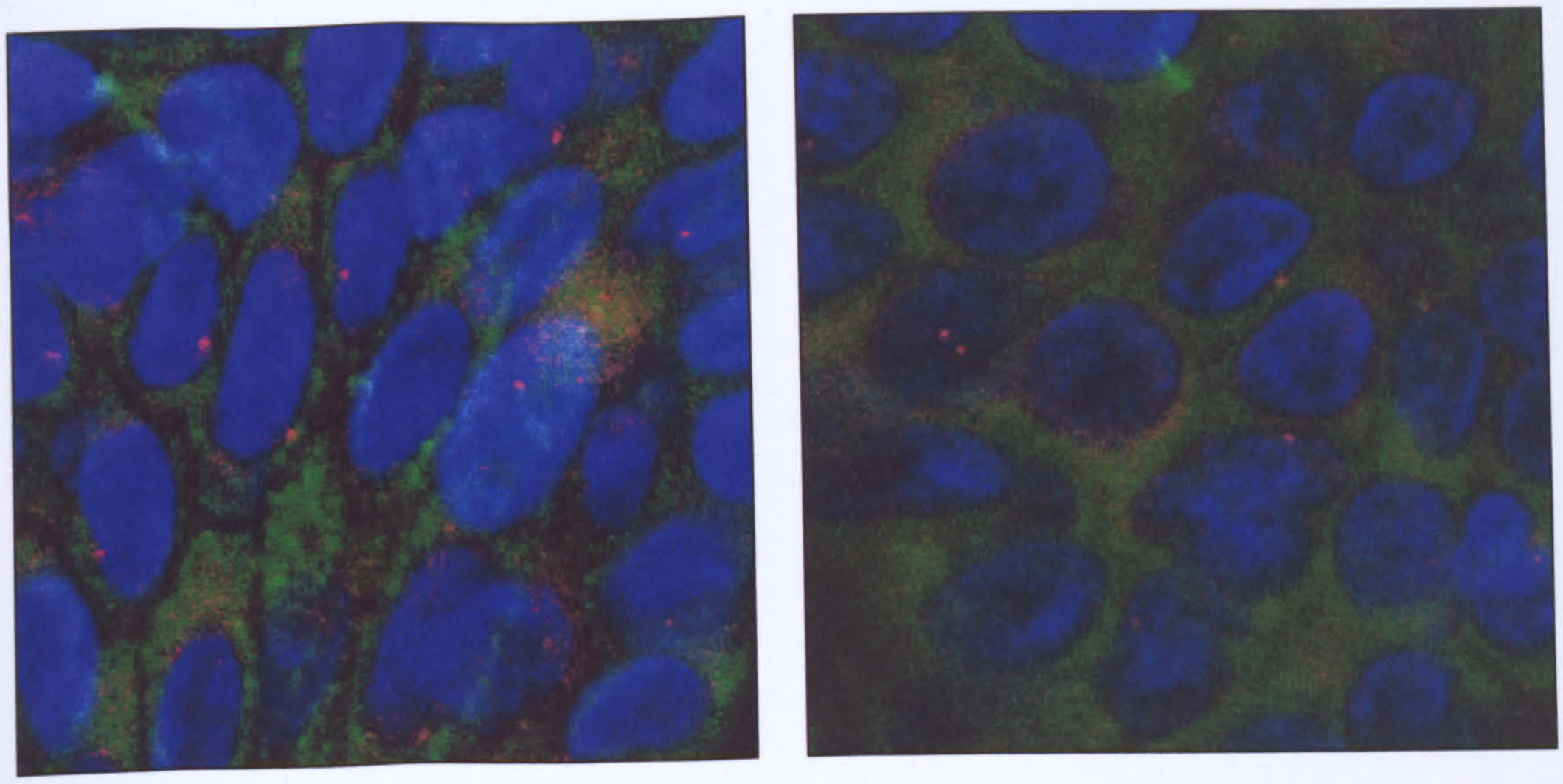

A B

Figure 5.1 Centrosomes in paraffin embedded normal oral tissue

Immunofluorescence image of a (A) single or (B) a pair of centrosomes at close proximity to each other, exhibiting punctate morphology, as usually observed in normal oral tissues. Centrosomes were detected using primary antibody against γ-tubulin and the epithelial cells were detected using antibody against cytokeratin. The primary antibodies were detected using Cyc3 (red; γ-tubulin) and FITC (green; cytokeratin) conjugated secondary antibodies. The nuclei were counterstained with DAPI (blue; x1000).

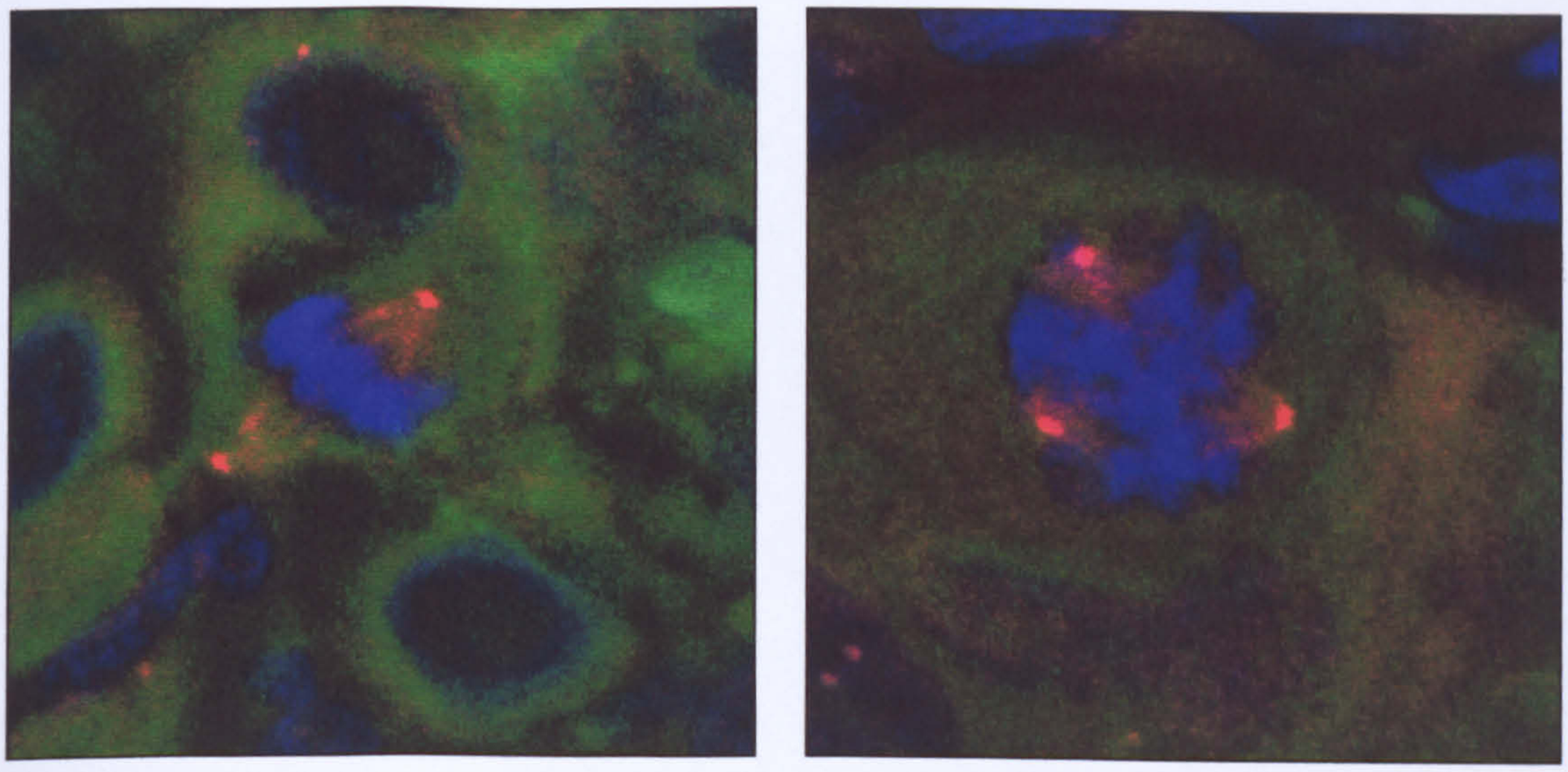

A B

Figure 5.2 Mitotic figures observed in oral carcinomas

Cells undergoing (A) normal mitosis exhibit distinct brightly stained bipolar mitotic spindles, whilst (B) abnormal mitosis consists of multipolar spindles (x2000). Centrosomes were detected using primary antibody against γ-tubulin and the epithelial cells were detected using antibody against cytokeratin. The primary antibodies were detected using Cyc3 (red; γ-tubulin) and FITC (green; cytokeratin) conjugated secondary antibodies. The nuclei were counterstained with DAPI (blue).

(A)

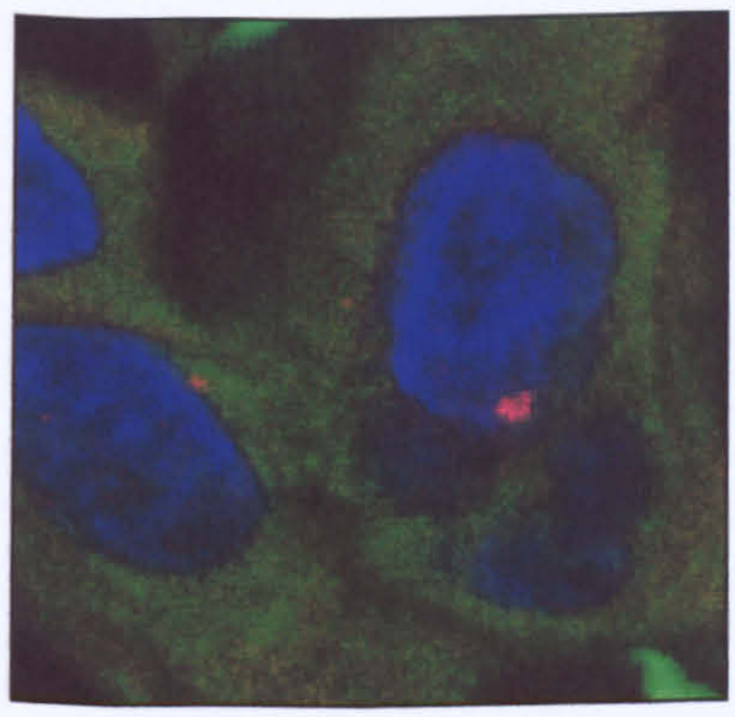

(B)

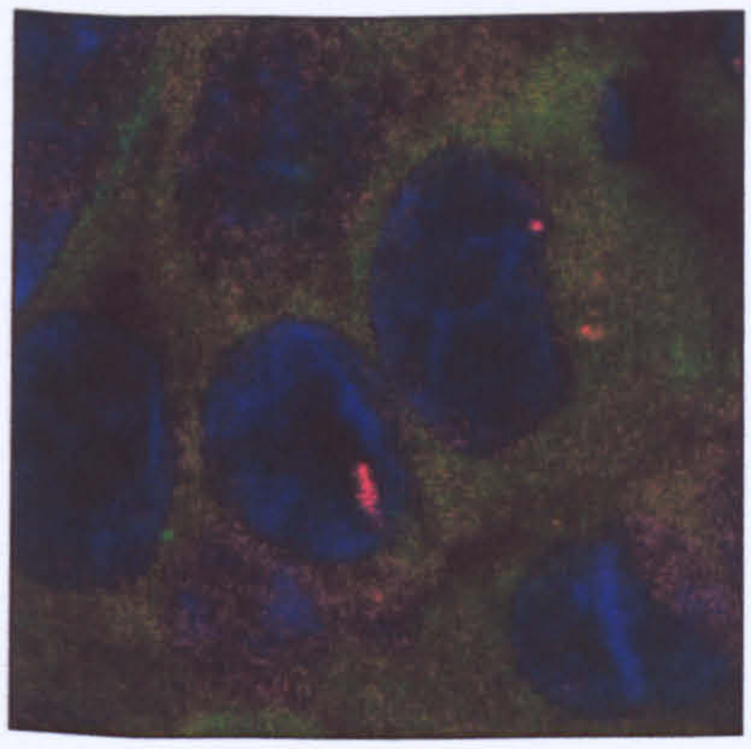

(C)

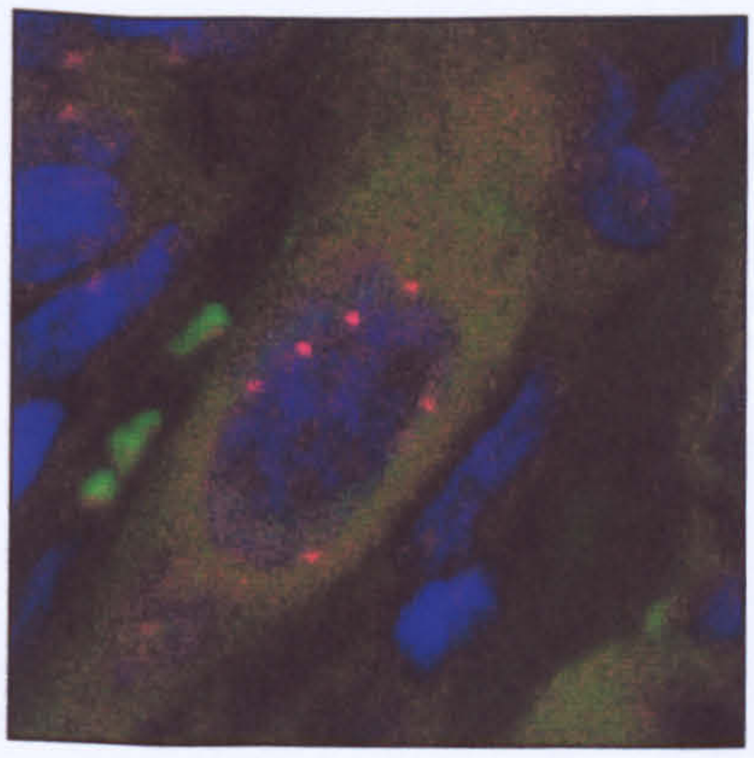

Figure 5.3 Centrosomal abnormalities observed in oral carcinomas

Centrosome abnormalities included (A) an increase in size, (B) alterations in shape resulting in elongated centrosomes and (C) increase in centrosome number (x2000). Centrosomes were detected using primary antibody against γ-tubulin and the epithelial cells were detected using antibody against cytokeratin. The primary antibodies were detected using Cyc3 (red; γ-tubulin) and FITC (green; cytokeratin) conjugated secondary antibodies. The nuclei were counterstained with DAPI (blue).

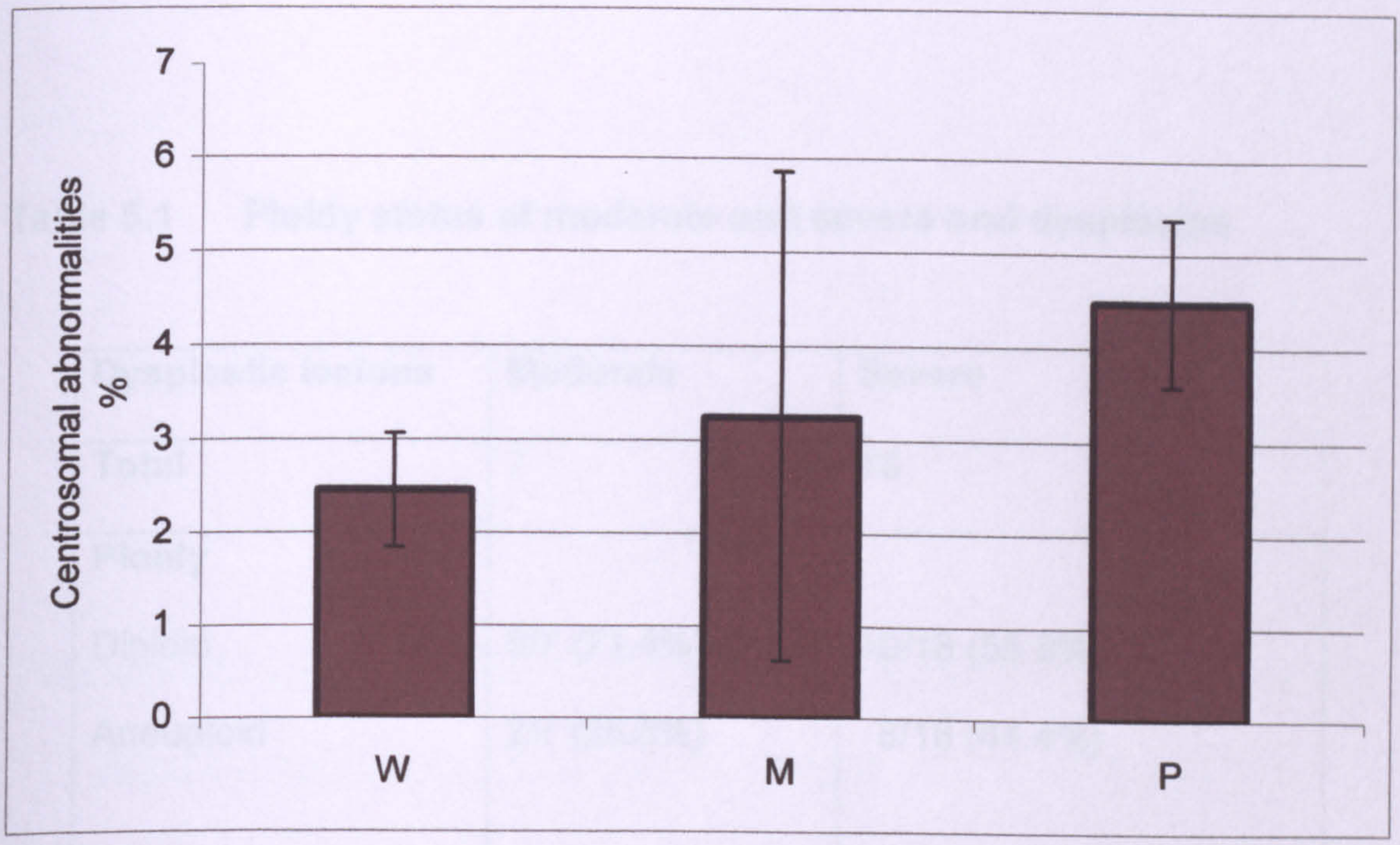

Figure 5.4 Centrosome abnormalities correlate with a loss of differentiation in oral SCCs

The presence of centrosome abnormalities was evaluated in a minimum of 200 cells per sample. The results represent the mean (± standard deviation) percentage of cells exhibiting centrosome abnormalities in well (W), moderate (M) and poorly (P) differentiated carcinomas. Statistical analysis (Kruskal-Wallis, $P<0.03$) showed a significant correlation between centrosome defects in carcinomas and loss of tumour cell differentiation.

Table 5.1 Ploidy status of moderate and severe oral dysplasias

Dysplastic lesions	Moderate	Severe
Total	7	18
Ploidy		
Diploid	5/7 (71.4%)	10/18 (55.6%)
Aneuploid	2/7 (28.6%)	8/18 (44.4%)

CHAPTER SIX

THE DEVELOPMENT OF PHIP RESISTANCE IN IMMORTALISED HUMAN NORMAL ORAL KERATINOCYTES RESULTS IN STABLE CHROMOSOME NUMBER ALTERATIONS BUT DOES NOT AFFECT THE RESPONSE TO IRRADIATION- INDUCED DNA DAMAGE

6.1 INTRODUCTION

Aneuploidy, or CIN, is ubiquitous and a dominant phenotype in cancer. Based on the presence of aneuploidy in premalignant lesions of a variety of cancers, CIN has been suggested to occur early and drive tumour progression (Pihan *et al.*, 2003). Although defects in mechanisms involving growth inhibition, DNA repair and chromosome segregation have been implicated in CIN, it is unclear whether such abnormalities are a cause or consequence of CIN. The development of an *in vitro* model of CIN would greatly facilitate the elucidation of the mechanisms involved in CIN and how they contribute towards tumorigenesis.

In the past, many studies have employed chemicals to demonstrate the ability of carcinogens to induce or select for aneuploidy. However, these studies were carried out either in rodent or cancer cell lines, which are naturally more susceptible to chemical manipulations. For example, treatment of the colorectal carcinoma cell line, HCT116, with the carcinogen PhIP was shown to induce CIN (Bardelli *et al.*, 2001). Normal human cells have historically proven to be difficult to transform in part because they have a short life span in culture (Rhim, 1991), but the development of immortalised human oral keratinocytes by the expression of hTERT, the catalytic subunit of the telomerase enzyme (Dickson *et al.*, 2000) means that essentially normal cells can now be used.

The aim of the present study was to determine if aneuploidy could be induced in an immortalised human normal oral keratinocyte cell line, OKF6/TERT-1, using PhIP. Having determined that the development of PhIP resistance was associated with the acquisition of consistent chromosomal gains, the study was

extended to determine whether the induction of carcinogen resistance produced cells that were resistant to DNA damage.

6.2 RESULTS

6.2.1 Generating PhIP-resistant clones

To generate PhIP-resistant cells, the immortalised normal epithelial cell line OKF6/TERT-1 was initially treated with 50 μM activated PhIP for 3 hours. Approximately $1x10^{-6}$-$2x10^{-6}$ cells survived the first treatment. After achieving exponential growth, the surviving cells were retreated with 50 μM PhIP and clonal populations of surviving cells were isolated. To identify PhIP-resistant clones, the cells were retreated with 50 μM PhIP and the plating efficiency was normalised against OKF6/TERT-1 parental cells treated with or without activated PhIP. Approximately $0.2x10^{-5}$–$1x10^{-5}$ cells survived the final PhIP treatment. Since PhIP treated parental cells frequently demonstrated very low colony forming efficiency, clones that formed more colonies compared to the parental cells following PhIP treatment were considered PhIP-resistant. From a total of thirty clones originally isolated, only four (clones 13, 16, 18 and 20) exhibited increased resistance to PhIP and were chosen for further analysis (Figure 6.1).

6.2.2 Cytogenetic analysis of PhIP-resistant clones.

To examine whether the development of PhIP resistance resulted in chromosomal imbalances, CGH analysis was performed on both low (4-5) and high (22-25) passage PhIP-resistant clones. Chromosomal losses and gains as

observed by CGH, in the parental OKF6-TERT/1 and PhIP-resistant clones are shown in Table 6.1.

The parental OKF6/TERT-1 cells exhibited gains of 1q22-qter and chromosome 5 and loss of 9p13-pter, associated with the acquisition of an immortal phenotype (Dickson *et al.*, 2000). Compared to parental OKF6/TERT-1 cells, all PhIP-resistant clones (clone 13, 16, 18 and 20) showed gains of chromosome 8, 9p21/22-qter and 20 at lower passage. An additional gain of chromosome 7 was seen in three of four clones (clone 13, 16 and 18) at higher passage. Clone 13 also exhibited an additional possible loss of 1q21-22, chromosome 2, 3 and 17. The consistency in the chromosomal alterations observed in the different PhIP-resistant clones suggests that the development of PhIP resistance in immortalised human oral keratinocytes resulted in aneuploidy in terms of consistent chromosomal gains and not a dynamic unstable karyotype typical of CIN.

6.2.3 Response to DNA damage in PhIP-resistant clones

Since no widespread CIN was seen in the OKF6-TERT/1 PhIP-resistant clones, we therefore hypothesised that the development of PhIP resistance was associated with resistance to other forms of DNA damage. Therefore, the cellular response to irradiation induced DNA damage in terms of cell viability, induction of apoptosis, activation of the p53 pathway and cell cycle arrest was assessed in both parental OKF6/TERT-1 cell lines and PhIP- resistant clones.

6.2.3.1 Cell viability

To analyse cell viability following DNA damage, MTT assays were performed 48 and 72 hours following 5Gy irradiation of parental OKF6/TERT-1 and the PhIP resistant clones.

Irradiation of the cells resulted in a similar reduction in yield of attached cells in both parental and PhIP resistant clones after 48 and 72 hours, indicating that PhIP resistant clones were no more radiosensitive than the parental cell line to irradiation (Figure 6.2).

6.2.3.2 Apoptosis

To determine the apoptotic response in the parental OKF6/TERT-1 and the PhIP resistant clones, FACS analyses were performed after 24, 48 and 72 hours following 5Gy irradiation. Apoptotic cells were detected using a FITC-conjugated annexin-V antibody.

A high proportion of early apoptotic cells were seen in both unirradiated and irradiated culture at all time points, which may have been due to enzymatic detachment of cells prior to FACS analysis. Nevertheless, an increase in annexin/propidium iodide positive signals signifying late apoptotic cells was observed 24 hours after irradiation in both parental OKF6/TERT-1 cells (Figure 6.3) and the PhIP-resistant clones (Figure 6.4). The lack of floating apoptotic cells in irradiated cultures of both parental and the PhIP-resistant clones, concurrent with an increase in early and a reduction in late apoptotic cells observed during FACS analysis, 48 and 72 hours following irradiation, suggests that these cells did not undergo apoptosis but re-entered the cell cycle.

6.2.3.3 p53 pathway

The integrity of the p53 pathway was analysed due to its importance as a regulator of cell cycle and apoptosis. Induction of the p53 protein and its transcriptional targets, MDM2, and p21 was assessed by western blot analysis in both parental OKF6/TERT-1 cell lines and the PhIP resistant clones at 0, 2, 4, 6 and 24 hours following 5Gy irradiation.

In both the parental OKF6/TERT-1 cells and PhIP resistant clones, p53 was induced within 2 hours of irradiation and the induction of p21 and MDM2 was seen within 4 hours following irradiation, indicating that the p53 pathway was functional. A representative western blot of p53, p21 and MDM2 for the PhIP resistant clone 18 is shown in Figure 6.5.

6.2.3.4 Cell cycle

To determine if the clones harbour defects in the ability to arrest in response to DNA damage, FACS analysis of cell cycle arrest was performed in both parental OKF6/TERT-1 and PhIP resistant clones, 24 and 48 hours following irradiation. Cell cycle analyses of parental OKF6/TERT-1 is shown in Figure 6.6 and a representative PhIP resistant clone 18 is shown in Figure 6.7.

Irradiated OKF6-TERT/1 cells exhibited cell cycle arrest at 24 hours following 5Gy radiation. The cells exited the arrest after 48 hours following irradiation and exhibited a similar FACS profile as asynchronous cultures (Figure 6.6). Similar arrest was observed in the PhIP resistant clones and the FACS profile of clone 18 is shown in Figure 6.7.

6.3 SUMMARY

This study examined the effect of treating an immortalised normal oral keratinocyte cell line, OKF6/TERT-1, with PhIP, a bulky adduct forming agent that has been shown previously to induce CIN in carcinoma cells (Bardelli *et al.*, 2000).

CGH analysis of PhIP resistant clones demonstrated a consistent gain of chromosomes 8, 9p21/22-qter and 20 in all clones at lower passage and an additional gain of chromosome 7 in three of the clones in higher passage, indicating that PhIP treatment resulted in consistent chromosomal alterations and not a dynamic CIN. It seems likely that the consistent gains observed in the PhIP-resistant clones are specific and sufficient to confer resistance to PhIP.

Examination of the cellular response to irradiation-induced DNA damage demonstrated that both parental OKF6/TERT-1 and PhIP resistant clones exhibited similar growth inhibitory and apoptotic responses, have an intact p53 pathway and are capable of cell cycle arrest following irradiation. The similarities between the parental cells and PhIP resistant clones in their response to DNA damage suggests that the induction of PhIP resistance is not also associated with resistance to irradiation induced DNA damage.

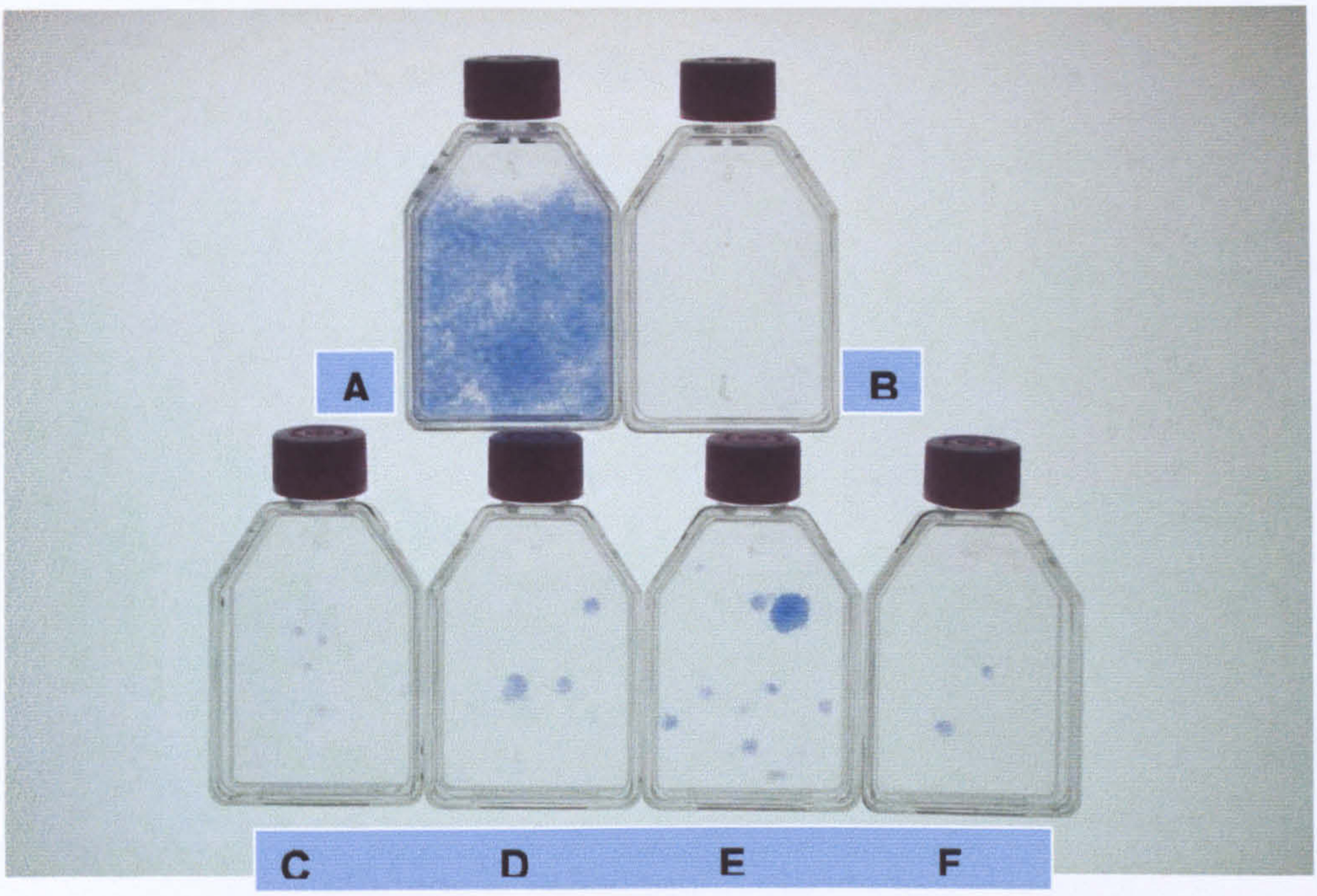

Figure 6.1 Resistance to PhIP

To identify PhIP resistant clones, 10^6 cells of individual PhIP clones were treated with 50μM PhIP and stained with methylene blue after 14 days. OKF6/TERT-1, parental cells were treated without PhIP (A) and with 50μM PhIP (B) as controls. The plating efficiency of the PhIP clones was normalised to the plating efficiency of PhIP treated control cells to identify PhIP resistant clones. Clones that formed more colonies in comparison to PhIP treated parental cells (B) were considered PhIP-resistant (C-F). PhIP treatment of the clones was repeated in order to confirm resistance to the carcinogen.

Table 6.1 Chromosomal alterations in PhIP resistant clones

	Low passage	Additional gains or losses at high passage
Parental OKF6/TERT-1	1q22-qter, 5, 9p13-pter	
PhIP clones		
Clone 13	1q23-qter, 5, 8, 9, 20	7, 9p22-qter, possible loss of 1q21-1q22, 2, 3, 17
Clone 16	1q23-qter, 5, 8, 9p22-qter, 20	7
Clone 18	1q21-qter, 5, 8, 9p22-qter, 20	7
Clone 20	1q24-qter, 5, 8, 9p21-qter, 20	None

CGH was performed on both low and high passage PhIP resistant clones. Relative to the parental cell line, OKF6/TERT-1, the PhIP resistant clones exhibited a consistent gain (green) of chromosome 8, 9p21/22-qter and 20 at low passage and 7 at high passage. Clone 13 also exhibited additional losses (red). Losses and gains were estimated at 99.5% confidence intervals.

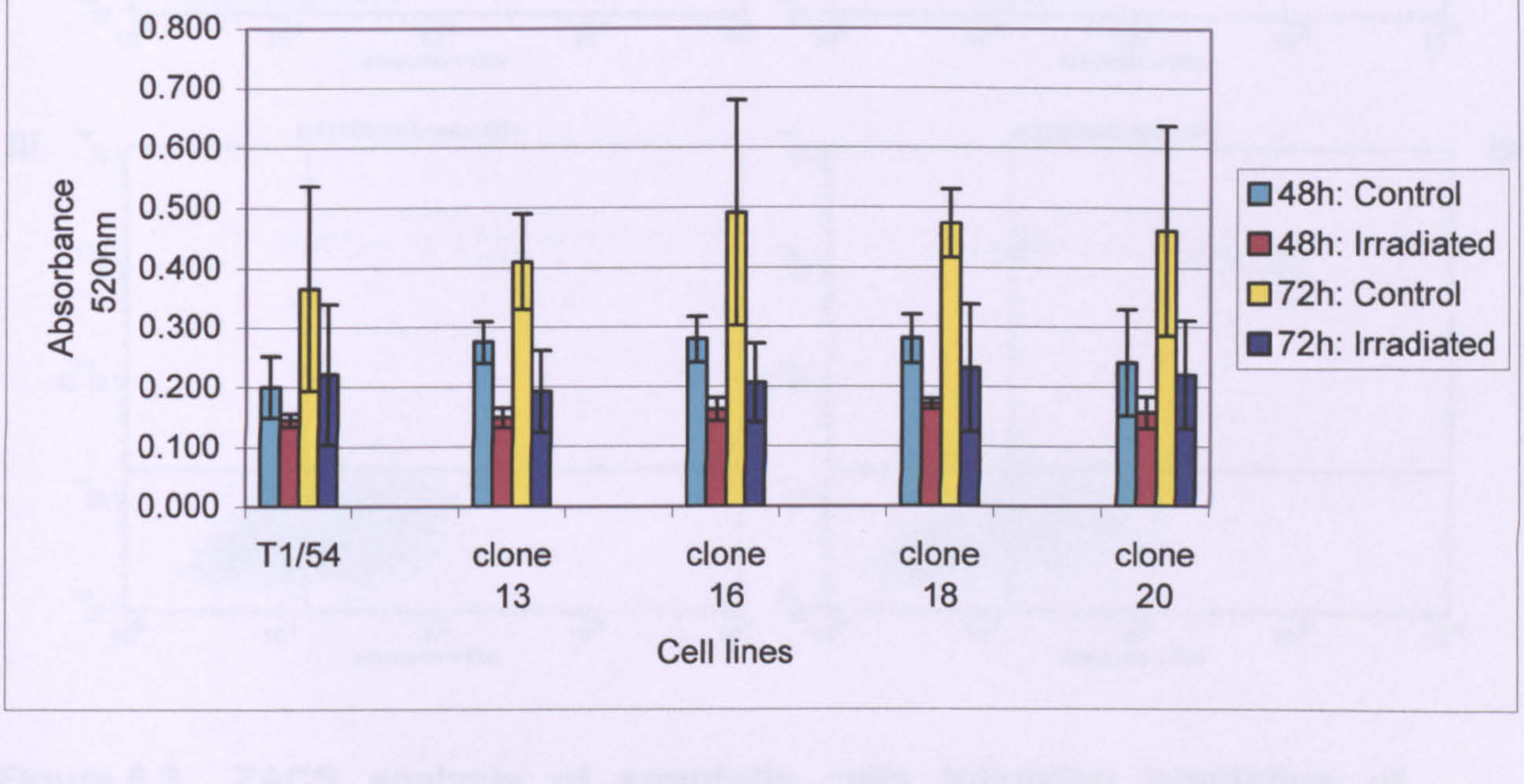

Figure 6.2 MTT assay for analysis of cell viability following irradiation

MTT assay were performed 48 and 72 hours following 5Gy irradiation. No difference in cell yield was seen between parental OKF6/TERT-1 (T1) and PhIP resistant clones at either time point following irradiation. Data points reflect the means (± standard deviation) of two separate experiments.

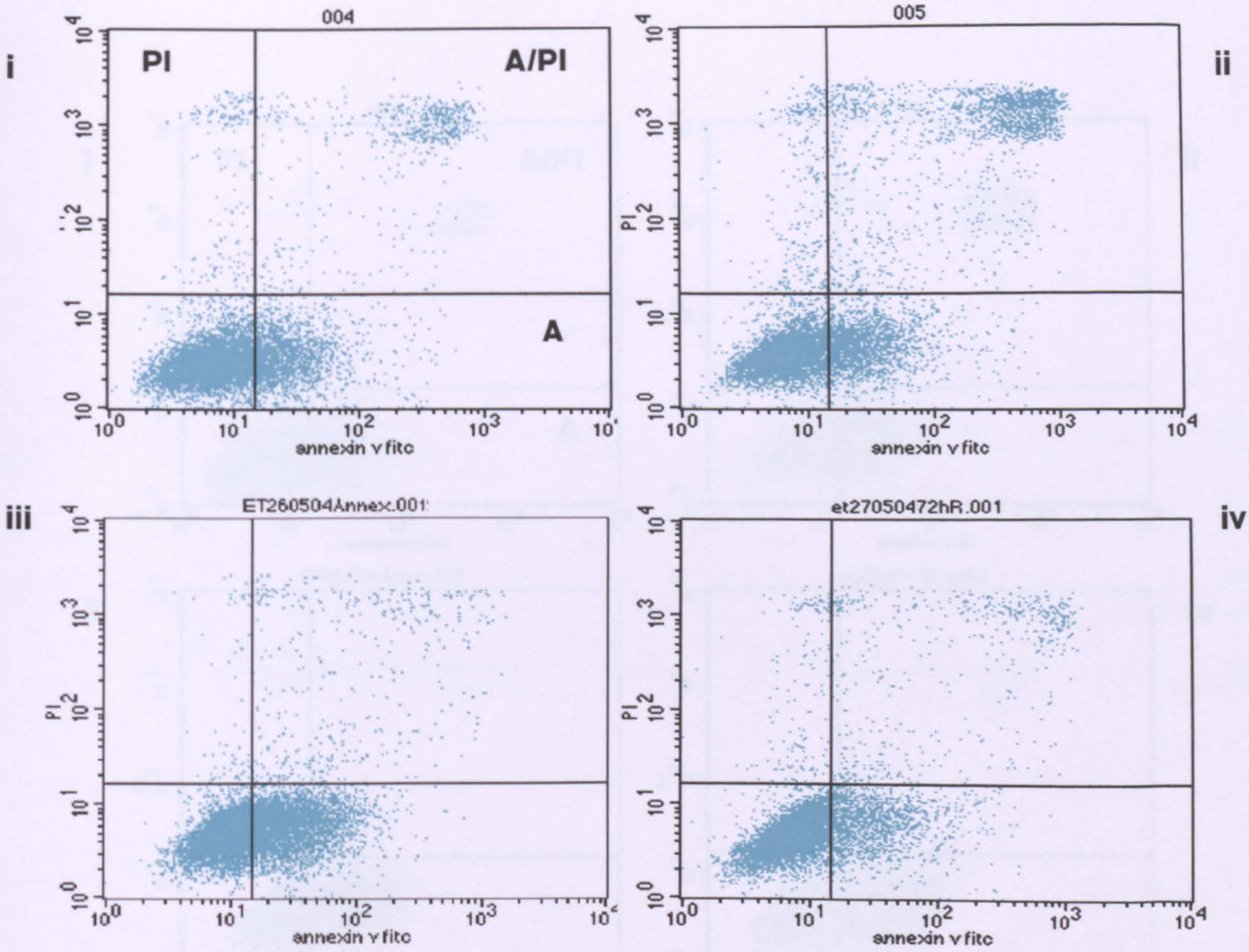

Figure 6.3 FACS analysis of apoptotic cells following irradiation of OKF6/TERT-1 parental cells

Cells were stained with FITC conjugated-annexin antibody and/or propidium iodide and the presence of apoptotic cells were examined in (i) unirradiated cells (ii) 24, (iii) 48 and (iv) 72 hours following 5Gy irradiation. Cells stained with annexin only (A) indicate early apoptotic cells, propidium iodide only (PI) indicate necrotic or dead cells and cells stained with both annexin and propidium iodide (A/PI) indicate late apoptotic cells. In contrast to unirradiated control, an increase in late apoptotic cells can be seen 24 hours following irradiation. These cells do not die but go on to cycle after 48 and 72 hours following irradiation, as seen by low number of PI stained cells.

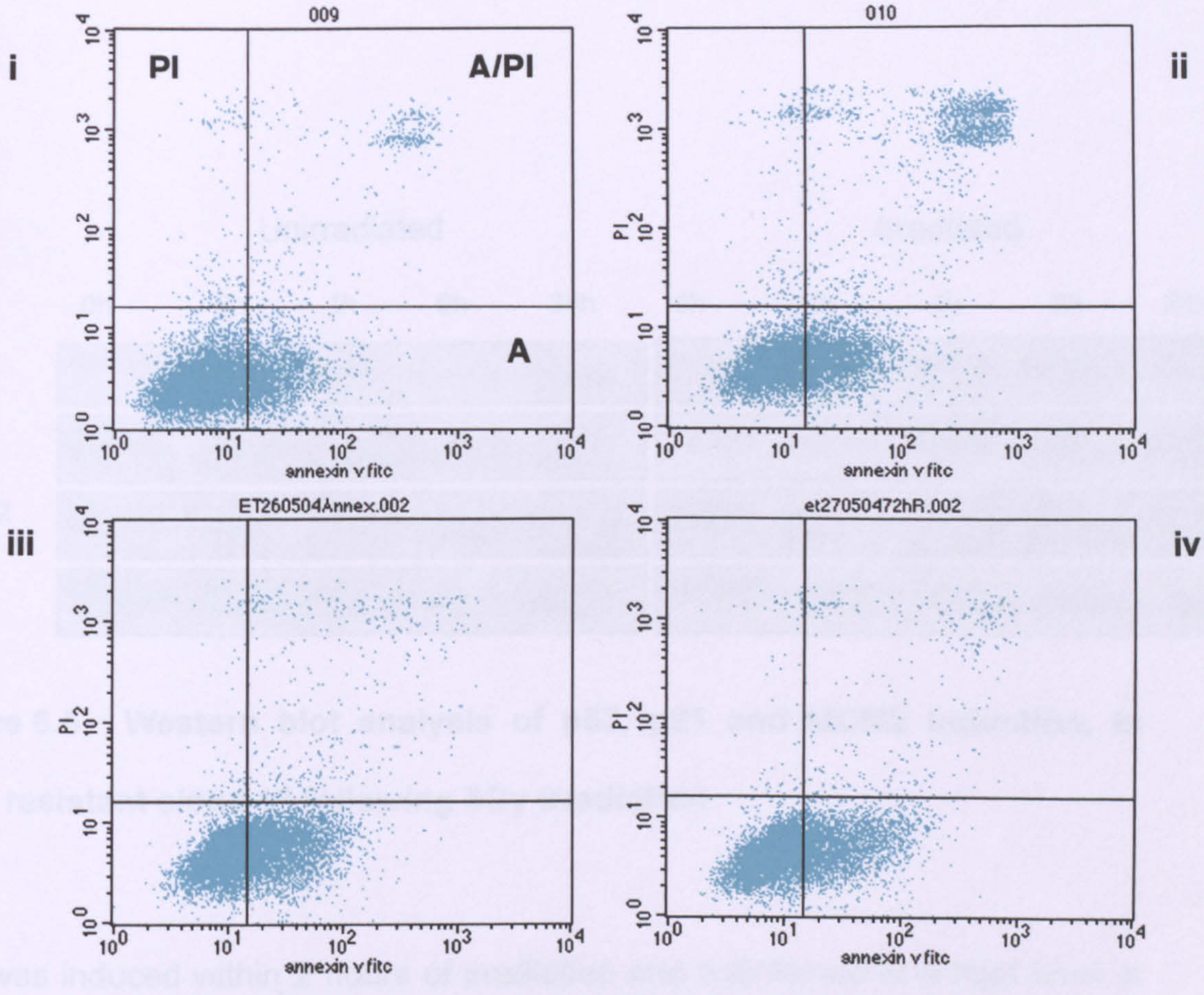

Figure 6.4 FACS analysis of apoptotic cells following irradiation of a PhIP resistant clone 18.

PhIP resistant clone 18 cells were similarly stained with FITC conjugated-annexin antibody and/or propidium iodide. By contrast to the (i) unirradiated PhIP resistant clone 18 cells, (ii) an increase in late apoptotic cells was seen 24 hours after irradiation, which diminished in number after (iii) 48 and (iv) 72 hours following irradiation.

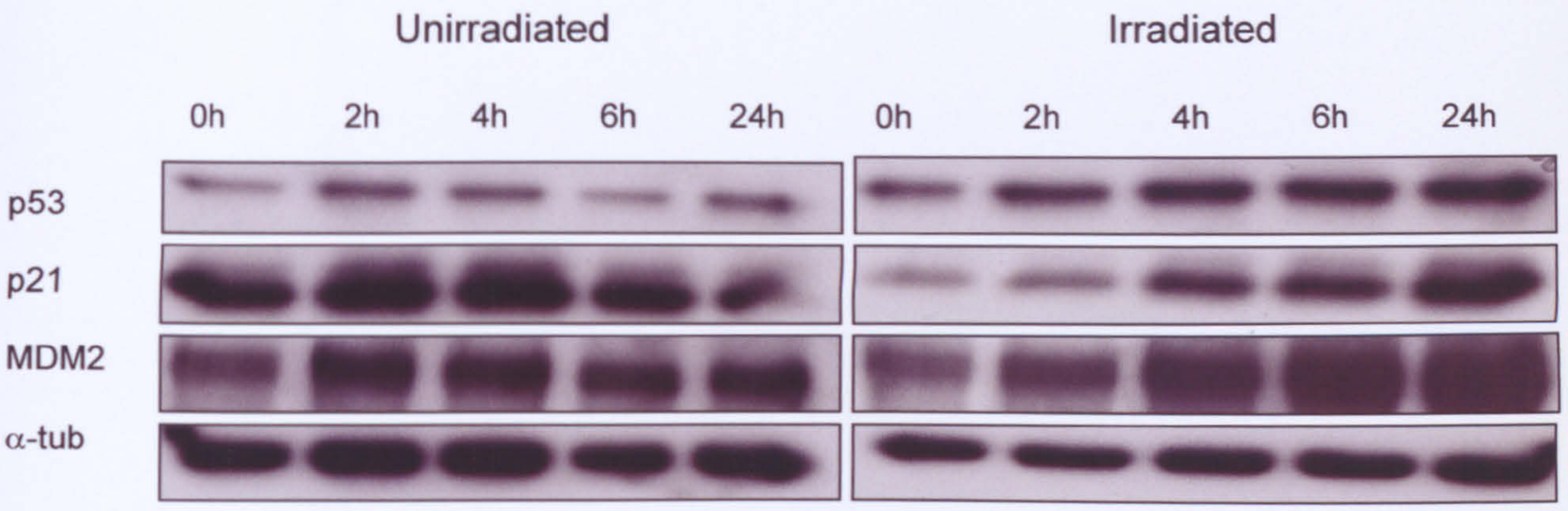

Figure 6.5 Western blot analysis of p53, p21 and MDM2 induction, in PhIP resistant clone 18 following 5Gy irradiation

p53 was induced within 2 hours of irradiation and maintained at a high level in comparison to unirradiated control. Both p21 and MDM2 were also induced within 4 hours of irradiation.

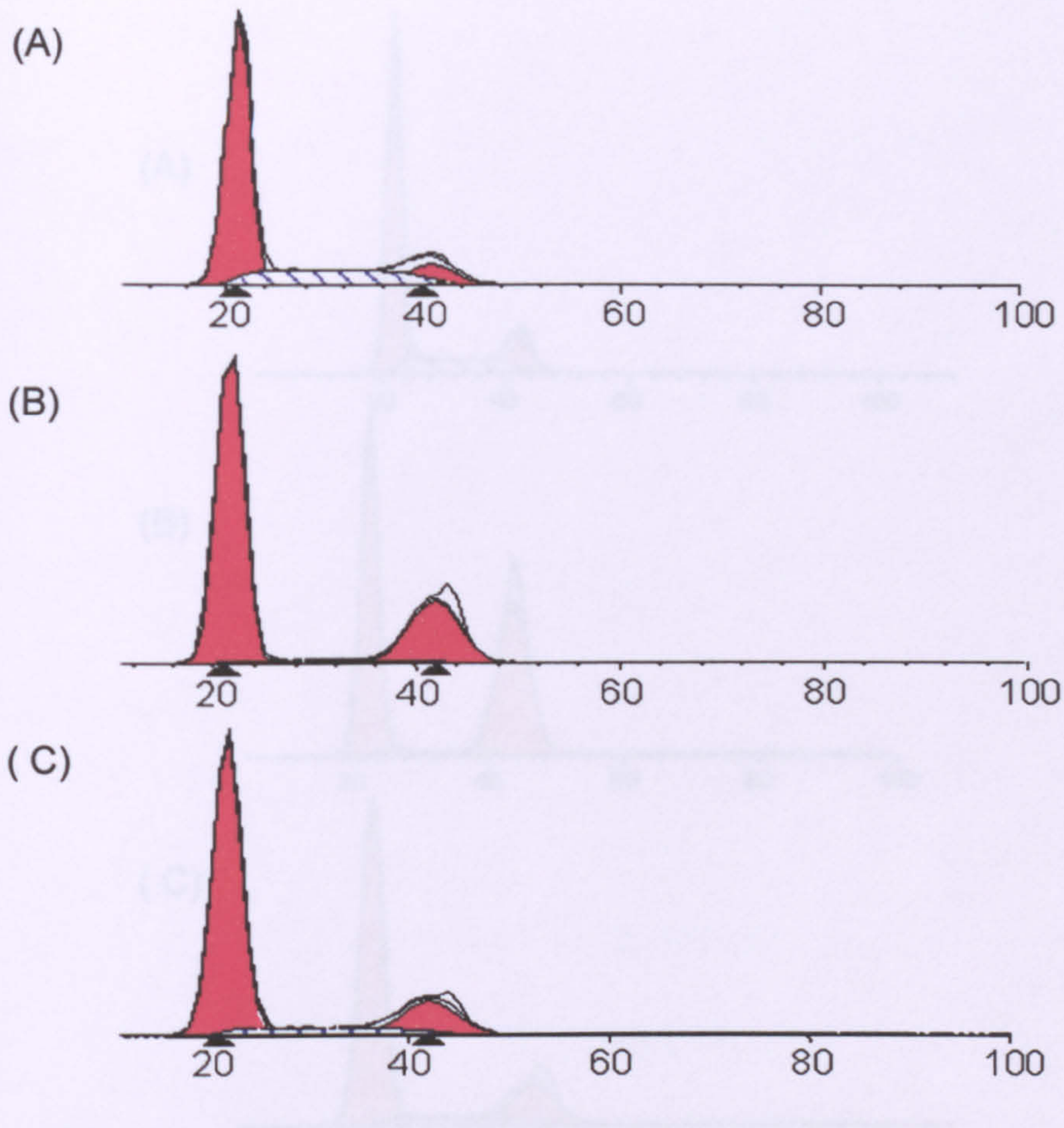

Figure 6.6 FACS analysis of cell cycle arrest in parental OKF6/TERT-1 cells

Unirradiated parental cells exhibited an asynchronous cell cycle profile. The cells arrested at both G0/G1 and G2/M phase arrest 24 hours after irradiation (B), exited arrest and began cycling to create an asynchronous population of cells similar to the unirradiated control, 48 hours following irradiation.

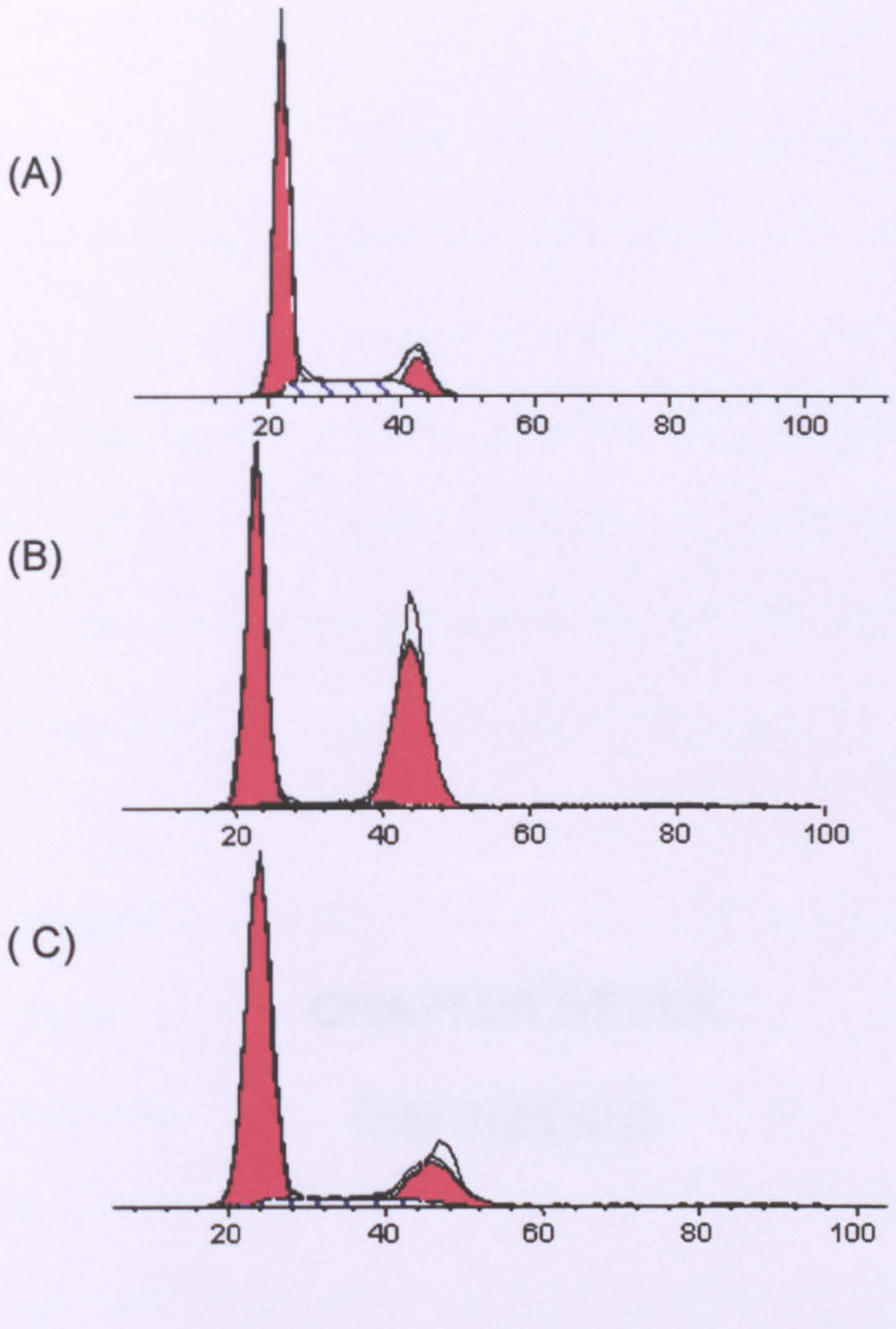

Figure 6.7 FACS analysis of cell cycle arrest in PhIP resistant clone 18

Unirradiated PhIP resistant cells exhibited an asynchronous cell cycle profile. The cells exhibited both G0/G1 and G2/M phase arrest 24 hours after irradiation (B), exited arrest and began cycling after 48 hours following irradiation. The FACS profile for cell cycle arrest was similar to the irradiated parental OKF6/TERT-1 cells.

CHAPTER SEVEN

DISCUSSION

7.1 INTRODUCTION

Evidence is accumulating to indicate that CIN occurs early in the neoplastic process and drives tumour progression (Shih *et al.*, 2001; Nowak *et al.*, 2002; Komarova *et al.*, 2003). The presence of aneuploidy in premalignant lesions of the oral cavity has been shown to correlate with malignant transformation (Sudbo *et al.*, 2001a; b), which suggests that CIN might facilitate the progression of oral cancer. The present study was initiated to investigate the mechanisms responsible for CIN in oral carcinogenesis.

This study examined the integrity of the chromosome segregation machinery, namely the mitotic checkpoint (Hartwell, 1992), the post-mitotic tetraploidy checkpoint (Andreassen *et al.*, 2001a) and centrosomes (Ghadimi *et al.*, 2000) in human oral cancer. The work was made possible by the availability of a series of human OSCC-derived cell lines that had previously been shown to harbour numerical and structural chromosome alterations (Patel *et al.*, 1993). Having determined that centrosome abnormalities were prevalent *in vitro*, the study was extended to examine the centrosome status of archival paraffin-embedded oral carcinomas and dysplasias; centrosome abnormalities in the dysplasias were also analysed in the context of DNA ploidy to examine if such abnormalities might be associated with malignant progression. In parallel studies, human immortalised normal oral keratinocytes were treated with the carcinogen PhIP in an attempt to develop an *in vitro* model of CIN.

For ease of interpretation, the Discussion has been subdivided such that consideration is given separately to the analysis of defects in the chromosomal segregation machinery *in vitro*, the analysis of centrosome abnormalities and

DNA ploidy in oral tissues *in vivo* and the development of an *in vitro* model of CIN in human immortalised normal oral keratinocytes. Proposals for future studies are included at the end of the Discussion.

7.2 ANALYSIS OF THE CHROMOSOMAL SEGREGATION MACHINERY IN HUMAN OSCC-DERIVED CELL LINES

7.2.1 Genetic instability in human OSCC-derived cell lines

The H-series of OSCC-derived cell lines have been shown previously to exhibit structural chromosomal aberrations including a high frequency of consistent chromosome breaks on chromosome 1, 7, 8, 9, 11 and X and the formation of isochromosomes 8, 9 and 11 (Patel *et al.*, 1993). Further, the cell lines also harboured numerical chromosomal aberrations; H103 exhibited a modal chromosome number of 41, whilst H157, H314, H357, H376, H400 and H413 exhibited a modal chromosome number that ranged between 72-91 (Patel *et al.*, 1993).

Although CIN and MIN have been suggested to be mutually exclusive (Lengaur *et al.*, 1998), exceptions to this rule have been reported (Ghadimi *et al.*, 2000). MIN cell lines are thought to be chromosomally stable and exhibit relatively few of the chromosome segregation defects related to the CIN phenotype (Ghadimi *et al.*, 2000; Tighe *et al.*, 2001). It was essential, therefore, to exclude the presence of MIN in the OSCC-derived cell lines to be used in this study. MIN has been shown to result from disruption of the MMR pathway and this has been mainly attributed to mutations of the *hMLH1* and *hMSH2* genes (Buermeyer *et al.*, 1999; Jiricny and Lahti, 2000). The results of the present study demonstrate that all seven OSCC-derived cell lines expressed both

hMLH1 and hMSH2 proteins, which strongly indicates that their MMR pathway is intact. Taken together with the chromosome alterations observed in these cell lines, these results indicate that the OSCC-derived cell lines used in this study exhibit exclusively CIN and not MIN. The data are entirely consistent with the observation that MIN is rare in oral cancer (Ishwad *et al.*, 1995).

7.2.2 Analysis of the mitotic and tetraploidy checkpoints in human OSCC-derived cell lines

7.2.2.1 Mitotic checkpoint

The mitotic checkpoint functions to monitor the process of kinetochore capture of metaphase chromosomes by spindle microtubules during mitosis to ensure an error free and even segregation of chromosomes (Skibbens *et al.*, 1998). Loss of this checkpoint has been shown to promote aneuploidy, result in chromosome missegregation and contribute to genomic instability in human cancers (Wassmann *et al.*, 2001).

The present study examined the integrity of the mitotic checkpoint in the H-series of OSCC-derived cell lines. The cells were treated with the microtubule depolymerising drug, nocodazole and the mitotic checkpoint examined following FACS analyses of the cell cycle and by quantification of mitotic indices. Analysis of the cell cycle after 18 hours of nocodazole treatment demonstrated a strong G2/M arrest in all the OSCC-derived cell lines, in a similar manner to the control cell line HCT116, indicating that the mitotic checkpoint was intact in these cells. Analysis of the mitotic indices, however, indicated a transient arrest of cells in mitosis in all of the cell lines after 18-24 hours of nocodazole treatment but only H357 and H400 cells behaved the same as control HCT116 cells; the mitotic

indices of the remaining five cell lines were lower than the control (37%-55% vs ≥70%). The percentage of cells in mitosis as determined by immunocytochemical staining for phospho-histone H3 was consistently lower than that indicated by FACS analysis. The discrepancy between the results obtained using these two techniques is likely to be due to the fact that the FACS analyses detected mitotic cells based on DNA content, whilst immunocytochemical analyses with the anti phospho-histone H3 antibody detects phosphorylated histone H3 proteins, which accumulate during mitosis. The percentage of cells arrested at G2/M as determined by FACS analysis includes cells at the end of S-phase, G2 and M phase, whilst the mitotic index analysis enables visualization and scoring of cells specifically in mitosis and, therefore, is a more accurate estimate of the number of mitotic cells. Taken together, the results indicate that the mitotic checkpoint is fully functional in two (H357 and H400) of the OSCC-derived cell lines and attenuated in the remaining five cell lines.

The results of the present study contrast with reports describing defective mitotic checkpoints in colon (Cahill *et al.*, 1998) and breast (Yoon *et al.*, 2002) cancer cell lines but are supported by the only other study to examine the mitotic checkpoint in head and neck squamous cell carcinoma (HNSCC) cell lines, which reported a similar attenuation of the checkpoint (Minhas *et al.*, 2003). Such discrepancies are likely to be due to inconsistent interpretation of the mitotic indices of cell lines [eg. Tighe *et al.*, (2001) vs Cahill *et al.*, (1998)]. Further, misinterpretation of the G0/G1 arrest and the consequential reduction in mitotic cells arrested at G2/M observed in some cell lines has been taken to indicate a defective mitotic checkpoint (Yoon *et al.*, 2002); this G0/G1 arrest has

been shown to be due to a nocodazole dose-dependent ability of some cell lines to arrest at G0/G1 and/or G2/M phase of the cell cycle rather than due to a *cancer-associated checkpoint loss (Blajeski et al., 2002).*

It has been proposed that a compromised mitotic checkpoint could mediate subtle rates of chromosome missegregation that is compatible with cell viability (Babu *et al.*, 2003; Michel *et al.*, 2001). In support of this theory, mutations in known spindle checkpoint genes are rare in human tumours (Cahill *et al.*, 1998) and complete suppression of the mitotic checkpoint has been demonstrated to result in lethality due to massive chromosome loss (Kops *et al.*, 2004). Further, studies have showed an elevated rate of chromosome missegregation in $Bub3^{+/-}$ mice (Babu *et al.*, 2003) and $Mad2^{+/-}$ human cancer cells (Michel *et al.*, 2001) and a compromised mitotic checkpoint in ovarian cancer cells with lowered expression of Mad2 (Wang *et al.*, 2002). These results indicate a role for haplo-insufficiency of mitotic checkpoint genes in compromising the fidelity of the checkpoint. The expression status of the mitotic checkpoint genes in the OSCC-derived cell lines used in the present study, however, is not known.

7.2.2.2 Tetraploidy checkpoint

The tetraploidy checkpoint is a post-mitotic checkpoint (Lanni and Jacks, 1998) that functions to elicit a G1 arrest in cells that exit mitosis with a tetraploid DNA content (Andreassen *et al.*, 2001a). In the present study, analysis of the cell cycle after 36 hours of nocodazole treatment indicated DNA reduplication in a high percentage of H357 and H376 cells, suggesting a defect in the ability of the cells to arrest with a tetraploid DNA content. Therefore, the tetraploidy checkpoint was assessed by FACS analysis of the cell cycle after releasing

cells from treatment with the cytokinesis inhibitor, DCB. The H400 cell line was chosen as a control for this assay, as it exhibited G2/M arrest during prolonged nocodazole treatment

Cell cycle analysis of DCB treated H400 cells showed that the cells were able to maintain G2/M arrest 18 hours after release into drug free medium. By contrast, a polyploid cell population was beginning to emerge in H357 and the presence of a polyploid cell population was evident in H376 after 18 hours release into drug free medium. However, the H400 cells exhibited formation of polyploid population of cells, similar to H357 and H376 cells, after 36 hours release from DCB treatment. This could potentially be attributed to the mutation(s) in the p53 gene harboured by all the OSCC-derived cell lines (Yeudall *et al.*, 1995), as p53 is thought to be important for maintenance of a post-mitotic arrest (Lanni and Jacks, 1998; Andreassen *et al.*, 2001a). The formation of a polyploid population of cells in all cell lines after prolonged release from DCB treatment, however, indicates that the checkpoint might also be attenuated in the H400 cells.

It is important to note that our understanding of the tetraploidy checkpoint is in its infancy. Recent evidence suggests that the arrest observed following the mitotic exit of tetraploid cells, which was reported to be caused by the tetraploidy checkpoint (Andreassen *et al.*, 2001a), was due to disorganization of the actin cytoskeleton by the high dose of DCB used that persists even after drug removal (Uetake *et al.*, 2004). Considering the controversy surrounding the tetraploidy checkpoint, this experiment, therefore, needs to be repeated using control cells with intact p53 and the ability of tetraploid cells to arrest should be

ascertained following induction of tetraploidization using methods other than inhibition of cytokinesis.

7.2.3 Analysis of centrosome abnormalities in human OSCC-derived cell lines

Although an impaired mitotic checkpoint is compatible with a low level of chromosome loss, it does not provide an explanation for the high chromosome number alterations observed in these cell lines. It is likely, therefore, that alternative mechanisms are also responsible for the CIN observed in these cell lines. The centrosome is the major microtubule-organizing centre (MTOC) of animal cells and its ability to form bipolar spindles is vital for accurate chromosome segregation into progeny cells. Centrosome defects have been suggested to drive CIN via their ability to mediate multipolar spindle formation and the consequential missegregation of chromosomes (Brinkley, 2001).

The results of this study showed that five of seven OSCC-derived cell lines exhibited centrosome abnormalities in terms of centrosome number, size and localization, suggesting that centrosome defects are common in oral cancer. This is the first study to examine centrosome abnormalities in OSCC-derived cell lines and the results are consistent with a number of reports using tumour-derived cell lines from a variety of other cancers (Ghadimi *et al.*, 2000; Sato *et al.*, 1999; 2001; D'Assoro *et al.*, 2002). The spectrum of centrosome defects observed in this study, namely, supernumerary centrosomes, increase in centrosome size, mislocalised centrosomes, abnormal mitoses and dispersed pericentrin staining are similar to those reported in other studies (Sato *et al.*, 1999; Ghadimi *et al.*, 2000). Importantly, centrosome defects occurred mainly in

the aneuploid cell lines used in this study, whilst the diploid HCT116 cells showed centrosome profile similar to normal cells; a similar correlation between centrosome abnormalities and aneuploidy has been reported in colon cancer cell lines (Ghadimi *et al.*, 2000). The increase in centrosome size due to increased pericentrin staining and dispersed pericentrin staining observed in the OSCC-derived cell lines has been suggested previously to cause accumulation of excess pericentriolar material, which might be associated with a highly anaplastic phenotype (Lingle and Salisbury, 1999). Breast tumours with excess pericentriolar material have been found to have higher frequency of abnormal mitosis (Lingle and Salisbury, 1999). It seems possible, therefore, that the excess centrosomes and pericentriolar material seen in the OSCC-derived cell lines could co-operate to perpetuate abnormal mitoses resulting in the altered chromosome number previously reported in these cell lines (Patel *et al.*, 1993)

It is interesting that H357 and H376 cells, which exhibited a centrosome profile similar to that seen in normal cells, also exhibited DNA reduplication following prolonged nocodazole arrest (Chapter Three). It is tempting to speculate that this could be caused by the specific p53 mutations carried by these cells, as studies have shown that conformational mutants of p53 can abrogate the spindle checkpoint leading to polyploidization (Gualberto *et al.*, 1998) and have varying effects on the centrosome (Tarapore *et al.*, 2001). Characterization of the effect of the p53 mutations, in H357 and H376 cells might shed some light upon how the protein regulates these two different aspects of the chromosome segregation machinery.

In addition to its role in chromosome segregation, the centrosome also coordinates other microtubule-related functions such as cell shape and polarity, through its control of number, polarity and distribution of microtubules (Fry *et al.*, 2000). Based on the hypothesis that cells showing a high level of centrosome hyperamplification would exhibit abnormalities in microtubule nucleation, centrosome function was examined in the present study by analysing the capacity of the centrosome(s) to nucleate microtubules following nocodazole-induced microtubule depolymerization. The results demonstrated a varied response amongst the OSCC-derived CIN lines, with 18.45% - 82.35% of cells nucleating microtubules 2 minutes after release from nocodazole. However, despite the delayed microtubule nucleation seen in some cell lines, the process was completed by 30 minutes in all cell lines. This observation is in contrast to the work by Ghadimi *et al.* (2000), who showed that centrosomes of aneuploid cells exhibited prolonged recovery time compared to that of diploid cells. The significance of the delayed microtubule nucleation observed in the present study in terms of centrosome function is not known.

During the assessment of centrosome function, microtubule nucleation consistently originated from one or two centrosomes only, despite the presence of supernumerary centrosomes in some cells. This suggests that not all supernumerary centrosomes have an equal potential to nucleate microtubules. Whether this inability of the supernumerary centrosomes to nucleate microtubules is restricted to the nucleation of interphase microtubules is not known, as they do nucleate microtubules during multipolar mitosis. The excessive microtubule nucleation and unorganised microtubule network observed in H413 and H357 cells following 2 minutes release from nocodazole

suggests that aspects other than the ability to nucleate microtubules, such as the ability to monitor the number of microtubules nucleated by the centrosome, might be compromised in some cell lines. Consistently, Lingle *et al.* (2002) showed that excessive microtubule nucleation, as determined by an increase in microtubule numbers nucleated by tumour centrosomes, correlated with a loss of tissue differentiation in breast tumours.

It has been assumed that cell death is the likely fate of progeny *cells generated* through an abnormal mitosis but no work has been carried out to support this hypothesis. In the present study, centrosome stability was examined in H413 cells because a high percentage of these cells exhibited centrosome abnormalities. The investigation of centrosome stability in H413 cells was initially undertaken to examine the fate of cells following an abnormal mitosis by video-microscopy of CETN2-EGFP tagged centrosomes. During the course of this work, cells with normal and abnormal number of centrosomes were observed in cloned populations of CETN2-EGFP transfected H413 cells. To ensure that this is not an artefact of transfection, cloned untransfected H413 cells were analysed and were shown to exhibit a similar combination of cells with normal and abnormal centrosome number. These observations suggest that centrosomes in H413 cells with high centrosomal abnormalities could be inherently unstable and this instability is apparent in cells with normal looking centrosomes. It is possible that centrosome instability could result in the formation of further cells containing centrosome abnormalities, which has potential to drive CIN through chromosome missegregation. There is some experimental support for this proposal because chromosome missegregation has been shown to be an incessant process, as observed through structural

variation in marker chromosomes in clonal populations of cancer cells (Reshmi *et al.*, 2004). Further evidence show that defects in chromosome segregation are intrinsic and inherited characteristics of the whole cell population in general and not just a subpopulation of cells (Reing *et al.*, 2004). The work to elucidate the fate of the progenies of an abnormal mitosis, using the CETN2-EGFP tagged H413 cells, is on going.

The question remains as to how cells survive with high centrosome numbers. A number of possible mechanisms have been proposed to explain this phenomenon. It is possible that somatic cells can use a centrosome independent pathway for spindle formation that is strong enough to drive bipolar spindle assembly (Khodjakov *et al.*, 2000). Alternatively, evidence of centrosomes clustering at the spindle poles was observed in the OSCC-derived cell lines used in this study, which suggests that supernumerary centrosomes coalesce to form a bipolar spindle (Lingle *et al.*, 1999). There is also some support for the possible acquisition of mutation(s) or clonal expansion of cells that have accrued mutation(s) that suppress centrosome abnormalities in order to enable accurate segregation of an acquired karyotype that is most conducive for survival *in vitro* (Chiba *et al.*, 2000). Finally, the hypothetical 'deamplification of centrosomes', whereby all but two dominant centrosomes are inactivated and/or eliminated, may also suppress the negative effects of centrosome hyperamplification (Brinkley, 2001).

7.3 ANALYSIS OF CENTROSOME ABNORMALITIES AND DNA PLOIDY IN ORAL DYSPLASIAS AND SCCs.

Centrosome abnormalities are common in many human cancers (Pihan *et al.*, 1998) and have been associated with tumour aggressiveness (D'Assoro *et al.*, 2002). Centrosome defects have been suggested to contribute to cancer development through the generation of CIN as these defects frequently coexist with aneuploidy in a variety of tumour types (Gustafson *et al.*, 2000, Sato *et al.*, 2001, Jiang *et al.*, 2003).

The results of Chapter Four demonstrated that centrosome abnormalities are common in OSCC-derived cell lines. In order to determine whether such abnormalities occur *in vivo*, a similar study was undertaken to examine centrosomes in oral premalignant and malignant tissues. The results demonstrate that centrosome abnormalities occur in both oral dysplasias and SCCs and were manifest as an increase in centrosome size, number and structural defects such as elongated centrosomes. These abnormalities are consistent with those documented in other studies (Pihan *et al.*, 1998; Jiang *et al.*, 2003; Pihan *et* al., 2003). Interestingly, increase in centrosome size and structural defects such as elongated centrosomes were observed more frequently *in vivo*, in contrast to the more prevalent numerical abnormalities observed in cultured cells.

In the present study, 100% (17/17) of the SCCs examined exhibited centrosome abnormalities, demonstrating that centrosome abnormalities are prevalent in oral cancer. The percentage of tumour cells exhibiting these abnormalities correlated significantly with increasing histological grade, whereby well

differentiated tumours exhibited the lowest (2.5%), whilst poorly differentiated tumours exhibited the highest percentage of cells (4.5%) with centrosome abnormalities. Similarly, a high prevalence of centrosome abnormalities and an increased incidence of centrosome abnormalities in high-grade tumours have also been reported in oral (Carroll *et al.*, 1999; Gustafson *et al.*, 2000) and various other cancers (Pihan *et al.*, 1998; Sato *et a*l., 1999; Pihan *et al.*, 2001; 2003; Jiang *et al.*, 2003). The correlation between centrosome abnormalities and a loss of tumour cell differentiation suggests that centrosome abnormalities might contribute to tumour aggressiveness (Sparano *et al.*, 2004). It has been proposed that centrosome dysfunction could cause modification of the microtubule cytoskeleton leading to cellular disorganization, creating cells that are predisposed to additional changes that could lead to aggressive tumour development (Pihan *et al.*, 2001) and tumour recurrence (Gustafson *et al.*, 2000).

Examination of centrosome abnormalities in the premalignant tissues showed that 100% (28/28) of oral dysplasias exhibited centrosomal abnormalities, although the percentage of cells exhibiting these abnormalities were low (1.7%-2.3%). The present study is the first to examine centrosome abnormalities in oral dysplasias and the results indicate that these abnormalities might occur early in oral cancer. To investigate whether centrosome abnormalities might be associated with malignant progression, these defects were examined in the context of DNA ploidy. It has been shown previously that aneuploidy is a reliable marker of malignant transformation in oral dysplasias (Sudbo *et al.*, 2001a; 2001b). In the present study, there was only a slight increase in the

prevalence of centrosome abnormalities in the aneuploid compared to the diploid lesions (2% vs 1.7%) and the difference was not statistically significant.

In the present study, 10/25 (40%) of dysplasias were classified as aneuploid, which is higher than that reported (17%) in the cohort of patients used by Sudbo *et al.* (2001a). Whether these differences reflect low sample numbers, the high number of severe dysplasias used and/or population-based differences is unknown. It is cautionary, however, to note that the findings of Sudbo and co-workers have not been verified in other laboratories. A longitudinal study using dysplasias with known outcomes is required to examine any association between centrosome abnormalities and malignant progression.

Due to the presence of centrosome abnormalities in all dysplasias regardless of ploidy status, it remains a possibility that centrosome abnormalities do not correlate with aneuploidy in early lesions of oral cancer. Support for this proposal comes from the observation that centrosome abnormalities have been observed in grade 1, diploid bladder cancer cells (Jiang *et al.*, 2003) and centrosome defects have been detected in carcinomas *in situ* that lacked CIN (Pihan *et al.*, 2003). This is in contrast to the many studies that have reported a strong correlation between centrosome abnormalities and aneuploidy (Jiang *et al.*, 2003; Pihan *et al.*, 2001; Lingle *et al.*, 2002; Pihan *et al.*, 1998). These interpretations were, however, based on the analyses of centrosome abnormalities and aneuploidy in malignant tumours and metastatic lesions (Jiang *et al.*, 2003; Pihan *et al.*, 2001; Lingle *et al.*, 2002; Pihan *et al.*, 1998) in which both phenotypes are found to be highly prevalent. It is possible that the centrosome abnormalities observed in diploid dysplasias in the present study

could have arisen as a consequence of the deregulated cellular growth and differentiation that is associated with the dysplastic phenotype.

It remains a possibility that centrosome abnormalities could potentially drive oral cancer progression by perpetuating CIN, based on the concomitant presence of centrosome abnormalities with abnormal mitoses in the oral lesions. It is also likely that additional mutations might be required before the centrosome abnormalities observed in the dysplasias could actively drive CIN and oral cancer progression. An increase in centrosome abnormalities was observed in this study during transition from dysplasias (1.7%-2.3%) to SCCs (2.5%-4.5%). The transition to the invasive phenotype has also been shown to be the period during which inactivation of p53 usually occurs in oral cancer (Shanavaz *et al.*, 2000) and centrosome abnormalities have been shown to occur in tandem with p53 inactivation in oral carcinomas (Carroll *et al.*, 1999) This suggests that inactivation of p53 might co-operate with centrosome defects leading to CIN and could potentially provide an explanation as to why the correlation between centrosome abnormalities and, aneuploidy is more prominent during the later stages of cancer (Jiang *et al.*, 2003; Pihan *et al.*, 2001; Lingle *et al.*, 2002; Pihan *et al.*, 1998). Centrosome abnormalities have also been observed following inactivation of downstream targets of p53, such as p21/Waf1 (Mantel *et al.*, 1999) and GAAD45 (Hollander and Fornace, 2002), overexpression of centrosome associated proteins such as aurora2/STK15/BTAK (Zhou *et al.*, 1998) and pericentrin (Pihan et al., 2001) and mutations in DNA repair genes such as BACR1 (Xu *et al.*, 1999) and BACR2 (Tutt *et al.*, 1999). It is currently not known which of these mechanisms are responsible for the centrosome

defects seen in the various cancers or if alternative mechanisms could be involved in mediating these effects.

7.4 THE DEVELOPMENT OF AN *IN VITRO* MODEL OF CIN IN IMMORTALISED HUMAN NORMAL ORAL KERATINOCYTES

The presence of CIN in cancer has been demonstrated unequivocally (Knuutila *et al.*, 1999). Whilst mutations in mitotic checkpoint genes such as BUB1 and MAD2 have been reported in a limited number of cancers, little is known about the mechanisms underlying CIN and how they facilitate cancer progression. The development of an *in vitro* model of CIN, therefore, would greatly facilitate the understanding of the cellular and molecular mechanisms underlying human carcinogenesis and would likely have implications for cancer therapy and prevention in the future.

Historically, the study of chemical carcinogenesis has relied heavily on the use of rodent (Li *et al.*, 1997; Duesberg *et al.*, 2000; Fabarius *et al.*, 2002) or malignant (Bardelli *et al.*, 2001) cells. These cells are more susceptible to chemical manipulations, as demonstrated by the induction of aneuploidy in a 100% of Chinese hamster cells after treatment with aromatic polycyclic hydrocarbons (Li *et al.*, 1997), but normal human cells have generally been shown to be resistant to neoplastic transformation (Rhim, 1991). The present study examined the potential of inducing CIN in human immortalised normal oral keratinocytes. PhIP, a bulky adduct forming agent belonging to the family of heterocyclic aromatic amines (HCA; Schut *et al.*, 1999) was chosen because it has been shown previously to induce CIN in malignant cells (Bardelli *et al.*, 2001). In the present study, human normal oral keratinocytes immortalised with

hTERT, the catalytic subunit of telomerase, were used because they have an infinite life span in contrast to normal cells that senesce in culture (Dickson *et al.*, 2000). Further, the results of this study show that these cells have acquired only a small number of genetic alterations, most likely associated with immortalisation. In the present study, the development of PhIP-resistance in human immortalised normal oral keratinocytes resulted in consistent chromosomal abnormalities, as determined by CGH. Compared to the parental OKF6/TERT-1 cells, all PhIP-resistant clones exhibited gains of chromosome 8, 9p21/22-qter and 20 at lower passage (4-5) and an additional gain of chromosome 7 in three clones at higher passage (22-25).

The results of the present study contrast with those of Bardelli *et al.* (2001) who showed that the development of PhIP resistance in colorectal cancer cells induced a dynamic CIN, which translated to loss or gain of one chromosome for every five cell division. These differences might be attributed to the techniques employed to evaluate CIN. Bardeli *et al.* (2001) used FISH to examine alterations in genome content, whilst CGH was used in the present study. FISH is more sensitive compared to CGH, as it is able to detect copy number changes of single chromosomes, whilst CGH detects gross changes in the genome. Therefore, if CIN was induced in only a small population of cells in the present study, it is possible that this might be too low to be detected by CGH. A preliminary FISH analysis using a centromeric probe to chromosome 11 revealed three times more monosomy of chromosome 11 in the PhIP-resistant cells compared to the parental cells (data not shown). Whether this reflects the presence of a population of cells with ongoing CIN is currently not known.

A recent two-step model of carcinogenesis proposed by Rasnick and Duesberg (1999) suggests that the initiation step of carcinogenesis involves the production of non-cancerous aneuploid cells, which is below the threshold for cancer and a latter promotion step allows the threshold of aneuploidy for cancer to be reached. It is, therefore, not unreasonable to speculate that the PhIP-resistant clones have only reached the initiation stage and it is possible that additional inactivation of vital genes, such as p53, might be required to breach the threshold for the induction of a dynamic CIN. For example, extensive aneuploidy was successfully induced using benzo[a]pyrene in SV40 immortalised nontumorigenic human lung fibroblast MRC-5 SV2 cells, which had inactivated p53 as a result of sequestration by SV40 (Zhu *et al.*, 2002). By contrast, the OKF6/TERT-1 cells used in this study have wild type p53 (Dickson *et al.*, 2000) and it would be of great interest to determine if abrogation of p53 in the PhIP-resistant clones could induce CIN in these cells or whether p53 inactivation might be required from the outset.

It remains a possibility that PhIP cannot induce CIN in normal cells and that the consistent chromosome gains observed in the PhIP-resistant clones are specific to the development of carcinogen resistance. This is not unprecedented because CGH analysis of PhIP-induced mammary carcinomas in rats showed consistent losses in regions of chromosome 2, 3, 11, 18 and X and these lesions were suggested to be potentially orthologous to regions of human chromosome 5q, 11p, 3p, 18q and X respectively, which harbour deletions in certain human breast cancers (Christian *et al.*, 2002).

Having determined that the induction of PhIP resistance resulted in only consistent chromosomal changes, the response of the PhIP-resistant clones to irradiation induced DNA damage was analysed to determine if the development of PhIP-resistance was associated with an altered response to other forms of DNA damage. The cellular response to irradiation was assessed in terms of cell viability, the induction of apoptosis, the activation of the p53 pathway and cell cycle arrest. Both parental and PhIP-resistant clones demonstrated similar growth inhibitory and apoptotic responses, had an intact p53 pathway and were capable of cell cycle arrest following irradiation. The similarities between the parental cells and PhIP resistant clones in their response to irradiation induced DNA damage indicate that the DNA damage response of these clones was not altered and, therefore, could not be associated with the induction of PhIP-resistance. Recently, Rubio *et al.* (2004) showed that telomerase activation confers resistance to genotoxic stresses such as irradiation and bleomycin. Since the OKF6/TERT-1 parental cells were immortalised through reactivation of telomerase, it is not certain if its protective mechanism could mask the presence of a damaged DNA response in the PhIP-resistant clones, thus conferring resistance to irradiation induced DNA damage. It is also possible that this protective mechanism may well have functioned from the beginning to prevent the induction of a dynamic CIN in the PhIP treated OKF6/TERT-1 cells.

7.5 CONCLUDING REMARKS

The results of the present study showed that H357 and H400 have an intact mitotic checkpoint, whilst the checkpoint could be attenuated in H103, H157, H314, H376 and H413 cells. H357 and H376 cells also exhibited a defective post-mitotic checkpoint. Although H357 and H376 exhibited centrosome profiles that were similar to normal cells, centrosome abnormalities were detected in all the remaining cell lines. Furthermore, the study showed that centrosomes in H357 and H413 might be defective in monitoring the number of microtubules nucleated and cells with high centrosome abnormalities might have an inherent defect in maintaining normal centrosome numbers. These results suggest that defects of the mitotic and post-mitotic checkpoints and centrosomes could singly or co-operatively perpetuate chromosome missegregation. It seems likely, therefore, that more than one route exist for the induction of aneuploidy and CIN in oral cancer.

The examination of centrosome abnormalities in the context of DNA ploidy in the dysplasias showed that centrosome abnormalities occurred irrespective of aneuploidy and increased during the transition from dysplasias to carcinomas. This suggests that centrosome abnormalities appear early and precede CIN in oral cancer and additional alterations might be required before these abnormalities can play an active role in driving oral tumour progression. In this study, centrosome abnormalities correlated with a loss of tumour cell differentiation in the SCCs suggesting that they could contribute towards tumour aggressiveness during the later stages of the disease.

Consistent with these observations, an increasing number of studies show that a defective post-mitotic or G1/S cell cycle checkpoint could lead to tetraploidization of the genome and the consequential inheritance of increased centrosome numbers (Borel *et al.*, 2002), which could synergise to destabilise the genome through chromosome missegregation. Telomere dysfunction could further synergise with these mechanisms in perpetuating CIN, as it has been shown to occur in conjunction with centrosome abnormalities and aneuploidy (Gisselsson *et al.*, 2002).

7.6 FUTURE WORK

During the course of this study, two areas of research have emerged that are likely to have important implications in our understanding of the mechanisms underlying CIN in oral cancer.

The results of Chapter Three have indicated that an attenuated rather than an *abrogated mitotic checkpoint* could be one of the mechanisms underlying CIN in oral cancer. Haplo-insufficiency of mitotic checkpoint genes has recently been reported to cause attenuation of the mitotic checkpoint (Michel *et al.*, 2001). The status of the mitotic checkpoint genes in oral cancer is largely unknown and the analysis of the expression of these genes in the OSCC-derived cell lines and oral carcinomas would extend the observations of the present study and indicate whether haplo-insufficiency of the mitotic checkpoint genes is common in oral cancer.

The results of the present study have indicated that the development of CIN in oral cancer is likely to involve multiple mechanisms or pathways. Telomere dysfunction is emerging as a potential mechanism leading to CIN as it occurs in conjunction with aneuploidy and centrosome abnormalities in head and neck tumours (Gisselsson *et al.*, 2002). The consequence of telomeric attrition on the stability of the genome and chromosome structure can be first examined *in vitro* using the system created by Rubio *et al.* (2002), which uses retroviral transduction of cells with a combination of Cre-recombinase flanked hTERT, catalytic subunit of telomerase, and TIN2, a negative regulator of telomere length, to create a population of cells with varying telomere length. The effect of short telomeres on the genome can then be investigated using CGH or

conventional karyotyping. Furthermore, this model could also be used to study telomeres in the context of the mitotic checkpoint or the centrosomes by using RNAi to knockdown genes that will lead to defects in these mechanisms, *in cells* with shortened centrosomes. Normal human oral fibroblasts or oral keratinocytes would be ideal for such studies, as genetic alterations caused by telomere dysfunction could be easily detected against the normal diploid genome of these cells.

REFERENCES

Abrieu A, Magnaghi-Jaulin L, Kahana JA, Peter M, Castro A, Vigneron S, Lorca T, Cleveland DW, Labbe JC. Mps1 is a kinetochore-associated kinase essential for the vertebrate mitotic checkpoint. *Cell* **106**: 83-93 (2001)

Ai H, Barrera JE, Meyers AD, Shroyer KR, Varella-Garcia M. Chromosomal aneuploidy precedes morphological changes and supports multifocality in head and neck lesions. *Laryngoscope* **111**: 1853-1858 (2001)

Andreassen PR, Martineau SN, Margolis RL. Chemical induction of mitotic checkpoint override in mammalian cells results in aneuploidy following a transient tetraploid state. *Mutation Research* **372**: 181-194 (1996)

Andreassen PR, Lohez OD, Lacroix FB, Margolis RL. Tetraploid state induces p53-dependent arrest of nontransformed mammalian cells in G1. *Molecular Biology of the Cell* **12**: 1315-1328 (2001a)

Andreassen PR, Lacroix FB, Lohez OD, Margolis RL. Neither $p21^{WAF1}$ nor 14-3-3sigma prevents G2 progression to mitotic catastrophe in human colon carcinoma cells after DNA damage, but $p21^{WAF1}$ induces stable G1 arrest in resulting tetraploid cells. *Cancer Research* **61**: 7660-7668 (2001b)

Andreassen PR, Lohez OD, Margolis RL. G2 and spindle assembly checkpoint adaptation, and tetraploidy arrest: Implications for intrinsic and chemically induced genomic instability. *Mutation Research* **532**: 245-253 (2003)

Artandi SE, DePinho RA. A critical role for telomeres in suppressing and facilitating carcinogenesis. *Current Opinion in Genetics and Development* **10**: 39-46 (2000)

Babu JR, Karthik B, Jeganathan, Baker DJ, Wu X, Kang-Decker N, van Deursen JM. Rae1 is an essential mitotic checkpoint regulator that cooperates with Bub3 to prevent chromosome missegregation. *Journal of Cell Biology* **160**: 341-353 (2003)

Balczon R. Centrosome replication in somatic cells: the significance of G_1 phase. *Current Topics in Developmental Biology* **49**: 251-265 (2000)

Bardelli A, Cahill DP, Lederer G, Speicher MR, Kinzler KW, Vogelstein B, Lengauer C. Carcinogen-specific induction of genetic instability. *Proceedings of the National Academy of Sciences USA* **98**: 5770 – 5775 (2001)

Bharadwaj R, Yu H. The spindle checkpoint, aneuploidy and cancer. *Oncogene* **23**: 2016-2027 (2004)

Blajeski AL, Phan VA, Kottke TJ, Kaufmann SH. G1 and G2 cell-cycle arrest following microtubule depolymerization in human breast cancer cells. *Journal of Clinical Investigation* **110**: 91-99 (2002)

Borel F, Lohez OD, Lacroix FB, Margolis RL. Multiple centrosomes arise from tetraploidy checkpoint failure and mitotic centrosome clusters in p53

and RB pocket protein-compromised cells. *Proceedings of National Academy of Sciences USA* **99**: 9819-9824 (2002)

Bradley G, Irish J, MacMillan C, Mancer K, Witterick I, Hartwick W, Gullane P, Kamel-Reid S, Benchimol S. Abnormalities of the ARF-p53 pathway in oral squamous cell carcinoma. *Oncogene* **20**: 654-8 (2001)

Brinkley BR. Managing the centrosome number game: from chaos to stability in cancer cell division. *Trends in Cell Biology* **11**: 18-21 (2001)

Buch SC, Notani PN, Bhisey RA. Polymorphism at GSTM1, GSTM3 and GSTT1 gene loci and susceptibility to oral cancer in an Indian population. *Carcinogenesis* **23**: 803-807 (2002)

Buermeyer AB, Deschenes SM, Baker SM, Liskay RM. Mammalian DNA mismatch repair. *Annual Review of Genetics* **33**: 533-64 (1999)

Cahill DP, Lengauer C, Yu J, Riggins GJ, Willson JK, Markowitz SD, Kinzler KW, Vogelstein B. Mutations of mitotic checkpoint genes in human cancers. *Nature* **392**: 300-303 (1998)

Cahill DP, da Costa LT, Carson-Walter EB, Kinzler KW, Vogelstein B, Lengauer C. Characterization of MAD2B and Other Mitotic Spindle Checkpoint Genes. *Genomics* **58**: 181-187 (1999)

Califano J, Riet P, Westra W, Nawroz H, Clayman G, Piantadosi RC, Lee D, Greenberg B, Koch W, and Sidransky D. Genetic progression model for Head and Neck Cancer: Implications for field cancerization. *Cancer Research* **56**: 2488-2492 (1996)

Campisi J, Kim S, Lim C, Rubio M. Cellular senescence, cancer, aging: the telomere connection. *Experimental Gerontology* **36**: 1619-1637 (2001)

Cancer Research Campaign. Cancer Stats: Oral-UK (2000)

Carroll PE, Okuda M, Horn HF, Biddinger P, Stambrook PJ, Gleich LL, Li YQ, Tarapore P, Fukasawa K. Centrosome hyperamplification in human cancer: chromosome instability induced by p53 mutation and/or Mdm2 overexpression. *Oncogene* **18**: 1935-1944 (1999)

Chan GKT, Jablonski SA, Sudakin V, Hittle JC, Yen TJ. Human BUBR1 is a mitotic checkpoint kinase that monitors CENP-E functions at kinetochores and binds the cyclosome/APC. *Journal of Cell Biology* **146**: 941-954 (1999)

Chan TA, Hwang PM, Hermeking H, Kinzler KW, Vogelstein B. Cooperative effects of genes controlling the G(2)/M checkpoint. *Genes and Development* **14**: 1584-1588 (2000)

Chen RH, Water JC, Salmon ED, Murray AW. Association of spindle assembly checkpoint component XMAD2 with unattached kinetochores. *Science* **274**: 242-246 (1996)

Chen TR. In situ detection of mycoplasma contamination in cell cultures by fluorescent Hoechst 33258 stain. *Experimental Cell Research* **104**: 255-262 (1997)

Chiba S, Okuda M, Mussman JG, Fukasawa K. Genomic convergence and suppression of centrosome hyperamplification in primary $p53^{-/-}$ cells in prolonged culture. *Experimental Cell Research* **258**: 310-321 (2000)

Christian AT, Snyderwine EG, Tucker JD. Comparative genomic hybridisation analysis of PhIP-induced mammary carcinomas in rats reveals a cytogenetic signature. *Mutation Research* **506-507**: 113-119 (2002)

Cruz IB, Snijders PJF, Meijer CJ, Braakhuis BJ, Snow GB, Walboomers JM, van der Waal I. p53 expression above the basal cell layer in oral mucosa is an early event of malignant transformation and has predictive value for developing oral squamous cell carcinoma. *Journal of Pathology* **184**: 360-368 (1998)

Cruz IB, Meijer CLJM, Snijders PJF, Snow GB, Walboomers JMM, van der Waal I. p53 immunoexpression in non-malignant oral mucosa adjacent to oral squamous cell carcinoma: potential consequence for clinical management. *Journal of Pathology* **191**: 132-137 (2000)

D'Assoro AB, Barrett SL, Folk C, Negron VC, Boeneman K, Busby R, Whitehead C, Stivala F, Lingle WL, Salisbury JL. Amplified centrosomes in breast cancer: a potential indicator of tumour aggressiveness. *Breast Cancer Research and Treatment* **75**: 25-34 (2002)

de Lange T. Protection of mammalian telomeres. *Oncogene* **21**: 532-540 (2002)

Crissman JD, Sakr WA. Squamous Intraepithelial Neoplasia of the Upper Aerodigestive Tract. In: *Diagnostic Surgical Pathology of the Head and Neck*. Ed. Douglas RG. W.B. Saunders Company. pp 1-17 (2001)

Dickson MA, Hahn WC, Ino Y, Ronfard V, Wu JY, Weinberg RA, Louis DN, Li FP, and Rheinwald JG. Human keratinocytes that express hTERT and also bypass a $p16^{INK4A}$ – enforced mechanism that limits life span become immortal yet retain normal growth and differentiation characteristics. *Molecular and Cellular Biology* **20**: 1436-1447 (2000)

Duesberg P, Rausch C, Rasnick D, Hehlmann R. Genetic instability of cancer cells is proportional to the degree of aneuploidy. *Proceedings of National Academy of Sciences USA* **95**: 13692-13697 (1998)

Duesberg P, Li R, Rasnick D, Rausch C, Willer A, Kraemer A, Yerganian G, and Hehlmann R. Aneuploidy Precedes and Segregates with Chemical Carcinogenesis. *Cancer, Genetics and Cytogenetics* **119**:83-93 (2000)

Duesberg P, Rasnick D. Aneuploidy, the somatic mutation that makes cancer a species of its own. *Cell Motility and Cytoskeleton* **47**: 81-107 (2000)

Duesberg P, Li R. Multistep carcinogenesis. A chain reaction of aneuploidizations. *Cell Cycle* **2**: 202-210 (2003)

Duesberg P, Fabarius A, Hehlmann R. Aneuploidy, the primary cause of the multilateral genomic instability of neoplastic and preneoplastic cells. *International Union of Biochemistry and Molecular Biology: Life* **56**: 65-81 (2004)

Dyer S, Prebble E, Davison V, Davies P, Ramani P, Ellison D, Grundy R. Genomic imbalances in paediatric intracranial ependymomas defines clinically relevant groups. *American Journal of Pathology* **161**: 2133-2141 (2002)

Fabarius A, Willer A, Yerganian G, Helhmann R, Duesberg P. Specific aneusomies in Chinese hamster cells at different stages of neoplastic transformation, initiated by nitrosomethylurea. *Proceedings of National Academy of Sciences USA* **99**: 6778-6783 (2002)

Fabarius A, Hehlmann R, Duesberg PH. Instability of chromosome structure in cancer cells increases exponentially with degrees of aneuploidy. *Cancer Genetics and Cytogenetics* **143**: 59-72 (2003)

Fry AM, Mayor T, Nigg EA. Regulating centrosomes by protein phosphorylation. *Current Topics in Developmental Biology* **49**: 291-312 (2000)

Fukasawa K. Introduction. *Oncogene* **21**: 6140-6145 (2002)

Gasco M, Crook T. The p53 network in head and neck cancer. *Oral Oncology* **39**: 222-231 (2003)

Ghadimi BM, Sackett DL, Difilippantonio MJ, Schrock E, Neumann T, Jauho A, Auer G, Ried T. Centrosome amplification and instability occurs exclusively in aneuploid, but not in diploid colorectal cancer cell lines, and correlates with numerical chromosomal aberrations. *Genes, Chromosomes and Cancer* **27**: 183-90 (2000)

Giesselsson D, Jonson T, Petersen A, Strombeck B, Cin PD, Hoglund M, *Mitelman F, Mertens F, Mandahl* N. Telomere dysfunction triggers extensive DNA fragmentation and evolution of *complex chromosome abnormalities in* human malignant tumours. *Proceedings of National Academy of Science USA* **98**: 12683-12688 (2001a)

Gisselsson D, Bjork J, Hoglund M, Mertens F, Cin PD, Akerman M, Mandahl N. Abnormal nuclear shape in solid tumors reflects mitotic instability. *American Journal of Pathology* **158**: 199-206 (2001b)

Gisselsson D, Jonson T, Yu C, Martins C, Mandahl N, Wiegant J, Jin Y, Mertens F, Jin C. Centrosomal abnormalities, multipolar mitoses and chromosomal instability in head and neck tumours with dysfunctional telomeres. *British Journal of Cancer* **87**: 202-207 (2002)

Gualberto A, Aldape K, Kozakiewicz K, Tlsty TD. An oncogenic form of p53 confers a dominant, gain-of-function phenotype that disrupts spindle checkpoint control. *Proceedings of National Academy of Sciences USA* **95**: 5166-5171 (1998)

Gustafson LM, Gleich LL, Fukasawa K, Chadwell J, Miller MA, Stambrook PJ, Gluckman JL. Centrosome hyperamplification in head and neck squamous cell carcinoma: A potential phenotypic marker of tumour aggressiveness. *Laryngoscope* **110**: 1798-1801 (2000)

Hardwich KG, Murray AW. Mad1p, a phosphoprotein component of the spindle assembly checkpoint in budding yeast. *Journal of Cell Biology* **131**: 709-720 (1995)

Hartwell L. Defects in a cell cycle checkpoint may be responsible for the genomic instability of cancer cells. *Cell* **71**: 543-546 (1992)

Harty LC, Capsraso NE, Hayes RB. Alcohol dehydrogenase 3 genotype and risk of the oral cavity and pharyngeal cancers. *Journal of National Cancer Institute* **89**: 1698-1705 (1997)

Haruki N, Saito H, Harano T, Nomoto S, Takahashi T, Osada H, Fujii Y, Takahashi T. Molecular analysis of the mitotic checkpoint genes BUB1, BUBR1 and BUB3 in human lung cancer. *Cancer Letters* **162**: 201-205 (2001)

Hempen PA, Kurpad H, Calhoun ES, Abraham S, Kern SE. A double missense variation of the BUB1 gene and a defective mitotic spindle checkpoint in the pancreatic cancer cell line Hs766T. *Human Mutation* **21**: 445-450 (2003)

Hermsen MAJA, Joenje H, Arwert F, Braakhuis BJM, Baak JPA, Westerveld A, Slater R. Assessment of chromosomal gains and losses in oral squamous cell carcinoma by comparative genomic hybridisation. *Oral Oncology* **33**: 414-418 (1997)

Hernando E, Orlow I, Liberal V, Nohales G, Benezra R, Cardo CC. Molecular analyses of the mitotic checkpoint components HSMAD2, HBUB1 and HBUB3 in human cancer. *International Journal of Cancer*. **95**: 223-227 (2001)

Hinchliffe EH, Li C, Thompson EA, Maller JL, Sluder G. Requirement of cdk2-cyclin E activity for repeated centrosome production in *Xenopus* egg extracts. *Science* **283**: 851-854 (1999)

Hinchcliffe EH, Miller FJ, Cham M, Khodjakov A, Sluder G. Requirement of a centrosomal activity for cell cycle progression through G1 into S phase. *Science* **291**: 1547-1550 (2001)

Hoeijmakers JHJ. Genome maintenance mechanisms for preventing cancer. *Nature* **411**: 366–374 (2001)

Hollander MC, Fornace AJ Genomic instability, centrosome amplification, cell cycle checkpoints and Gadd45a. *Oncogene* **21**: 6228-6233 (2002)

Hyot MA, Totis L, Roberts BT. S.cerevisiae genes requires for cell cycle arrest in response to loss of microtubule function. *Cell* **66**: 507-517. (1991)

Ishwad CS, Ferrell RE, Rossie KM, Apple BN, Johnson JT, Myers EN, Law JC, Srivastava S, Gollin SM. Microsatellite instability in oral cancer. *International Journal of Cancer* **20**: 332-335 (1995)

Jang SJ, Chiba I, Hirai A, Hong WK, Mao L. Multiple oral squamous epithelial lesion: are they genetically related? *Oncogene* **20**: 2235-2242 (2001)

Jiang WW, Fujii H, Shirai T, Mega H, Takagi M. Accumulative increase of loss of heterozygosity from leukoplakia to foci of early cancerization in leukoplakia of the oral cavity. *Cancer* **92**: 2349-2356 (2001)

Jiang F, Caraway NP, Sabichi AL, Zhang HZ, Ruitrok A, Grossman B, Gu J, Lerner SP, Lippman S, Katz RL. Centrosomal abnormality is common in and a potential biomarker for bladder cancer. *International Journal of Cancer* **106**: 661-665 (2003)

Jiricny, J. Replication errors: Cha(lle)nging the genome. *EMBO Journal* **17**: 6427-6436 (1998)

Jiricny J, Lahti MN. Mismatch repair defects in cancer. *Current Opinion in Genetics and Development* **10**: 157-161 (2000)

Kasai T, Iwanaga Y, Iha H, Jeang KT. Prevalent loss of mitotic spindle checkpoint in adult T-cell leukaemia confers resistance to microtubule inhibitors. *Journal of Biology and Chemistry* **277**: 5187-5193 (2002)

Kawamura K, Izumi H, Ma Z, Ikeda R, Moriyama M, Tanaka T, Nojima T, Levin LS, Yamamoto KF, Suzuki K, Fukasawa K. Induction of centrosome amplification and chromosome instability in human bladder cancer cells by p53 mutation and cyclin E overexpression. *Cancer Research* **64**: 4800-4809 (2004)

Khodjakov A, Cole RW, Oakley BR, Rieder CL Centrosome-independent mitotic spindle formation in vertebrates. *Current Biology* **10**: 59-67 (2000)

Kim MM, Califano JA. Molecular pathology of head-and-neck cancers. *International Journal of Cancer* **112**: 545-553 (2004)

Knuutila S, Aalto Y, Autio K, Bjorkqvist AM, El-Rifai W, Hemmer S, Huhta T, Kettunen E, Kiuru-Kuhlefelt S, Larramendy ML, Lushnikova T, Monnin O, Pere H, Tapper J, Tarkkanen, Varis A, Wasenius VM, Wolf M, Zhu Y. DNA copy number losses in human neoplasms. *American Journal of Pathology* **155**: 683-694 (1999)

Komarova NL, Sengupta A, Nowak M. Mutation-selection networks of cancer initiation: tumour suppressor genes and chromosomal instability. *Journal of Theoretical Biology* **223**: 433-450 (2003)

Kops GJPL, Foltz DR, Cleveland DW. Lethality to human cancer cells through massive chromosome loss by inhibition of the mitotic checkpoint. *Proceedings of National Academy of Science USA* **101**: 8699-8704 (2004)

Kuo MYP, Huang JS, Hsu HC, Chiang CP, Kok SH, Kuo YS. Hong CY. Infrequent p53 mutations in patients with areca quid chewing-associated oral squamous cell carcinomas in Taiwan. *Journal of Oral Pathology and Medicine* **28**: 221-225 (1999)

Lacey KR, Jackson PK, Searns T. Cyclin-dependent kinase control of centrosome duplication. *Proceedings of National Academy of Sciences USA* **96**: 2817-2822 (1999)

Langdon JD. Mouth cancer and jaw tumours. In: Malignant Tumours of the Mouth, Jaw and Salivary Gland eds. JD Langdon and JM Henk. Edward Arnold London pp 36-44 (1995)

Langerod A, Stromberg M, Chin K, Kristen VN, Borresen-Dale AL. BUB1 infrequently mutated in human breast carcinomas. *Human Mutation* **22**: 420-424 (2003)

Lanni JS, Jacks T. Characterization of the p53-dependent postmitotic checkpoint following spindle disruption. *Molecular and Cellular Biology* **18**: 1055-1064 (1998)

Lee JJ, Hong WK, Hittelman WN, Mao L, Lotan R, Shin DM, Benner SE, Xu XC, Lee JS, Papadimitrakopoulou VM, Geyer C, Perez C, Martin JW, El-Naggar AK, Lippman SM. Predicting cancer development in oral leukoplakia: ten years of translational research. *Clinical Cancer Research* **6**: 1702-1710 (2000)

Lengaur C, Kinzler KW, Vogelstein B. Genetic instability in colorectal cancers. *Nature* **386**: 623-627 (1997).

Lengauer C, Kinzler KW, Vogelstein B. Genetic Instabilities in Human Cancers. *Nature* **396**: 643-649 (1998)

Levine DS, Sanchez CA, Rabinovitch PS, Reid BJ. Formation of the tetraploid intermediate is associated with the development of cells with more than four centrioles in the elastase-simian virus 40 tumour antigen transgene mouse model of pancreatic cancer. *Proceedings of National Academy of Sciences USA* **88**: 6427-6431 (1991)

Li R, Murray AW. Feed back control of mitosis in budding yeast. *Cell* **66**: 519-531 (1991)

Li Y, Benezra R. Identification of human mitotic checkpoint gene: hsMAD2. *Science* **274**: 246-248 (1996)

Li R, Yerganian G, Duesberg P, Kraemer A, Willer A, Rausch C, Hehlmann R. Aneuploidy correlated 100% with chemical transformation of Chinese hamster cells. *Proceedings of National Academy of Sciences USA* **94**: 14506-14511 (1997).

Li R, Sonik A, Stindl R, Rasnick D, Duesberg P. Aneuploidy vs. gene mutation hypothesis of cancer: Recent study claims mutation but is found to support aneuploidy. *Proceedings of National Academy of Sciences USA* **97**: 3236-3241 (2000)

Lingle WL, Lutz WH, Ingle JN, Maihle N.J, Salisbury JL. Centrosome hyperthrophy in human breast tumors: Implications for genomic instability and cell polarity. *Proceedings of National Academy of. Sciences USA* **95**: 2950-2955 (1998).

Lingle WL, Salisbury JL. Altered centrosome structure is associated with abnormal mitoses in human breast tumours. *American Journal of Pathology* **155**: 1941-1951 (1999)

Lingle WL, Barret SL, Negron VC, D'Assoro AB, Boeneman K, Liu W, Whitehead CM, Reynolds C, Salisbury JL. Centrosome amplification drives chromosomal instability in breast tumor development. *Proceedings of National Academy of Science USA* **99**: 1978-1983 (2002)

Lippman SM, Hong WK. Molecular markers of the risk of oral cancer. *New England Journal of Medicine* **344**: 1323-1326 (2001)

Loeb LA. A mutator phenotype in cancer. *Cancer Research* **61**: 3230-3239 (2001)

Loeb LA, Loeb KR, Anderson JP. Multiple mutations and cancer. *Proceedings of National Academy of Sciences USA* **100**: 776-781 (2003)

Mantel C, Braun SE, Reid S, Henegariu O, Liu L, Hangoc G, Broxmeyer HE. p21 cip-1/waf-1 deficiency causes deformed nuclear architecture, centriole overduplication, polyploidy and relaxed microtubule damage checkpoints in human hematopoietic cells. *Blood* **93**: 1390-1398 (1999).

Mao L, Lee JS, Fan YH, Ro JY, Batsakis JG, Lippman S, Hittelman W, Hong WK. Frequent microsatellite alterations at chromosomes 9p21 and 3p14 in oral premalignant lesions and their value in cancer risk assessment. *Nature Medicine* **2**: 682-685 (1996)

Mao L. Leukoplakia: molecular understanding of pre-malignant lesions and implications for clinical management. *Molecular Medicine Today* **3**: 442-448 (1997)

Margolis RL, Lohez OD, Andreassen PR. G1 tetraploidy checkpoint and the suppression of tumorigenesis. *Journal of Cellular Biochemistry* **88**: 673-683 (2003)

Masayesva BG, Ha P, Garrett-Mayer E, Pilkington T, Mao R, Pevsner J, Speed T, Benoit N, Moon CS, Sidransky D, Westra WH, Califano J. Gene

expression alterations over large chromosomal regions in cancer include multiple genes unrelated to malignant progression. *Proceedings of the National Academy of Sciences USA* **101**: 8715-8720 (2004)

Maser RS, DePinho RA. Connecting chromosome, crisis and cancer. *Science* **297**: 565-569 (2002)

Meeker AK, Hicks JL, Iacobuzio-Donahue CA, Montgomery EA, Westra WH, Chan TY, Ronnett BM, Marzo AMD. Telomere length abnormalities occur early in the initiation of epithelial carcinogenesis. *Clinical Cancer Research* **10**: 3317-3326 (2004)

Meraldi P, Lukas J, Fry AM, Bartek J, Nigg EA Centrosome duplication in mammalian somatic cells requires E2F and Cdk2-CyclinA. *Nature Cell Biology* **1**: 88-93 (1999)

Meraldi P, Honda R, Nigg EA. Aurora-A overexpression reveals tetraploidization as a major route to centrosome amplification in p53-/- cells. *EMBO Journal* **21**: 483-492 (2002)

Michel LS, Liberal V, Chatterjee A, Kirchwegger R, Paschel B, Gerald W, Dobles M, Sorger PK, Murty VVVS, Benezra R. MAD2 haplo-insufficiency causes premature anaphase and chromosome instability in mammalian cells. *Nature* **409**: 355-359 (2001)

Minhas KM, Singh B, Jiang W, Sidransky D, Califano JA. Spindle assembly checkpoint defects and chromosomal instability in head and neck squamous cell carcinoma. *International Journal of Cancer* **107**: 46–52 (2003)

Murti PR, Warnakulasuriya KAAS, Johnson NW, Bhonsle RB, Gupta PC, Daftary DK. Mehta FS. p53 expression in oral precancer as a marker for malignant potential. *Journal of Oral Pathology and Medicine* **27**:191-196 (1998).

Nakayama K, Nagahama H, Minamishima YA, Matsumoto M, Nakamichi I, Kitagawa K, Shirane M, Tsunematsu R, Tsukiyama T, Ishida N, Kitagawa M, Nakayama K, Hatakeyama S. Targeted disruption of *Skp2* results in accumulation of cyclin E and $p27^{Kip1}$, polyploidy and centrosome overduplication. *EMBO Journal* **19**: 2069-2081(2000)

Nevins JR. The Rb/E2F pathway and cancer. *Human Molecular Genetics* **10**: 699-703 (2001)

Nowak MA, Komorova N, Sengupta A, Jallepalli P, Shih IM, Vogelstein B, Lengaur C. The role of chromosomal instability in tumour initiation. *Proceedings of National Academy of Sciences USA* **99**: 16226-16231 (2002)

O'Hagan RC, Chang S, Maser RS, Mohan R, Artandi SE, Chin L, DePinho RA. Telomere dysfunction provokes regional amplification and deletion in cancer. *Cancer Cell* **2**: 149-155 (2002)

Okafuji M, Ita M, Hayatsu Y, Shinozaki F, Oga A, Sasaki K. Identification of genetic aberrations in cell lines from oral squamous cell carcinomas by

comparative genomic hybridisation. *Journal of Oral Pathology and Medicine* **28**: 241-245 (1999)

Okami K, Reed AL, Cairns P, Koch WM, Westra WH, Wehage S, Jen J, Sidransky D. Cyclin D1 amplification is independent of p16 inactivation in head and neck squamous cell carcinoma. *Oncogene* **18**: 3541-3545 (1999)

Ouyang X, Wang X, Xu K, Jin DY, Cheung ALM, Tsao SW, Wong YC. Effect of p53 on centrosome amplification in prostate cancer cells. *Biochimica et Biophysica Acta* **1541**: 212-220 (2001)

Ouyang B, Knauf JA, Ain K, Nacev B, Fagin JA. Mechanisms of aneuploidy in thyroid cancer cell lines and tissues: evidence for mitotic checkpoint dysfunction without mutations in BUB1 and BUBR1. *Clinical Endocrinology* **56**: 341-350 (2002)

Parkin MD, Pisani P, Ferlay J. Estimates of the worldwide incidence of 25 major cancers in 1990. *International Journal of Cancer* **80**: 827-841 (1999)

Partridge M, Emilion G, Pateromichelakis S, A'Hern R, Philips E, Langdon J. Allelic imbalance at chromosomal loci implicated in the pathogenesis of oral precancer, cumulative loss and its relationship with progression to cancer. *Oral Oncology* **34**: 77-83 (1998)

Partridge M, Emilion G, Pateromichelakis S, Phillips E, Langdon J. Field Cancerisation of the Oral Cavity: Comparison of the Spectrum of Molecular Alterations in Cases Presenting with Both Dysplastic and Malignant Lesions. *Oral Oncology* **33**: 332-337 (1997)

Patel V, Yeudall WA, Gardner A, Mutlu S, Scully C, Prime SS. Consistent Chromosomal Anomalies in Keratinocyte Cell Lines Derived From Untreated Malignant Lesions of the Oral Cavity. *Genes, Chromosomes and Cancer* **7**: 109-115 (1993)

Paterson IC, Eveson JW. Prime SS. Molecular Changes in Oral Cancer May Reflect Aetiology and Ethnic Origin. *Oral Oncology European Journal of Cancer* **32**: 150-153 (1996)

Percy MJ, Myre KA, Neeley CK, Azm JN, Ether SP, and Petty EM. Expression and Mutational Analyses of the Human MAD2L1 Gene in Breast Cancer Cells. *Genes, Chromosomes and Cancer* **29**: 356-362 (2000)

Peters JM. The anaphase-promoting complex: proteolysis in mitosis and beyond. *Molecular Cell* **9**: 931-943 (2002)

Piel M, Nordberg J, Euteneuer U, Bornens M. Centrosome–dependent exit of cytokinesis in animal cells. *Science* **291**: 1550-1553 (2001)

Pihan GA, Purohit A, Wallace J, Knecht H, Woda B, Quesenberry P, Doxey SJ. Centrosome defects and genetic instability in malignant tumours. *Cancer Research* **58**: 3974-3985 (1998)

Pihan GA, Purohit A, Wallace J, Malhotra R, Liotta L, Doxey SJ. Centrosome defects can account for cellular and genetic changes that characterize prostate cancer progression. *Cancer Research* **61**: 2212-2219 (2001)

Pihan GA, Wallace J, Zhou Y, Doxey SJ. Centrosome abnormalities and chromosome instability occur together in pre-invasive carcinomas. *Cancer Research* **63**: 1398-1404 (2003)

Prime SS, Nixon SVR, Crane IJ, Stone A, Matthews JB, Maitland NJ, Remnant L, Powell SK, Game SM, Scully C. The behaviour of human oral squamous cell carcinoma in cell culture. *Journal of Pathology* **160**: 259-269 (1990)

Prime SS, Matthews JB, Patel V, Game SM, Donnelly M, Stone A, Paterson IC, Sandy JR, Yeudall WA. TGF-β receptor regulation mediates the response to exogenous ligand but is independent of the degree of cellular differentiation in human oral keratinocytes. *International Journal of Cancer* **56**: 406-412 (1994)

Prime SS, Eveson JW, Stone AM, Huntley SP, Davies M, Paterson IC, Robinson CM. Metastatic dissemination of human malignant oral keratinocyte cell lines following orthotopic transplantation reflects response to TGF-β1. *Journal of Pathology* **203**: 927-932 (2004)

Rajagopalan H, Lengauer C. CIN-ful cancers. *Cancer Chemotherapy and Pharmacology* **54**: S65-S68 (2004)

Rasnick D, Duesberg PH. How aneuploidy affects metabolic control and causes cancer. *Biochemical Journal* **340**: 621-630 (1999)

Reibel J. Prognosis of oral pre-malignant lesions: significance of clinical, histopathological and molecular biological characteristics. *Critical Review in Oral Biology and Medicine* **14**: 47-62 (2003)

Reing JE, Gollin SM, Saunders WS. The occurrence of chromosome segregational defects is an intrinsic and heritable property of oral squamous cell carcinoma cell lines. *Cancer, Genetics and Cytogenetics* **150**: 57-61 (2004)

Reis RM, Nakamura M, Masuoka J, Watanabe T, Colella S, Yonekawa Y, Kleihues P, Ohgaki H. Mutation analysis of hBUB1, hBUBR1 and hBUB3 genes in glioblastoma. *Acta Neuropathology* **101**: 297-304 (2001)

Reshmi SC, Saunders WS, Kudla DM, Ragin CR, Gollin SM. Chromosomal instability and marker chromosome evolution in oral squamous cell carcinoma. *Genes, Chromosomes and Cancer* **41**: 38-46 (2004)

Rheinwald JG, Beckett MA. Tumorigenic keratinocyte cell lines requiring anchorage and fibroblast support cultured from human squamous cell carcinomas. *Cancer Research* **41**: 1657-1663 (1981)

Rhim JS. Current state-of-the-art in human cell transformation in culture. *Yonsei Medical Journal* **32**: 195-206 (1991)

Rieder CL, Schultz A, Cole R, Sluder G. Anaphase onset in vertebrate somatic cells is controlled by a checkpoint that monitors sister kinethochore attachment to the spindle. *Journal of Cell Biol*ogy **127**: 1301-1310 (1994)

Rieder CL, Cole RW, Khodjakov A, Sluder G. The checkpoint delaying anaphase in response to chromosome monoorientation is mediated by an inhibitory signal produced by unattached kinetochores. *Journal of Cell. Biology* **130**: 941-948 (1995)

Roberts BT, Farr KA, Hyot MA. The Saccharomyces cerevisiae checkpoint gene BUB1 encodes a novel protein kinase. *Molecular and Cellular Biology* **14**: 8282-8291 (1994)

Rosin MP, Cheng X, Poh C, Lam WL, Huang Y, Lovas J, Berean K, Epstein JB, Priddy R, Le ND, Zhang L. Use of allelic loss to predict malignant risk for low-grade oral epithelial dysplasia. *Clinical Cancer Research* **6**: 357-362 (2000)

Rousseau A, Lim MS, Lin Z, Jordan RCK. Frequent cyclin D1 gene amplification and protein overexpression in oral epithelial dysplasias. *Oral Oncology* **37**: 268-275 (2001)

Rubio MA, Kim SH, Campisi J. Reversible manipulation of telomerase expression and telomere length. *Journal of Biological Chemistry* **277**: 28609-28617 (2002)

Rubio MA, Davalos AR, Campisi J. Telomere length mediates the effects of telomerase on the cellular response to genotoxic stress. *Experimental Cell Research* **298**: 17-27 (2004)

Rudolph KL, Millard M, Bosenberg MW, DePinho RA. Telomere dysfunction and evolution of intestinal carcinoma in mice and humans. *Nature Genetics* **28**: 155-159 (2001)

Saeki A, Tamura S, Ito N, Kiso S, Matsuda Y, Yabuuchi I, Kawata S, Matsuzawa Y. Frequent impairment of the spindle assembly checkpoint in hepatocellular carcinoma. *Cancer* **94**: 2047 – 54 (2002)

Sambrook J, Fritsch EF, Maniatis T. Molecular Cloning: A Laboratory Manual (2nd Edition). Cold Spring Harbour: Cold Spring Laboratory Press. (1989)

Sato N, Mizumoto K, Nakamura M, Nakamura K, Kusumoto M, Niiyama H, Ogawa T, Tanaka M. Centrosome abnormalities in pancreatic ductal carcinoma. *Clinical Cancer Research* **5**: 963-970 (1999)

Sato M, Sekido Y, Horio Y, Takahashi M, Saito H, Minna JD, Shimokata K, Hasegawa. Infrequent mutation of the hBUB1 and hBUBR1 genes in human lung cancer. *Japan Journal of Cancer Research* **91**: 504-509 (2000)

Sato N, Mizumoto K, Nakamura M, Maehara N, Minamishima YA, Nishio S, Nagai E, Tanaka M. Correlation between centrosome abnormalities and chromosomal instability in human pancreatic cancer cells. *Cancer Genetics and Cytogenetics* **126**:13-19 (2001)

Schut HAJ, Snyderwine EG. DNA adduct of heterocyclic amine food mutagens: implications for mutagenesis and carcinogenesis. *Carcinogenesis* **20**: 353-368 (1999)

Schwartz SM, Doody DR, Fitzgibbons ED, Ricks S, Porter PL, Chen C. Oral squamous cell cancer risk in relation to alcohol consumption and alcohol dehydrogenase-3 genotype. *Cancer Epidemiology Biomarker and Prevention* **10**: 1137-1144 (2001)

Scully C, Field JK, Tanzawa H. Genetic aberrations in oral or head and neck squamous cell carcinoma 2: chromosomal aberrations. *Oral Oncology* **36**; 311-327 (2000)

Shackney SE, Smith CA, Miller BW, Burholt DR, Murtha K, Giles HR, Ketterer DM, Pollice AA. Model for the genetic evolution of human solid tumors. *Cancer Research* **49**: 3344-3354 (1989)

Shahnavaz SA, Regezi JA, Bradley G, Dube ID, Jordan RCK. p53 gene mutations in sequential oral epithelial dysplasias and squamous cell carcinoma. *Journal of Pathology* **190**: 417-422 (2000)

Shahnavaz SA, Bradley G, Regezi JA, Thakker N, Gao L, Hogg D, Jordan RCK. Patterns of CDKN2A gene loss in sequential oral epithelial dysplasias and carcinomas. *Cancer Research* **61**: 2371-2375 (2001)

Shichiri M, Yoshinaga K, Hisatomi H, Sugihara K, Hirata Y. Genetic and epigenetic inactivation of mitotic checkpoint genes hBUB1 and hBUBR1 and their relationship to survival. *Cancer Research* **62**: 13-17 (2002)

Shih IM, Zhou W, Goodman SN, Lengauer C, Kinzler KW, Vogelstein B. Evidence that genetic instability occurs at an early stage of colorectal tumorigenesis. *Cancer Research* **61**: 818-822 (2001)

Shintani S, Nakahara Y, Mihara M, Ueyama Y, Matsumura T. Inactivation of the p14ARF, p15INK4B and p16INK4A genes is a frequent event in human oral squamous cell carcinomas. *Oral Oncology* **37**: 498-504 (2001)

Shono M, Sato N, Mizumoto K, Maehara N, Nakamura M, Nagai E, Tanaka M. Stepwise progression of centrosome defects associated with local tumor growth and metastatic process of human pancreatic carcinoma cells transplanted orthotopically into nude mice. *Laboratory Investigation* **81**: 945-952 (2001)

Skibbens RV, Hieter P. Kinetochores and the checkpoint mechanism that monitors for defects in the chromosome segregation machinery. *Annual Review in Genetics* **32**: 307-337 (1998)

Skoufias DA, Andreassen PR, Lacroix FB, Wilson L, Margolis RL. Mammalian mad2 and bub1/bubR1 recognize distinct spindle-attachment and kinetochore-tension checkpoints. *Proceedings of National Academy of Science USA* **98**: 4492-4497 (2001)

Sluder G, Hinchcliffe EH. The coordination of centrosome reproduction with nuclear events during cell cycle. *Current Topics in Developmental Biology* **49**: 268-289 (2000)

Sparano A, Weinstein G, Chalian A, Yodul M, Weber R. Multivariate predictor of occult neck metastasis in early oral tongue cancer. *Otolaryngology-Head and Neck Surgery* **131**: 472-476 (2004)

Stearns T. Centrosome duplication: A centriolar Pas de Deux. *Cell* **105**: 417-420 (2001)

Stewart ZA, Leach SD, Pietenpol JA. p21 Waf1/Cip1 inhibition of cyclin E/Cdk" activity prevents endoreduplication after mitotic spindle disruption. *Molecular and Cellular Biology* **19**: 205-215 (1999)

Sudbo, J., Kildal, W., Risberg, B., Koppang, H.S., Danielsen, H.E., and Reith,A. DNA content as a prognostic marker in patients with oral leukoplakia. *New England Journal of Medicine* **344**: 1270-1278 (2001a)

Sudbo, J., Ried,T., Bryne, M., Kildal, W., Danielsen, H., and Reith, A. Abnormal DNA content predicts the occurrence of carcinomas in non-dysplastic oral white patches. *Oral Oncology* **37**: 558-565 (2001b)

Sudbo J, Bryne M, Johannessen AC, Kildal W, Danielsen HE, Reith A. Comparison of histological grading and large scale genomic status (DNA ploidy) as prognostic tools in oral dysplasia. *Journal of Pathology* **194**: 303-310 (2001c)

Sudbo J, Lippman SM, Lee JJ, Mao L, Kildal W, Sudbo A, Sagen S, Bryne M, El-Naggar A, Risberg B, Evensen JF, Reith A. The influence of resection and aneuploidy on mortality in oral leukoplakia. *New England Journal of Medicine* **350**: 1405-1413 (2004)

Sugiyama M, Speight PM, Prime SS, Watt FM. Comparison of integrin expression and terminal differentiation capacity in cell lines derived from oral squamous cell carcinomas. *Carcinogenesis* **14**: 2171-2176 (1993)

Tarapore P, Tokuyama Y, Horn HF, Fukasawa K. Difference in the centrosome duplication regulatory activity among p53 'hot spot' mutants: potential role of Ser 315 phosphorylation-dependent centrosome binding of p53. *Oncogene* **20**: 6851-6863 (2001)

Taylor SS, McKeon F. Kinetochore Localization of Murine Bub1 Is Required for Normal Mitotic Timing and Checkpoint Response to Spindle Damage. *Cell* **89**: 727-735 (1997)

Tighe A, Johnson VL, Albertella M, Taylor SS. Aneuploid colon cancer cells have a robust spindle checkpoint. *EMBO Reports* **21**: 609-614 (2001)

Tomlinson IPM, Novell MR, Bodmer WF. The mutation rate and cancer. *Proceedings of National Academy of Sciences USA* **93**: 14800-14803 (1996)

Tsukasaki K, Miller CW, Greensoun E, Eshaghian S, Kawabata H, Fujimoto T, Tomonaga M, Sawyers C, Said JW, Koeffler HP. Mutations in the mitotic checkpoint gene, Mad1L1, in human cancers. *Oncogene* **20** 3301-3305 (2001)

Tutt A, Gabriel A, Bertwistle D, Connor F, Paterson H, Peacock J, Ross G, Ashworth A. Absence of Brca2 causes genome instability by chromosome breakage and loss associated with centrosome amplification. *Current Biology* **9**: 1107-1110 (1999)

Uetake Y, Sluder G. Cell cycle progression after cleavage failure: mammalian somatic cells do not possess a "tetraploidy checkpoint". *Journal of Cell Biology* **165**: 609-615 (2004)

Vogelstein B, Lane D, Levine AJ. Surfing the p53 network. *Nature* **408**: 307-310. (2001)

Wang X, Jin DY, Ng RWM, Feng HF, Wong YC, Cheung ALM, Tsao SW. Significance of MAD2 expression to mitotic checkpoint control in ovarian cancer cells. *Cancer Research* **62**: 1662 – 1668. (2002)

Warnakulasuriya, S. Lack of molecular markers to predict malignant potential of oral precancer. *Journal of Pathology* **190**: 407-409. (2000)

Wassmann K, Benezra R. Mitotic checkpoints: from yeast to cancer. *Current Opinion in Genetics and Development* **11**: 83-90 (2001)

Weber RG, Scheer M, Born IA, joos S, Cobbers JMJL, Hofele C, Reifenberger G, Zoller JE, Lichter P. Recurrent chromosomal imbalances detected in biopsy *material from oral premalignant* and malignant lesions by combined tissue microdissection, universal *DNA amplification, and* comparative genomic hybridisation. *American Journal of Pathology* **153**: 295-303 (1998)

Weiss E, Winey M. The Saccharomyces cerevisiae spindle pole body duplication gene MPS1 is part of a mitotic checkpoint. *Journal of Cell Biology* **132**: 111-123 (1996)

Wu CI, Roz L, McKown S, Sloan P, Read AP, Holland S, Porter S, Scully C, Paterson I, Tavassoli M, Thakker N. DNA studies underestimate the major role of CDKN2A inactivation in oral and orophyrangeal squamous cell carcinomas. *Genes, Chromosomes and Cancer* **25**: 16–25 (1999)

Xu XL, Weaver Z, Linke SP, Li CL, Gotay J, Wang XW, Harris CC, Ried T, Deng CX. Centrosome amplification and a defective G(2)-M cell cycle checkpoint induce genetic instability in BRCA1 exon 11 isoform-deficient cells. *Molecular Cell* **3**: 389-395 (1999)

Yamaguchi K, Okami K, Hibi K,. Wehage SL, Jen J, Sidransky D. Mutational analysis of hBUB1 in aneuploid HNSCC and lung cancer cell lines. *Cancer Letters* **139**: 183-187 (1999)

Yamasaki H, Mironov N. Genomic instability in multistage carcinogenesis. *Toxicology Letters* **112-113**: 251-256 (2000)

Yamazaki Y, Chiba I, Hirai A, Sugiura C, Notani K, Kashiwazaki H, Tei K, Totsuka Y, Fukuda H. Specific p53 mutations predict poor prognosis in oral squamous cell carcinoma. *Oral Oncology* **39**: 163-169 (2003)

Yeudal WA, Torrance LK, Elsegood KA, Speight P, Scully C, Prime SS. *ras* gene point mutation is a rare event in premalignant and malignant lesions of the oral cavity. *Oral Oncology European Journal of Cancer* **29**: 63-68 (1993)

Yeudall WA, Paterson IC, Patel V, Prime SS. Presence of human papillomavirus sequences in tumour-derived human oral keratinocytes expressing mutant p53. *Oral Oncology European Journal of Cancer* **31**: 136-143 (1995)

Yoon DS, Wersto RP, Zhou W, Chrest FJ, Garrett ES, Kwon TK, Gabrielson E. Variable levels of chromosomal instability and mitotic spindle checkpoint defects in breast cancer. *American Journal of Pathology* **161**: 391-397 (2002)

Yu H. Regulation of APC-Cdc20 by the spindle checkpoint. *Current Opinion in Cell Biology* **14**: 706-714 (2002)

Zhou H, Kuang J, Kuo W, Gray *JW, Sahin A, Brinkley BR, Sen S. Tumour* amplified kinase STK15/BTAK induces centrosome amplification, aneuploidy and transformation. *Nature Genetics* **20**: 189-(1998)

Zhu H, Gooderham N. Neoplastic transformation of human lung fibroblast MRC-5 SV2 cells induced by benzo[a]pyrene and confluence culture. *Cancer Research* **62**: 4605-4609 (2002)

Zimonjic D, Brooks MW, Popescu N, Weinberg RA, Hahn WC. Derivation of human tumor cells in vitro without widespread genomic instability. *Cancer Research* **61**: 8838-8844 (2001)

APPENDICES

APPENDIX I

INDEX OF MAIN SUPPLIERS

Alexis Corporation (UK)
3 Moorbridge Court,
Moorbridge Road East,
Bingham, Nottingham
NG13 8QG United Kingdom

Amersham International Plc.
Amersham Place
Little Chalfont
Buckinghamshire
HP7 9NA United Kingdom

Applied Imaging
Stretton Scientific Ltd.
Stretton House, Highstairs Lane
Stretton, Derbyshire
DE55 6FD United Kingdom

BDH
VWR International Ltd.
Merck House
Poole, Dorset,
BH15 1TD United Kingdom

BD Biosciences (BD-Pharmingen)
21 Between Towns Road
Cowley, Oxford
OX4 3LY United Kingdom

Beckman Coulter (U.K.) Ltd.
Oakley Court
Kingsmead Business Park
London Road, High Wycombe
Buckinghamshire
HP11 1JU United Kingdom

Berkeley Antibody Company (BabCO)
1223 South 47th Street
Richmond, California,
94804 USA

Bibby Sterilin Ltd.
Tilling Drive Stone,
ST15 0SA Staffordshire
United Kingdom

Bio-Rad Laboratories Ltd.
Bio-Rad House
Maylands Avenue
Hemel Hampstead, Hertfordshire
HP2 7TD United Kingdom

BioWhittaker UK, Ltd.
1 Ashville Way
Wokingham
RG41 2PL United Kingdom

APPENDIX I

Calbiochem
EMD Biosciences, Inc
10394 Pacific Center Court
San Diego, CA 92121
United States

Clontech
1020 East Meadow Circle
Palo Alto, CA 94303-4230

Corning Limited
The Guildway, Old Portsmouth Road,
Artington, Surrey
GU3 1LR United Kingdom

European Collection of Animal Cell Cultures
Division of Biologics, PHLS
Centre for Applied Microbiology & Res
Porton Down, Salisbury, SP4 0JG

Fairfield Imaging Ltd.,
1 Orchard Place,
Nottingham Business Park,
Nottingham
NG8 6PX United Kingdom

Fisher Scientific UK Ltd
Bishop Meadow Road
Loughborough, Leicestershire
LE11 5RG United Kingdom

Greiner Bio-One Ltd.
Brunel Way,
Stroudwater Business Park,
Stonehouse, Gloucestershire
GL10 3SX United Kingdom

Hoefer Scientific Instrument
654 Minnesota Street
San Francisco CA 94107

Invitrogen Life Technologies Ltd.
3 Fountain Drive
Inchinnan Business Park, Paisley
PA4 9RF United Kingdom

ICN Pharmaceuticals Ltd.
Cedarwood,
Chineham Business Park,
Crockford Lane,
Basingstoke, Hampshire
RG24 8WD United Kingdom

Jackson ImmunoResearch Lab.,Inc
Stratech Scientific Ltd.
Unit 4, Northfield Business Park,
Northfield Road, Soham,
CB7 5UE Cambridgeshire, United Kingdo

Kodak UK
Professional Customer Services
PO Box 66, Station Road
Hemel Hempstead, Hertfordshire
HP1 1JU United Kingdom

APPENDIX I

Leica Microsystems (UK) Ltd
Davy Avenue, Knowlhill
Milton Keynes,
MK5 8LB United Kingdom

New England Biolabs (UK) Ltd.
73 Knowl Piece, Wilbury Way
Hitchin, Herts
SG4 0TY United Kingdom

Merck Biosciences, Ltd
Boulevard Industrial Park,
Padge Road,
Beeston, Nottingham
NG9 2JR United Kingdom

Olympus UK Ltd
2-8 Honduras Street
London
EC1Y 0TX United Kingdom

Microflow
Dent & Hellyer, Walworth Road
Andover, Hampshire
SP10 5AA United Kingdom

PAA Laboratories Ltd
1 Technine, Guard Avenue
Houndstone Business Park,
Yeovil, Somerset
BA22 8YE United Kingdom

Millipore (U.K.) Ltd
Units 3&5 The Courtyards
Hatters Lane, Watford
WD18 8YH United Kingdom

PE Applied Biosystems
Chalfont Road, Seer Green,
Beaconsfield Bucks HP9 2FX
United Kingdom

Moltox Inc.
P.O box 1189
Boone, NC8607 USA

Promega
Delta House
Chilworth Science Park
Southampton SO16 7NS
United Kingdom

MWG Biotech (UK) Ltd
Mill Court, Featherstone Road,
Wolverton Mill South, Milton Keynes,
MK12 5RD United Kingdom

Qiagen Ltd.
Fleming Way,
Crawley, West Sussex
RH10 9NQ United KIngdom

APPENDIX I

Roche Products Limited
P.O. Box 8, 40 Broadwater Road
Welwyn Garden City
Hertfordshire
AL7 3AY United Kingdom

Upstate Cell Signalling Solutions
Unit 3 Mill Square
Wolverton Mill South, Milton Keynes,
MK12 5YU United Kingdom

Shimadzu UK
Mill Court,
Featherstone Road, Milton Keynes
United Kingdom

Vysis
Abbott Laboratories Ltd.
Diagnostic Division
Abbott House, Norden Road,
Maidenhead, Berkshire
SL6 4XL United Kingdom

Sigma-Aldrich Company Ltd.
Fancy Road,
Poole, Dorset
BH12 4QH United Kingdom

Whatmann International Ltd
20/20 Whatman House
St Leonards Road
Maidstone, Kent
ME16 0LS United Kingdom

APPENDIX II

CETN2 SEQUENCE

agtgtacacg tcggttgcct aacaaccggc agcggactcc **tttggctatg gcctccaact ttaagaaggc aaacatggca tcaagttctc agcgaaaaag aatgagccct aagcctgagc ttactgaaga gcaaaagcag gagatccggg aagcttttga tcttttcgat gcggatggaa ctggcaccat agatgttaaa gaactgaagg tggcaatgag ggccctgggc tttgaaccca agaaagaaga aattaagaaa atgataagtg aaattgataa ggaagggaca ggaaaaatga actttggtga ctttttaact gtgatgaccc agaaaatgtc tgagaaagat actaaagaag aaatcctgaa agctttcaag ctctttgatg atgatgaaac tgggaagatt tcgttcaaaa atctgaaacg cgtggccaag gagttgggtg agaacctgac tgatgaggag ctgcaggaaa tgattgatga agctgatcga gatggagatg gagaggtcag tgagcaagag ttcctgcgca tcatgaaaaa gaccagcctc tattaa**gatc agtgtcttct ttttctactg caagcacatg taactagatt tagtgcctgc catggtgtga aatctggctt ttgagaacac aaacttttcc cccacggacc tccctttatc actttaatag tgaccttgag cctattttag ccgtttggaa gtgttctttg atattacagt tctttgtaaa atgacctgcg aattacccta attctcaaaa gcaaaacaag agcacacaag cgtgaagaaa aggatcttaa agctttgagc acctgccatt ttgccttgca tcgtttccct cgtcatgcat ttccacatat ccacaaacac agaacgactt tagacaagca catgttacac ctgtgttgcc acaagcagtc attcttgacg gctccagttt ttatttgaca cttgagttta gttttctctt ttataaaccc agtgaactcc tgcactggca tttggatgtg tgttaatgct atttgttttg tcttaaaagt aaaaccttte tcagtttgaa aaaaaaa**

Coding sequence in **bold**

APPENDIX III

PUBLICATIONS ARISING DURING CANDIDATURE

Thirthagiri E, Huntley S, Cowpe JG, Patterson I. Quantitative cytophotometry of monolayers of archival oral tissue samples. *Journal of Dental Research* **82**: 566 (2003)

Thirthagiri E, Prime SS, Paterson IC. **Mechanisms of genomic instability in oral** cancer. *Journal of Pathology* **201**: 36A (2003)